



**HYDROLOGICAL MODELING AND  
FORECASTING USING HEC-HMS SOIL  
MOISTURE ACCOUNTING FOR A SNOW  
DOMINATED BASIN IN TURKEY**  
Master of Science Thesis

**Bahlakoana Daniel KIKINE**  
Eskişehir, 2017

**HYDROLOGICAL MODELING AND FORECASTING  
USING HEC-HMS SOIL MOISTURE ACCOUNTING  
FOR A SNOW DOMINATED BASIN IN TURKEY**

**Bahlakoana Daniel KIKINE**

**MASTER OF SCIENCE THESIS**

**Department of Civil Engineering**

**Supervisor: Assoc. Prof. Dr. Aynur ŞENSOY ŞORMAN**

**Eskişehir**

**Anadolu University**

**Graduate School of Sciences**

**February, 2017**

## THESIS APPROVAL

This thesis entitled “Hydrological Modeling and Forecasting Using HEC-HMS Soil Moisture Accounting for a Snow Dominated Basin in Turkey” has been prepared and submitted by Bahlakoana Daniel KIKINE in partial fulfillment of the requirements in “Anadolu University Directive on Graduate Education and Examination” for the Degree of Master of Science in Civil Engineering Department has been examined and approved on 01/02/2017.

### Committee Members

### Signature

Member (Supervisor)	Assoc. Prof. Dr. AYNUR ŞENSOY ŞORMAN	.....
Member	Assoc. Prof. Dr. YAKUP DARAMA	.....
Member	Assist. Prof. Dr. ALİ ARDA ŞORMAN	.....

.....

Date

.....

Director

Graduate School of Sciences

## ABSTRACT

### HYDROLOGICAL MODELING AND FORECASTING USING HEC-HMS SOIL MOISTURE ACCOUNTING FOR A SNOW DOMINATED BASIN IN TURKEY

**Bahlakoana Daniel KIKINE**

**Department of Civil Engineering**

**Anadolu University, Graduate of School of Sciences, February, 2017**

**Supervisor: Assoc. Prof. Dr. Aynur ŞENSOY ŞORMAN**

The ever increasing world population, climate change, floods and droughts make an effective management of water resources a crucial subject in hydrologic science. Advancements in hydrologic modeling, snow modeling and streamflow forecasting technologies are significant to the efficient water resources management, minimizing flood and drought risk and increased hydropower generation in mountainous regions.

Karasu (Upper Euphrates) Basin (10,275 km<sup>2</sup>), a headwater of Euphrates River is selected as the pilot basin in this study. The aim of the study is to perform a forward-oriented deterministic streamflow forecasting with Numerical Weather Prediction data for Karasu Basin using Soil Moisture Accounting (SMA) and snow routine. A conceptual hydrological model HEC-HMS is calibrated and validated for 2002-2008 and 2009-2015, respectively. Furthermore, streamflow is forecasted for 2015 water year snowmelt period. Both event and continuous hydrologic modeling approaches are employed to determine the model parameters. Continuous modeling is done using conventional and start-state approaches which help to utilize multi method application. Also the satellite products for Snow Covered Area and Soil Moisture are used to assess the consistency of model results on Snow Water Equivalent and Soil Moisture. The model produced NSE and RMSE of 0.88 and 29.52 m<sup>3</sup>/s for calibration and 0.82 and 25.65 m<sup>3</sup>/s for validation, respectively.

The study applies SMA model in a snow dominated basin and draws internal consistency evaluations of state variables with satellite data. The study sets precedence with continuous SMA and streamflow forecasting for applied hydrology.

**Keywords:** Upper Euphrates Basin, Soil Moisture Accounting, HEC-HMS, Hydrologic Modeling, Runoff Forecasting.

## ÖZET

### TÜRKİYE’DE KAR AĞIRLIKLIL BİR HAVZADA HEC-HMS TOPRAK NEMİ YÖNTEMİ KULLANILARAK HİDROLOJİK MODELLEME VE TAHMİN

**Bahlakoana Daniel KIKINE**

**İnşaat Mühendisliği Anabilim Dalı**

**Anadolu Üniversitesi, Fen Bilimleri Enstitüsü, Şubat, 2017**

**Danışman: Doç. Dr. Aynur ŞENSOY ŞORMAN**

Artan dünya nüfusu, iklim değişikliği, taşkınlar ve kuraklıklar su kaynaklarının etkin yönetimini hidroloji biliminde kritik bir konu haline getirmektedir. Hidrolojik modelleme, kar modellemesi ve akım tahmini teknolojilerindeki gelişmeler dağlık bölgelerdeki su kaynaklarının etkin yönetimi, taşkın ve kuraklık riskini azaltmak ve hidroelektrik enerji üretimi için önemlidir.

Fırat Nehri'nin membasında bulunan Karasu (Yukarı Fırat) Havzası (10,275 km<sup>2</sup>) uygulama alanı olarak seçilmiştir. Çalışmanın amacı, Sayısal Hava Tahmin verileri ile toprak nemi ve kar yöntemleri kullanılarak Karasu Havzası için ileriye yönelik deterministik akım tahmini yapmaktır. HEC-HMS kavramsal hidrolojik modeli 2002-2008 ve 2009-2015 yıllarında sırasıyla kalibre edilmiş ve doğrulanmıştır. Ayrıca, 2015 su yılının erime döneminde akım tahmini yapılmıştır. Model parametrelerini belirlemek için hem olay bazlı hem de sürekli hidrolojik modelleme yaklaşımları kullanılmıştır. Sürekli modelleme, geleneksel ve 'başlangıç-durum' yaklaşımları kullanarak yapılmıştır. Aynı zamanda, modelin kar su eşdeğeri ve toprak nemi sonuçlarının tutarlılığını değerlendirmek amacıyla karla kaplı alan ve toprak nemi uydu ürünleri kullanılmıştır. Model, kalibrasyon döneminde 0.88 NSE ve 29.52 m<sup>3</sup>/s RMSE ve doğrulama döneminde 0.82 NSE ve 25.65 m<sup>3</sup>/s RMSE performansı sağlamıştır

Bu çalışmada kar ağırlıklı bir havzada toprak nemi modeli uygulanmakta ve durum değişkenlerinin içsel tutarlılığının değerlendirmesi uydu ürünleri ile yapılmaktadır. Çalışma, sürekli yaklaşımla toprak nemi yöntemi ve deterministik akım tahmini ile uygulamalı hidroloji alanında önemli bir örnek oluşturmaktadır.

**Anahtar Kelimeler:** Yukarı Fırat Havzası, Yoprak Nemi, HEC-HMS, Hidolojik Modelleme, Akım Tahmini.



*To my mother, 'Mathabang Rose Kikine  
And my late father, Ts'eliso Polaki Kikine...*

## ACKNOWLEDGEMENT

I would like to pass my heartfelt gratitude to Assoc. Prof. Dr. Aynur ŞENSOY ŞORMAN and Asst. Prof. Dr. Ali Arda ŞORMAN. Your wisdom always shined an optimistic light not only in my studies but my life during the course of my MSc studies. This study would have not been possible had it not been for your mentoring, guidance and patience, for that I am eternally grateful.

I would also like to thank Assoc. Prof. Dr. Yakup DARAMA for the valuable review of the thesis.

Special thanks to Cansaran ERTAŞ, Gökçen UYSAL and Bulut AKKOL for their valuable contribution to the study.

I would like to extend my gratitude to my colleagues and officemates Didem Özkan, Miyase İrem Topçu and Oğulcan Doğan for their motivation and encouragement, you are indeed the friends in need.

I would like express my sincere appreciation to my beloved Jeniffer Galenda NAGUDI for her motivation and faith in my dreams and aspirations, I am a blessed man to have you in my life.

Finally, I would like to thank my mother 'Mathabang Rose KIKINE, my brother Thabang Joseph KIKINE, my lovely sister Mats'eliso Adele KIKINE, my extended family and friends for their motivation and insightful advices. Because of you, I am a testament that indeed it takes a village to raise a child. Thank you.

Bahlakoana Daniel KIKINE

February, 2017

**STATEMENT OF COMPLIANCE WITH ETHICAL PRINCIPLES AND RULES**

I hereby truthfully declare that this thesis is an original work prepared by me; that I have behaved in accordance with the scientific ethical principles and rules throughout the stages of preparation, data collection, analysis and presentation of my work; that I have cited the sources of all the data and information that could be obtained within the scope of this study, and included these sources in the references section; and that this study has been scanned for plagiarism with “scientific plagiarism detection program” used by Anadolu University, and that “it does not have any plagiarism” whatsoever. I also declare that, if a case contrary to my declaration is detected in my work at any time, I hereby express my consent to all the ethical and legal consequences that are involved.

.....  
Bahlakoana Daniel KIKINE



## TABLE OF CONTENTS

	<u>Page</u>
TITLE PAGE.....	i
THESIS APPROVAL.....	ii
ABSTRACT .....	iii
ÖZET .....	iv
DEDICATION .....	v
ACKNOWLEDGEMENT .....	vi
STATEMENT OF COMPLIANCE WITH ETHICAL PRINCIPLES AND RULES.....	vii
TABLE OF CONTENTS.....	viii
LIST OF FIGURES .....	x
LIST OF TABLES .....	xiii
ABBREVIATIONS AND SYMBOLS .....	xv
<b>1. INTRODUCTION.....</b>	<b>1</b>
<b>1.1. Importance of the Study.....</b>	<b>1</b>
<b>1.2. Aim of the Study.....</b>	<b>2</b>
<b>1.3. Thesis Guideline .....</b>	<b>3</b>
<b>2. LITERATURE REVIEW .....</b>	<b>4</b>
<b>2.1. Previous Studies in the Pilot Area .....</b>	<b>4</b>
<b>2.2. Soil Moisture Accounting Studies .....</b>	<b>5</b>
<b>2.3. Hydrologic Modeling and Streamflow Forecasting .....</b>	<b>7</b>
<b>3. STUDY AREA AND DATA .....</b>	<b>10</b>
<b>3.1. Karasu Basin .....</b>	<b>10</b>
<b>3.2. Hydro-meteorological data .....</b>	<b>15</b>
<b>3.3. Numerical Weather Predictions .....</b>	<b>23</b>
<b>3.4. Satellite Products .....</b>	<b>26</b>
<b>3.4.1. Soil moisture product .....</b>	<b>26</b>
<b>3.4.2. Snow cover product .....</b>	<b>27</b>
<b>4. HYDROLOGICAL MODEL .....</b>	<b>29</b>
<b>4.1. Hydrological Model Description .....</b>	<b>29</b>
<b>4.2. Hydrological Model Structure .....</b>	<b>31</b>
<b>4.2.1. Loss method .....</b>	<b>33</b>

4.2.2.	Transform method.....	37
4.2.3.	Baseflow method.....	39
4.2.4.	Temperature index method.....	39
4.2.5.	Start-state condition.....	41
4.2.6.	Runoff forecast module.....	42
5.	MODEL APPLICATION AND RESULTS.....	45
5.1.	Model Parameter Estimation.....	45
5.1.1.	Loss parameter estimation .....	47
5.1.2.	Baseflow parameter estimation .....	51
5.1.3.	Snowmelt parameter estimation.....	52
5.1.4.	Transform parameter estimation .....	57
5.2.	Model Results.....	57
5.2.1.	Discharge.....	57
5.2.2.	Snow water equivalent .....	67
5.2.3.	Soil moisture .....	74
5.3.	Streamflow Forecasting .....	79
6.	CONCLUSION AND RECOMMENDATIONS .....	81
	REFERENCES .....	84
	APPENDIX A .....	91

CV

## LIST OF FIGURES

	<u>Pages</u>
<b>Figure 3.1.</b> Karasu Basin's location and elevation map .....	11
<b>Figure 3.2.</b> Karasu Basin elevation zone map .....	12
<b>Figure 3.3.</b> Karasu Basin aspect map .....	13
<b>Figure 3.4.</b> Karasu Basin slope map .....	14
<b>Figure 3.5.</b> Karasu Basin land use map .....	15
<b>Figure 3.6.</b> Hydro-meteorological stations in and around Karasu Basin .....	16
<b>Figure 3.7.</b> Average total monthly precipitation for Karasu Basin (2002-2015) .....	17
<b>Figure 3.8.</b> Average total annual precipitation for Karasu Basin (2002-2005) .....	17
<b>Figure 3.9.</b> Average monthly temperature for Karasu Basin (2002-2015) .....	18
<b>Figure 3.10.</b> Average annual temperature for Karasu Basin (2002-2015) .....	19
<b>Figure 3.11.</b> Karasu Basin hydrograph for different water years .....	20
<b>Figure 3.12.</b> Observed and WRF precipitation data in Turkey for 06 June 2013 .....	24
<b>Figure 3.13.</b> Observed and WRF temperature data in Turkey for 06 June 2013 .....	24
<b>Figure 3.14.</b> Observed and WRF temperature data for Karasu Basin, 2015 .....	25
<b>Figure 3.15.</b> Observed and WRF precipitation data for Karasu Basin, 2015 .....	25
<b>Figure 3.16.</b> Global H-14 Soil Moisture data for 23 December 2016 .....	26
<b>Figure 3.17.</b> H-14 Soil Moisture data for Karasu Basin, 2015 .....	27
<b>Figure 3.18.</b> Snow depletion curves for Karasu Basin.....	28
<b>Figure 4.1.</b> Computational process of a hydrologic model .....	29
<b>Figure 4.2.</b> HEC-HMS basin model schematic (USACE, 2015) .....	30
<b>Figure 4.3.</b> Spatial characterization on rainfall-runoff models (Jones, 1997) .....	32
<b>Figure 4.4.</b> HEC-HMS schematic diagram for SMA (USACE, 2015) .....	34

<b>Figure 4.5.</b> Component editor for SMA (USACE, 2015) .....	36
<b>Figure 4.6.</b> Transformation of excess precipitation into a hydrograph (Musy, 2001) .....	37
<b>Figure 4.7.</b> Component editor for Clark unit hydrograph (USACE, 2015) .....	38
<b>Figure 4.8.</b> Component editor for linear reservoir (USACE, 2015) .....	39
<b>Figure 4.9.</b> Component editor for the temperature index (USACE, 2015) .....	40
<b>Figure 4.10.</b> Component editor for saved state (USACE, 2015) .....	42
<b>Figure 4.11.</b> Component editor for forecast alternative (USACE, 2015) .....	43
<b>Figure 5.1.</b> Event based simulation of 2002 snowmelt period .....	55
<b>Figure 5.2.</b> Observed and event based simulated hydrographs for Karasu Basin (2002 – 2007) .....	56
<b>Figure 5.3.</b> Observed and conventional simulated hydrographs for Karasu Basin, 2002 .....	59
<b>Figure 5.4.</b> Observed and start-state simulated hydrographs for Karasu Basin, 2002 .....	60
<b>Figure 5.5.</b> Observed and start-state simulated hydrographs for Karasu Basin, calibration period.....	61
<b>Figure 5.6.</b> Observed, start-state and conventional simulated hydrographs for Karasu Basin, calibration period .....	62
<b>Figure 5.7.</b> Observed and start-state simulated hydrograph for Karasu Basin, validation period .....	63
<b>Figure 5.8.</b> Observed, start-state and conventional simulated hydrograph for Karasu Basin, validation period .....	64
<b>Figure 5.9.</b> Snow Depletion Curve and start-state simulated SWE for Karasu Basin, 2002 .....	67
<b>Figure 5.10.</b> Start-state simulated SWE and Snow Depletion Curve for Karasu Basin, calibration period .....	70

<b>Figure 5.11.</b> Conventional and start-state simulated SWE for Karasu Basin, calibration period.....	71
<b>Figure 5.12.</b> Start-state simulated SWE and Snow Depletion Curve for Karasu Basin, validation period .....	72
<b>Figure 5.13.</b> Conventional and start-state simulated SWE for Karasu Basin, validation period .....	73
<b>Figure 5.14.</b> Simulated and satellite based soil moisture for Karasu Basin, 2013.....	76
<b>Figure 5.15.</b> Linear regression of soil moisture for Karasu Basin, 2013.....	76
<b>Figure 5.16.</b> Simulated and satellite based soil moisture for Karasu Basin, 2014.....	77
<b>Figure 5.17.</b> Linear regression of soil moisture for Karasu Basin, 2014.....	77
<b>Figure 5.18.</b> Simulated and satellite based soil moisture for Karasu Basin, 2015.....	78
<b>Figure 5.19.</b> Linear regression of soil moisture for Karasu Basin, 2015.....	78
<b>Figure 5.20.</b> Runoff forecasting with observed and Numerical Weather Prediction data for Karasu Basin, 2015.....	80

## LIST OF TABLES

	<u>Pages</u>
<b>Table 3.1.</b> Karasu Basin topographic properties .....	12
<b>Table 3.2.</b> Karasu Basin aspect distribution .....	13
<b>Table 3.3.</b> Karasu Basin slope distribution .....	14
<b>Table 3.4.</b> Karasu Basin land use distribution .....	15
<b>Table 3.5.</b> Karasu Basin water year classification .....	22
<b>Table 4.1.</b> Component editor for ATI meltrate function .....	41
<b>Table 5.1.</b> Range of SMA parameters used in HEC-HMS .....	48
<b>Table 5.2.</b> Sensitivity analysis for maximum infiltration, 2007 .....	49
<b>Table 5.3.</b> Sensitivity analysis for soil storage, 2007 .....	49
<b>Table 5.4.</b> Sensitivity analysis for tension storage, 2007 .....	49
<b>Table 5.5.</b> Sensitivity analysis of soil percolation, 2007 .....	50
<b>Table 5.6.</b> Soil moisture accounting model parameter set for Karasu Basin .....	50
<b>Table 5.7.</b> Linear reservoir baseflow parameter set for Karasu Basin .....	51
<b>Table 5.8.</b> Constant monthly baseflow parameter set for Karasu Basin .....	52
<b>Table 5.9.</b> Temperature index parameter ranges .....	53
<b>Table 5.10.</b> Adjustment coefficients for snow water equivalent (SWE) distribution in Karasu Basin .....	54
<b>Table 5.11.</b> Temperature index parameter set for Karasu Basin .....	54
<b>Table 5.12.</b> Clark unit hydrograph parameter set for Karasu Basin .....	57
<b>Table 5.13.</b> Model performance assessment for Karasu Basin .....	65
<b>Table 5.14.</b> The consistency analysis of simulated SWE and satellite derived SCA (>0) for Karasu Basin .....	68

<b>Table 5.14 (b).</b> The consistency analysis of simulated SWE and satellite derived SCA (>3) for Karasu Basin .....	68
<b>Table 5.15. (a).</b> Model performance for snow state .....	69
<b>Table 5.16 (b).</b> Model performance for snow state.....	69
<b>Table 5.16.</b> Pearson R performance results for Karasu Basin .....	75
<b>Table 5.17.</b> Forecast model performance with different data sets .....	79



## ABBREVIATIONS AND SYMBOLS

<b>ATI</b>	: Antecedent Temperature Index
<b>AWOS</b>	: Automated Weather Observation Stations
<b>DK</b>	: Detrended Krigging
<b>DSI</b>	: General Directorate of State Hydraulic Works
<b>DSS</b>	: Data Storage System
<b>ET</b>	: EvapoTranspiration
<b>EUMETSAT</b>	: European Organization for the Exploitation Meteorological Satellites
<b>GIS</b>	: Geographic Information Systems
<b>HEC-HMS</b>	: Hydrologic Engineering Center's Hydrologic Modeling System
<b>H-SAF</b>	: Satellite Application Facility on Support to Operational Hydrology and Water Management
<b>MGM</b>	: Turkish General Directorate of Meteorology
<b>MM5</b>	: Mesoscale Model 5
<b>MODIS</b>	: Moderate Resolution Imaging Spectroradiometer
<b>NASA</b>	: National Aeronautics and Space Administration
<b>NATO</b>	: The North Atlantic Treaty Organization
<b>NSE</b>	: Nash-Sutcliffe Efficiency
<b>NWP</b>	: Numerical Weather Predictions
<b>RMSE</b>	: Root Mean Square Error
<b>SCA</b>	: Snow Covered Area
<b>SM</b>	: Soil Moisture
<b>SMA</b>	: Soil Moisture Accounting
<b>SNOTEL</b>	: Snow Telemetry
<b>SRTM</b>	: Shuttle Radar Topographic Mission
<b>SWE</b>	: Snow Water Equivalent
<b>TC</b>	: Time of Concentration
<b>TCKB</b>	: The Turkish Ministry of Development
<b>TSMS</b>	: Turkish State Meteorological Services



**USACE** : Unites States Army Corps of Engineers

**WRF** : Weather Research and Forecasting



# 1. INTRODUCTION

## 1.1. Importance of the Study

Water as the source of life has influenced the settlements of civilizations for centuries. However, the ever increasing world population, the effects of climate change and global warming pose a significant threat to the hydrological cycle and water resources. Therefore, the development and advancement of technologies in hydrological sciences and snow modeling are of great importance in the mountainous snow dominated regions. This will increase the efficiency of water resources management and minimize the effects of droughts and floods through the use of planning and operation assisted by the hydrological models based on runoff forecasting.

Despite been enclosed by three seas, the mean elevation of 1130 m shows that Turkey is a mountainous country. The mountainous Eastern Anatolia region of Turkey experiences precipitation during the winter seasons in the form of snow and snowmelt is a major contributor to the streamflows. The Euphrates River with two major tributaries as Karasu and Murat in the eastern part of Turkey, is one of the important and longest rivers of Southeast Asia with important large reservoirs located on the river, Keban, Karakaya, Atatürk, Birecik and Karkamış reservoirs. The Upper Euphrates Basin as a headwater of Euphrates River is selected as a pilot site for the study. The Euphrates River Basin has a runoff potential of 17% and the area of 127 304 km<sup>2</sup> making it the largest basin in Turkey.

The Euphrates River Basin's importance stretches far beyond the Turkish borders into the riparian countries as it is also their major water source. Hence improving hydrological modeling and the streamflow forecasting capabilities will result in effective management of water resources, hydropower and minimize the effects of drought and flooding in this region.

On the other hand, Turkey has one of the largest populations in Europe, and therefore higher water demands. Turkey's water resources management systems are not only affected by the rapid growth of its major cities but also floods and droughts can be equally disastrous. Therefore, basin management systems, long-term continuous hydrologic modeling, operational runoff forecasting and flood control system are essential. Application of new technologies in hydrologic modeling implemented in this

study, the Soil Moisture Accounting (SMA), satellite data for Snow Covered Area (SCA) and Numerical Weather Prediction form an important area of research in Turkey. The MODIS SCA with resolution of 500 m (<https://modis.gsfc.nasa.gov/>) is applied to assess the Snow Water Equivalent (SWE) performance and the H-14 root zone soil moisture index satellite product with 25 km resolution (<http://hsaf.meteoam.it/description-sm-das-2.php>) is used to evaluate the HEC-HMS model's soil moisture consistency.

## **1.2. Aim of the Study**

Reliability of streamflow forecasting is very important for operational hydrology in regard to reservoir management, hydropower generation and flood control. For the consistent streamflow forecasting, the accurately calibrated and validated hydrological models (i.e. rainfall runoff models) are essential. Therefore, in this study a conceptual hydrological model is applied in the Upper Euphrates Basin.

Hydrologic Engineering Center's Hydrologic Modeling System (HEC-HMS) Version 4.1 (USACE, 2015) developed by the US Army Corps of Engineers (USACE) is selected to be applied in the pilot basin. The model is employed in a lumped and continuous form with the soil moisture accounting and snow components. SMA approach is used for the first time in a snow dominated basin in Turkey. Moreover, the satellite data is used to validate the consistency of the simulated results to check the internal validity of state variables. The Moderate Resolution Imaging Spectroradiometer (MODIS), Snow Covered Area (SCA) product is used to inspect the Snow Water Equivalent (SWE) consistency. On the other hand, the soil moisture product of Satellite Application Facility on Support to Operational Hydrology and Water Management (H-SAF) established by the European Organization for the Exploitation of Meteorological Satellites (EUMETSAT), H14 (Root Zone Soil Moisture Profile) is used to check the consistency of soil moisture.

The other purpose of the study is the deterministic daily streamflow forecasting using the Numerical Weather Predictions (NWP) as input to the model. The daily temperature and precipitation data of the Weather Research and Forecasting (WRF) are used to forecast streamflow. The forecasted results are compared with the observed discharges and analyzed. The results obtained from the study could be used to support reservoir operations downstream and also optimize the water resources management and flood warning systems.

### **1.3. Thesis Guideline**

The thesis is divided into 6 chapters. The subject matter of each chapter with the exception of introduction is as follows:

The literature review is discussed in Chapter 2. First the survey on the previous studies on the study area are highlighted, then the literature on the Soil Moisture Accounting (SMA) component of HEC-HMS are discussed briefly. And finally the literature on the hydrologic modeling and streamflow forecasting are provided.

Study area is discussed with details in Chapter 3, also all the data sources and types used in the study are explained.

The description and all components of the hydrologic model are given in detail within Chapter 4.

Chapter 5 includes the model application procedures, outputs and assessment of results.

Chapter 6 provides the conclusion and recommendations of the thesis. It highlights the main findings of the study with suggested future studies.

## **2. LITERATURE REVIEW**

The research on literature is briefly summarized under three main topics. First, the previous research on the study area is reviewed. Then, the applications of HEC-HMS with Soil Moisture Accounting (SMA) are taken into account. And finally, literature on the hydrological modeling streamflow forecasting is highlighted.

### **2.1. Previous Studies in the Pilot Area**

The hydrological applications and studies depend on the meteorological data of the area. The high elevations and remote mountainous locations of the snow-dominated watersheds make these studies rather difficult. Their remote locations bring about challenges as the easy access locations such as towns and cities house the majority of the meteorological stations' networks in Turkey. The first step to the studies in the mountainous Eastern Anatolia region was the extension and enhancement of the meteorological networks. Several research projects were undertaken to upgrade the networks.

The installation of the Automated Weather Observation Stations (AWOS) and Snow Telemetry (SNOTEL) was pioneered by NATO SFS and Middle East Technical University (METU) research projects (Kaya, 1999; Uzunoğlu, 1999; Şensoy, 2000; Tekeli, 2000; Beşer, 2002). The stations installations were followed by the hydrological modeling in the area. Turkish Ministry of Development (TCKB) then issued a financial support to the subsequent research projects. Two governmental agencies, the Turkish General Directorate of Meteorology (MGM) and the General Directorate of State Hydraulic Works (DSI) collaborated while working on these projects. The collaborations led to further extensions of the network with the improvement of quality through additional sensors installation.

A few research studies in thesis format on the region include Şensoy (2005), Şorman (2005) and Tekeli (2005). Their studies covered amongst others the data collection, data analysis and streamflow forecasting. The isotope samples are analyzed with the research projects sponsored by Anadolu University. Also in 2012, within a scope of a Scientific and Technological Research Council of Turkey (TÜBİTAK) project (108Y161) one day lead time deterministic forecast were made using Meso-scale Version

5 (MM5) data. Yamankurt (2010) and Gözel (2011) includes hydrological modeling examples with different conceptual models.

Studies on water balance for the Tigris-Euphrates basin for the crucial historic flood and drought conditions as well as the effects of different water resource uses on the water balance were investigated (Chen et al., 2011 and Ohara et al., 2011). Further studies on the pilot basin (Ertaş, 2014; Çoşkun, 2016; Akkol, 2016) used the forecast system based on deterministic and probabilistic Numerical Weather Predictions to estimate the average-range flow forecasts with different modeling approaches.

Moreover, there has been a contribution of satellite applications pioneered by the study area in Turkey. The ground observations are used to validate the satellite snow products (MODIS, MSG-SEVRI and IMS) (Tekeli et al., 2005 and Tekeli et al., 2006; Çoşkun, 2016).

The international project of the Operational Hydrology and Water Management Satellite Application (HSAF) supported by the European organization for the Exploration of Meteorological Satellites (EUMESAT) commenced in 2005 and will continue with the third phase until 2023 in this study area (<http://hsaf.meteoam.it/>). Montero Alvarado et al., (2016) applied an adaptational method based on the Moving Horizon Estimation (MHE) to HBV model. They assimilated the remotely sensed Snow Water Equivalent (SWE), Snow Covered Area (SCA) and Soil Moisture (SM) through a hydrological model. Their studies also pioneered the use of H-SAF products through data assimilation (DA) and verified its added value to hydrological forecasting systems in German and Turkish test watersheds.

On the other hand, TÜBİTAK (113Y075) research project aimed at improving the hydrological forecasting using satellite data in the pilot basin was made a part of COST Action ES1404. An international Harnosnow Joint Event was organized in the pilot basin in March 2016 with the focus on harmonization of snow measurements, snow depth and snow water equivalent ([http://www.cost.eu/COST\\_Actions/essem/ES1404](http://www.cost.eu/COST_Actions/essem/ES1404)).

## **2.2. Soil Moisture Accounting Studies**

Complex theories describing the hydrologic process become applicable using computer simulations, and vast quantities of observed data are reduced to summary statistics for better understanding of the hydrological phenomena (Chow et al., 1988).

HEC-HMS (USACE, 2015) is one such computer simulation program, it is a free public software developed to simulate event-based or continuous precipitation-runoff of dendritic watersheds. It does not only delineate watersheds but also it calculates their hydrologic properties (Chow et al., 1988; Olivera, 2001; USACE, 2015)

The developments both in quality and quantity of the digital maps from publicly available databases, provided the derivation of model parameters using Geographic Information Systems (GIS) and increased their value in hydrological models. The complex soil moisture accounting parameters can be derived into multi-parameter sets which then improve the model performance. GIS is also a useful tool for storing, analyzing and integration of spatial data and attributing information related to slope, runoff and watershed drainage (Fleming and Neary 2004; Ramakrishnan and Steinman 2009).

Event based hydrological modeling highlights the watershed's response to an individual precipitation event. Fine-scale hydrologic models such as event-based hourly simulation modeling are particularly useful for understanding the detailed hydrologic processes and identifying the relevant parameter sets that can be later applied in a coarse-scale continuous modeling and streamflow predictions (Yener, 2006; Chu and Steinman, 2009).

The continuous hydrological modeling synthesizes hydrologic process over both wet and dry conditions and is suitable for daily, monthly and seasonal streamflow simulations. HEC-HMS utilizes the Soil Moisture Accounting (SMA) to account for the watershed's soil moisture balance over these long periods. This can be used to recreate the historical streamflows as the model's algorithm simulates long-term relationship between precipitation, evapotranspiration, soil losses and the streamflow (Fleming and Neary, 2004; Chu and Steinman, 2009; Bashar and Zaki, 2010; Gyawali and Watkins, 2013).

Unfortunately, extensive work on the Soil Moisture Accounting (SMA) with HEC-HMS has not been undertaken yet. Fleming and Neary (2006) used the Geographic Information Systems (GIS) based HEC-HMS to model and calibrate parameters of Soil Moisture Accounting (SMA) loss method. Their study showed that the model

performance of the GIS based HEC-HMS calibration and parameterization is significantly improved and functioned perfectly in the Cumberland River Basins, USA.

Chu and Steinman (2009) applied a combined hydrologic modeling of both the event-based and continuous approaches to the Mona Lake Watershed in Western Michigan, USA. The event based model was used for parameter calibration and the determined parameters are used in the continuous model application. Their studies concluded that the use of intensive data in event-based modeling provided both well-calibrated and accurate parameter sets which intern improved the performance of the continuous model.

Yilmaz et al. (2012) applied continuous model simulation to the snow-dominated Upper Euphrates Basin, Turkey. To conceptualize the snow-runoff relation with the aim of computing the snowmelt, the temperature index/ degree day approach was applied. The application employed the initial and constant loss method and was limited with the number of meteorological stations of low altitudes.

Gyawali and Watkins (2013) applied the soil moisture accounting and the temperature index snowmelt components within the HEC-HMS to model the Great Lakes Watersheds. In their study, they used the geospatial databases to estimate the physically based parameters. They compared the results with the National Oceanic and Atmospheric Administration (NOAA) large basin runoff model (LBRM) for historical conditions.

De Silva et al. (2014) made a joint study of event-based and continuous hydrological modeling in Kelani River Basin in Sri Lanka. In an event-based approach, extreme rainfall events were used both to calibrate and validate model parameters. It is shown that the intensive field data supported event-based modeling is effective in deriving model parameters for continuous modeling.

### **2.3. Hydrologic Modeling and Streamflow Forecasting**

Hydrologic modeling dates back to the ancient Egyptian civilization, but rainfall-runoff modelling in a broad sense can be attributed to the arising response to urban sewer design, land drainage systems and the reservoir spillway design with the design discharge being of major interest in the nineteenth century. The concept of the rational method for determining flood peak discharge from measurements of rainfall depths owes its origins to Mulvaney (Mulvaney, 1850).



The Sherman's concept of simple unit hydrograph in 1932 (Sherman, 1932) became a major step forward in hydrological analysis, and many breakthroughs followed then after when hydrologists became aware of system engineering approaches used for the analysis of complex dynamic systems. The computer revolution towards the end of the twentieth century saw the increased computerization of hydrologic modelling and the computer applications in hydrology making it possible for large scale analysis.

Even though runoff forecasting is performed using the HEC-HMS forecast component in this study, there are a few applications with this model components. Because of this reason, the literature review will take a broad approach investigating runoff forecasting with different hydrological models.

Anderson et al. (2002) used the Mesoscale Model (MM5) to transfer the 48 hour ahead precipitation forecast provided by the operational National Center for Environmental Prediction Eta model to suitable spatial and time scales for HEC-HMS streamflow forecasting in the Calaveras River watershed in Northern California.

Zhao et al. (2009) forecasted 24 hour snowmelt runoff with the Distributed Hydrology Soil Vegetation Model (DHSVM) and the Weather Research and Forecasting (WRF) modelling system in Juntanghu watershed in Xinjiang China.

Abudu et al. (2011) used the telemetry (SNOTEL) precipitation and Snow Water Equivalent (SWE) using transfer-function noise (TFN) model to investigate the monthly runoff forecasting during the spring summer season in the Rio Grande Headwaters Basin in Colorado.

Johansson et al. (2001) provided the five days temperature and precipitation data to HBV to forecast streamflow at a mountainous region within the HydAlp in Sweden. To calibrate the model, they used the runoff and observed snow cover area. It was discovered that the short-term forecasting resulted in more accurate predictions. In other HBV model forecasting applications, forecasting data (MM5) was found to be helpful in planning for water resources by Jónsdóttir and Þórarinnsson (2004). Also in a similar study, Kunstmann and Stadler (2005) used numerical weather forecasting data as an input into the HBV model in Germany.

Şorman et al. (2009) applied the multi-purpose calibration aimed at discharge data and MODIS snow covered area. The study employed the MM5 forecast data for

streamflow predictions. Şensoy et al. (2016) developed a Decision Support System (DSS) to reduce the risk of flooding incorporating snowmelt in real-time and applied HEC-HMS to forecast runoff in Yuvacık Dam Basin, Turkey.

On the other hand, previous applications of continuous hydrologic models in the pilot basin did not implement the SMA. In this study, the combination of event based and continuous hydrologic modeling with SMA is employed in the Karasu Basin. Soil Moisture Accounting and temperature index snowmelt components are utilized together. Also, since Karasu Basin is snow dominated, satellite products of MODIS Snow Covered Area and ASCAT root zone are used to validate the consistency of simulated Snow Water Equivalent and soil moisture. Moreover, deterministic Numerical Weather Prediction (WRF model data) are correlated and employed to forecast streamflows.

### **3. STUDY AREA and DATA**

#### **3.1. Karasu Basin**

Access to fresh water bodies has influenced the population settlements over the years and Turkey is not an exception. Turkey is geographically divided into seven regions, Marmara, Black Sea, Aegean, Mediterranean, Central Anatolia, Eastern Anatolia and Southeastern Anatolia Regions. The harsh winter conditions in the Eastern Anatolia region have resulted in low population density despite its large surface area. The Eastern Anatolia is home to some of the important streams in Turkey, Euphrates, Tigris, Aras and Kura streams.

The Euphrates and Tigris rivers were key to the early settlements in the Mesopotamia. These two rivers together form the large trans-boundary rivers running from Turkey, Syria, Iran, and Iraq through Saudi Arabia. These rivers are significant to water supply, irrigation and hydropower generation. Euphrates and Tigris are fed by snow in the mountainous eastern Anatolia region with most of the precipitation occurring in winter as snow. The melting snow results in the concentration of high discharges during spring and early summer.

Euphrates River is the longest in Southern West Asia, it is 2700 km in length, 1236 km within Turkish borders and has a monthly flow potential of 36.5 billion cubic meters (Aytemiz and Kodaman, 2006). Euphrates River is also home to several large reservoirs, Keban, Karakaya, Atatürk, Birecik and Karkamış.

Upper Euphrates (Karasu) Basin, the headwater of Euphrates River Basin is selected for this study. Karasu Basin is a North to South oriented basin; the basin streams and its tributaries originate from the northern mountainous parts of the basin and join together at the outlet South-West of the basin. The snow dominated nature of Karasu Basin encourages the snow studies and it is one of the reasons to be selected for the study. However, despite its prominence and a wealth of existing infrastructure, Karasu Basin can be classified as a data scarce region in terms of hydrometeorological networks.

Karasu Basin is geographically located between 39° 23' to 40° 24' Northern Latitudes and 38° 58' to 41° 38' Eastern Longitudes and has the drainage area of 10,275 km<sup>2</sup> (Figure 3.1). The basin elevation ranges in between 1136 m to 3497 m and has the hypsometric mean elevation of 1983 m.

The General Directorate of State Hydraulic Works (DSI) operates the streamflow station (E21A019 – Kemah) that controls the Karasu Basin outlet.

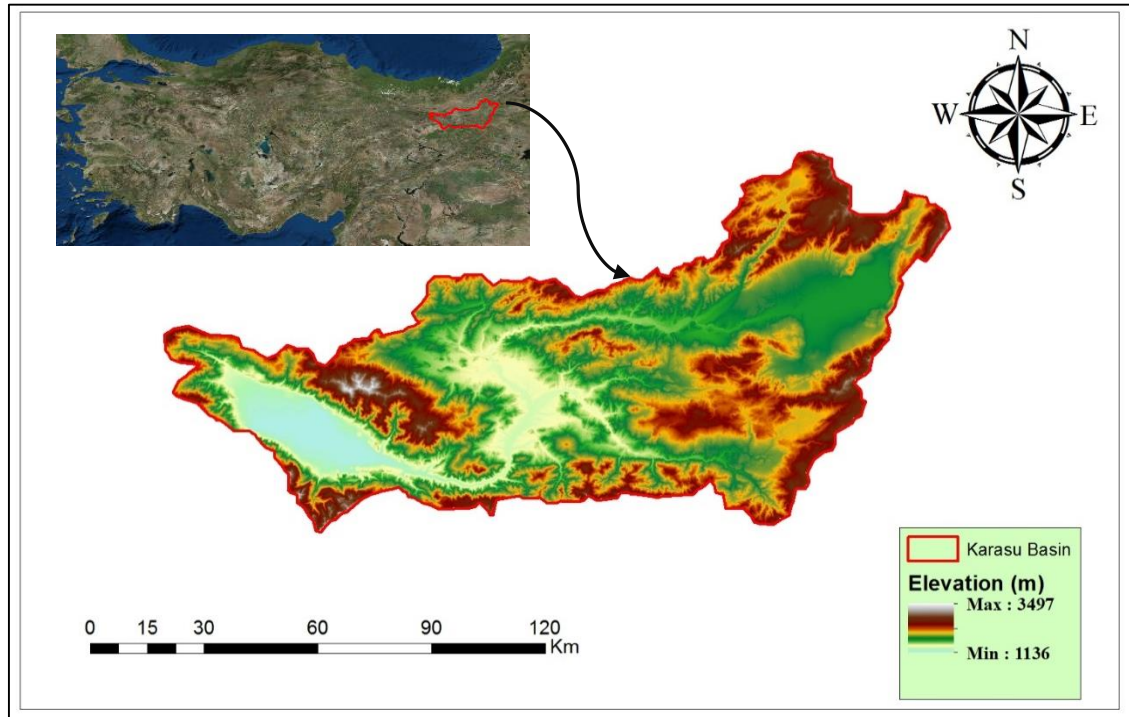


**Figure 3.1.** *Karasu Basin's location and elevation map.*

Karasu Basin is divided into five elevation zones, Zone A (<1500 m) to Zone E (>2900 m). The Geographic Information System (GIS) is used with ESRI ArcMap (Version 10.2.2) (<http://www.esri.com/arcgis/about-arcgis>) to determine the topographic properties of the basin from the National Aeronautics and Space Administration (NASA) Shuttle Radar Topographic Mission (SRTM) 90 Digital Elevation Data (<https://earthexplorer.usgs.gov/>). Topographic properties of the basin according to each elevation zone is represented in Table 3.1 and Figure 3.2.

**Table 3.1.** *Karasu Basin topographic properties.*

Zone	Elevation Range (m)	Area (km <sup>2</sup> )	Area (%)
A	1136-1500	1093.9	10.6
B	1501-1900	3264.7	31.8
C	1900-2300	3466.3	33.7
D	2301-2900	2277.8	22.2
E	2901-3497	172.3	1.7
Whole Basin	1136-3497	10275	100

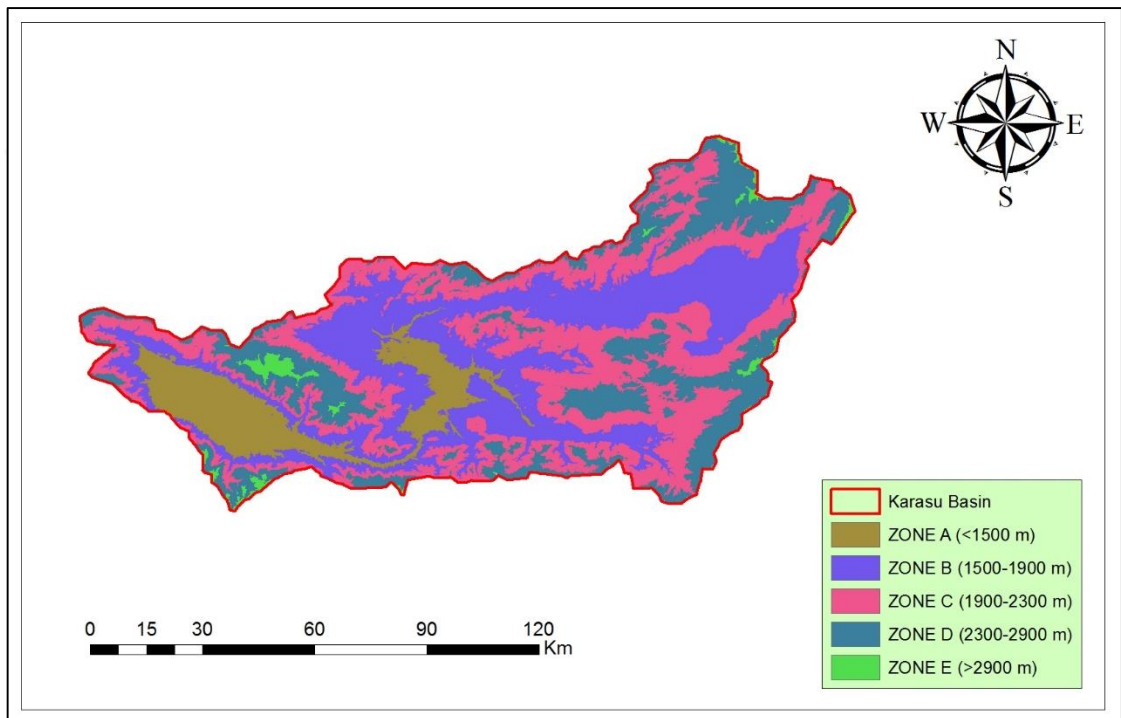


**Figure 3.2.** *Karasu Basin elevation zone map.*

The watershed's aspect has a significant effect on snowmelt as it represents the direction of exposure to the sunlight. So the GIS platform is used to derive the Karasu Basin aspect map (Table 3.2 and Figure 3.3).

**Table 3.2.** *Karasu Basin aspect distribution.*

Aspect	Area (km <sup>2</sup> )	Area (%)
Flat	52.1	0.5
NorthEast	2293.5	22.3
SouthEast	2797.5	27.2
SouthWest	2472.8	24.1
NorthWest	2659.1	25.9
Whole Basin	10275	100

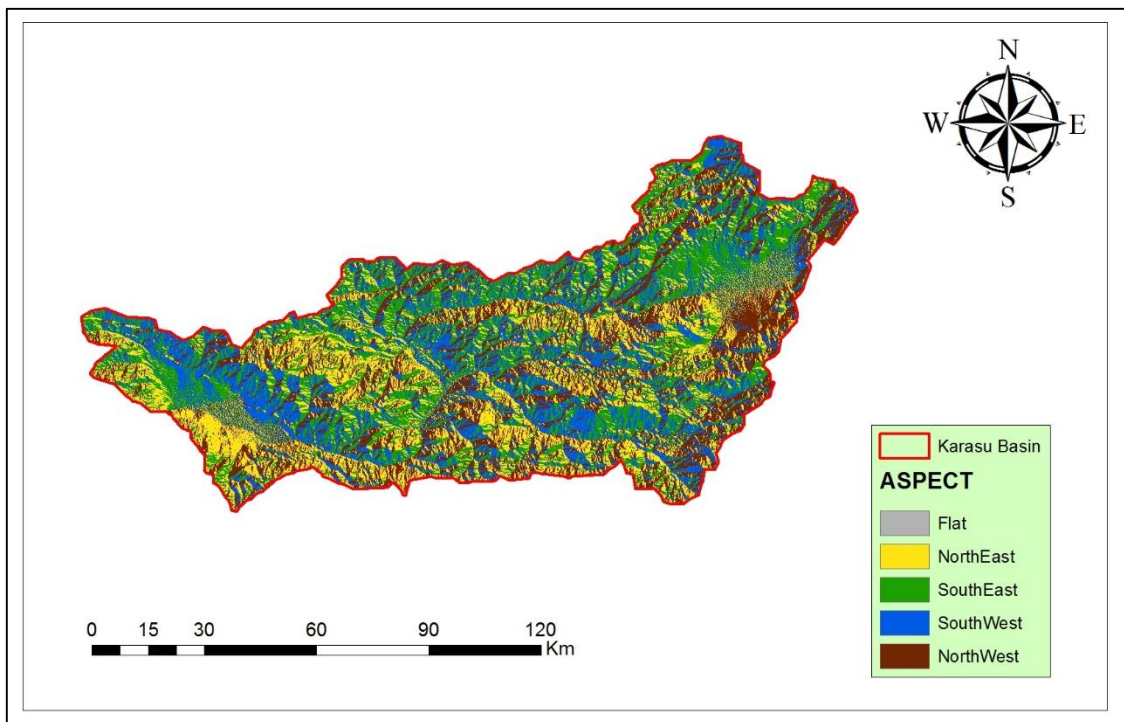


**Figure 3.3.** *Karasu Basin aspect map.*

The slope of a watershed has a great impact on the surface runoff velocity as well as the erosion. The solar radiation on the watershed is affected when the slope and the aspect (directional orientation) of the watershed are taken into account. This in turn, influences the distribution of the precipitation and the snowmelt (Singh, 1988). Karasu Basin has more than half of its elevation above 15 percent slope. Both the steep slope and the elevation ranges of the Karasu Basin are a clear indication that the basin is located in a mountainous region. So the GIS platform was used to derive the Karasu Basin slope map (Table 3.3 and Figure 3.4).

**Table 3.3.** *Karasu Basin slope distribution.*

Slope	Area (km <sup>2</sup> )	Area (%)
0-4	2231.9	21.7
4-10	2912.1	28.3
10-15	2097	20.2
15-25	2325	22.6
25-40	692	7.0
>40	17	0.2
Whole Basin	10275	100

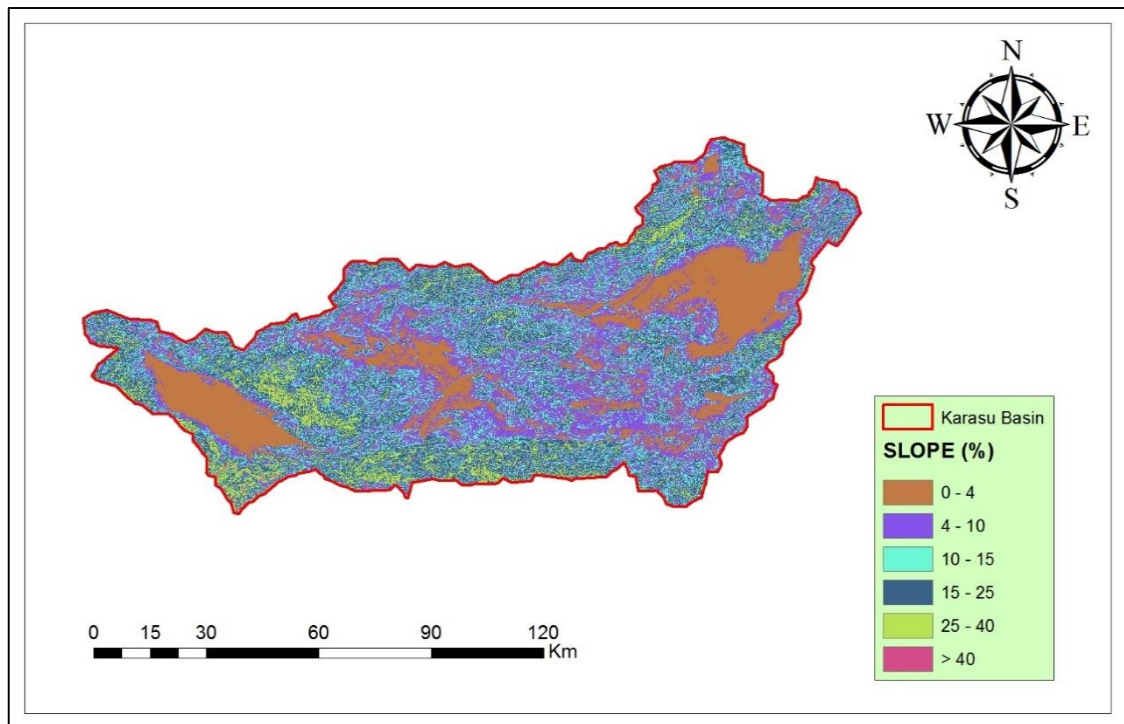


**Figure 3.4.** *Karasu Basin slope map.*

The land use of a watershed is fundamental to the computation of its infiltration capacity and runoff potential. The direction of the watershed's slopes affects the evapotranspiration and runoff. Dense vegetation creates a barrier shielding the precipitation from the surface while barelands on the other hand receive all the precipitation. The European Environment Agency's Corine land use classification map ([www.eea.europa.eu](http://www.eea.europa.eu)) shows the basin to be mainly agricultural and grasslands covering more than 60% of the watershed. So the GIS platform was used to derive the Karasu Basin land use map (Table 3.4 and Figure 3.5).

**Table 3.4.** *Karasu Basin land use distribution.*

Land Use	Area (km <sup>2</sup> )	Area (%)
Urban	189.1	1.8
Water Bodies	67.8	0.7
Agriculture	3236.6	31.5
Forest	359.6	3.5
Grasslands	3596.3	35
Sparse Vegetation	2825.6	27.5
Whole Basin	10275	100

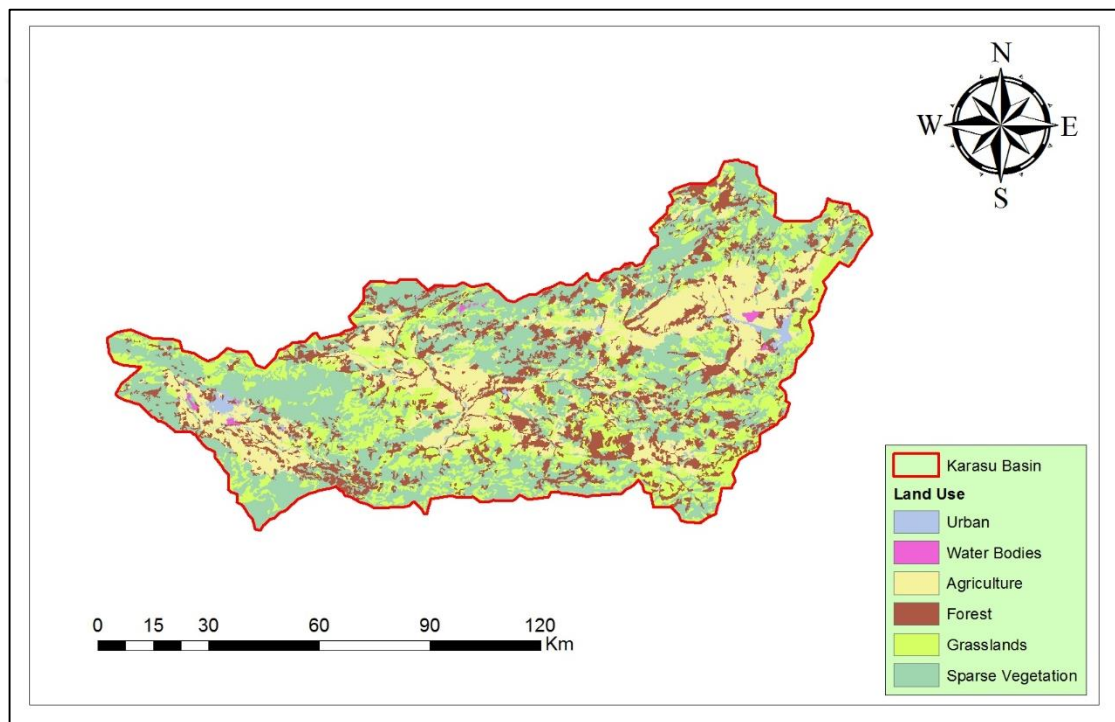


**Figure 3.5.** *Karasu Basin land use map.*

### 3.2. Hydro-meteorological Data

Hydro meteorological data are fundamental for a study on hydrological science and its applications. They can be used to estimate the water potential in reservoir management, flood prevention and water quality control management. Therefore the data acquisition in terms of both quality and quantity is very important. In Turkey, the General Directorate of Meteorology (MGM) and the General Directorate of State Hydraulic Works (DSI) are in charge of the acquisition and storage of the data. Several difficulties can be encountered while obtaining data especially from mountainous snow dominated watersheds during the winter seasons.



Most of the data are collected from a station point and distributed across the watershed with different methods to utilize the areal averages. Seventeen meteorological stations in and around the watershed used in this study (Figure 3.6). Two of these stations measure temperature alone. The remaining fifteen measure both the precipitation and temperature.

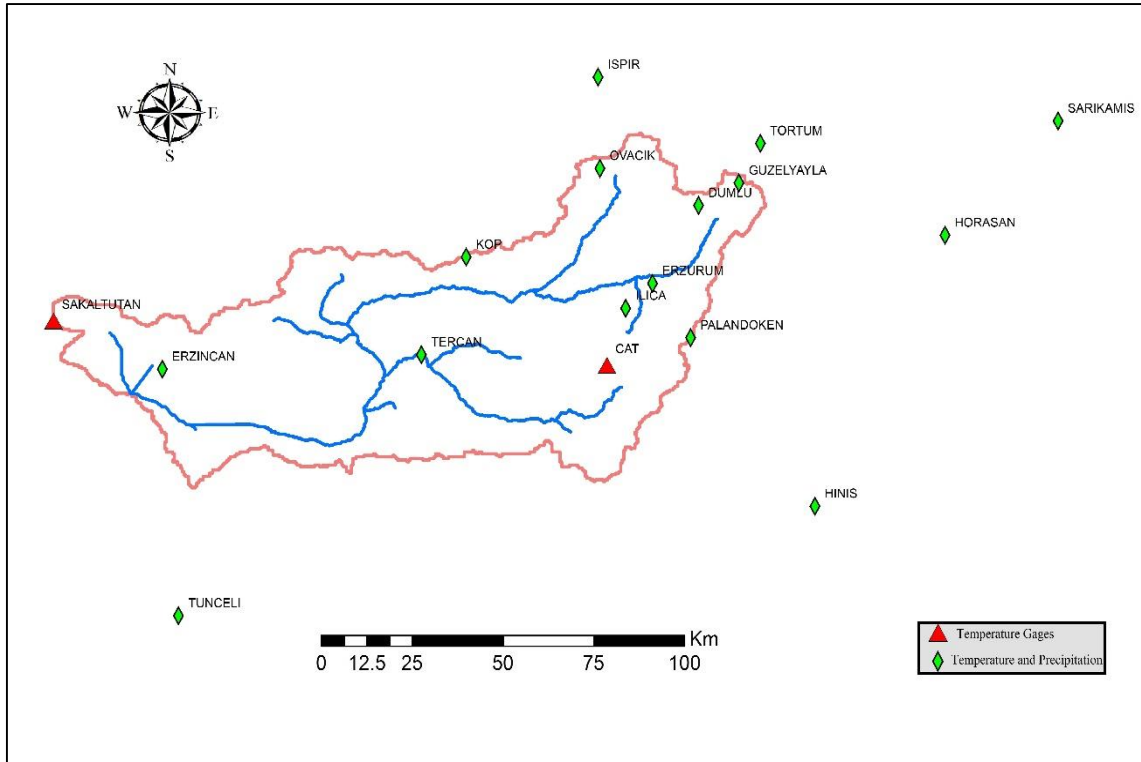


**Figure 3.6.** *Hydro-meteorological stations in and around Karasu Basin.*

The meteorological data spanning fourteen years (2002 – 2015) are assessed and used in the model. Total daily precipitation and average daily temperature values observed at meteorological stations (Figure 3.6) are distributed over the whole basin using Detrended Krigging (DK) approach (Garen et al., 1994). Then the overall average values are used in the analysis and modeling.

The average total monthly and total annual precipitation records for Karasu Basin are shown in Figure 3.7 and Figure 3.8, respectively. The precipitation analysis are performed for the fourteen years (2002 – 2015) data set. It can be interpreted from Figure 3.7 that the highest precipitation occurs during the snowmelt period. This results in high peak discharges as the rain falling on the snowpack accelerates the melting process. The lowest average precipitation is observed during the summer months as expected.

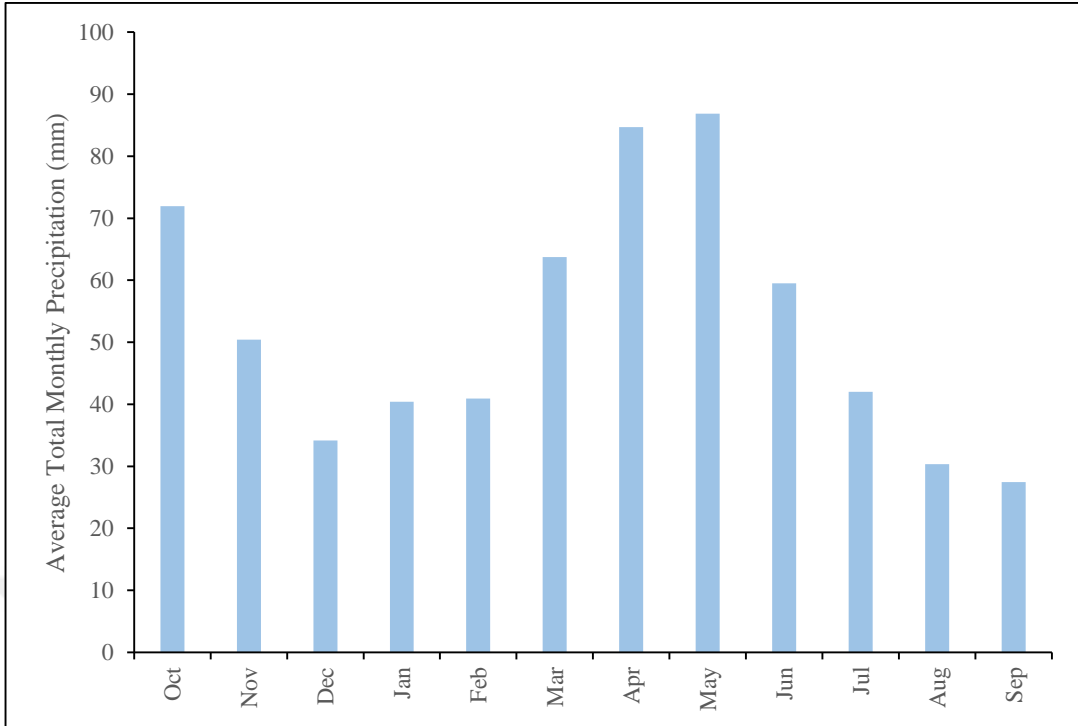


**Figure 3.7.** Average total monthly precipitation for Karasu Basin (2002 – 2015).

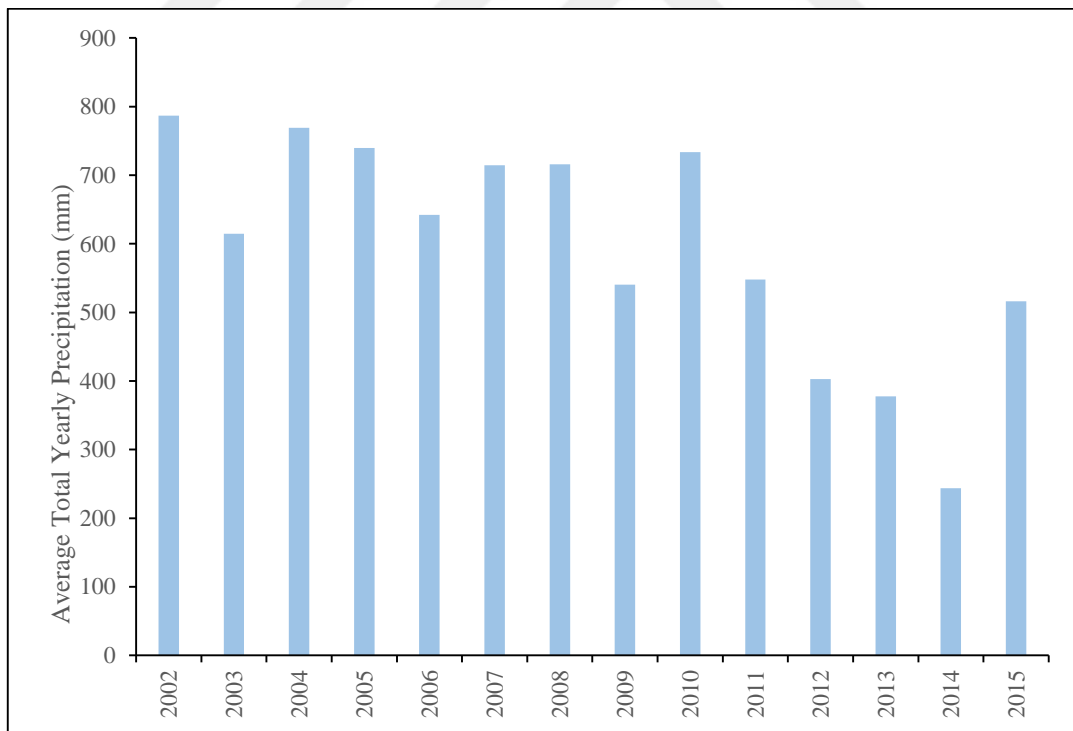


**Figure 3.8.** Average total annual precipitation for Karasu Basin (2002 – 2015).

In modeling a snow dominated basin, temperature plays a vital role to determine whether precipitation is snowfall or rainfall. Also temperature is the dominant variable to control whether or not the conditions are suitable for snowmelt. The average total monthly and total annual temperature records for Karasu Basin (at 2098 m) are shown in Figure 3.9 and Figure 3.10, respectively. The snowfall period represented by the negative temperatures spans from November to March followed by the snowmelt as explained earlier.

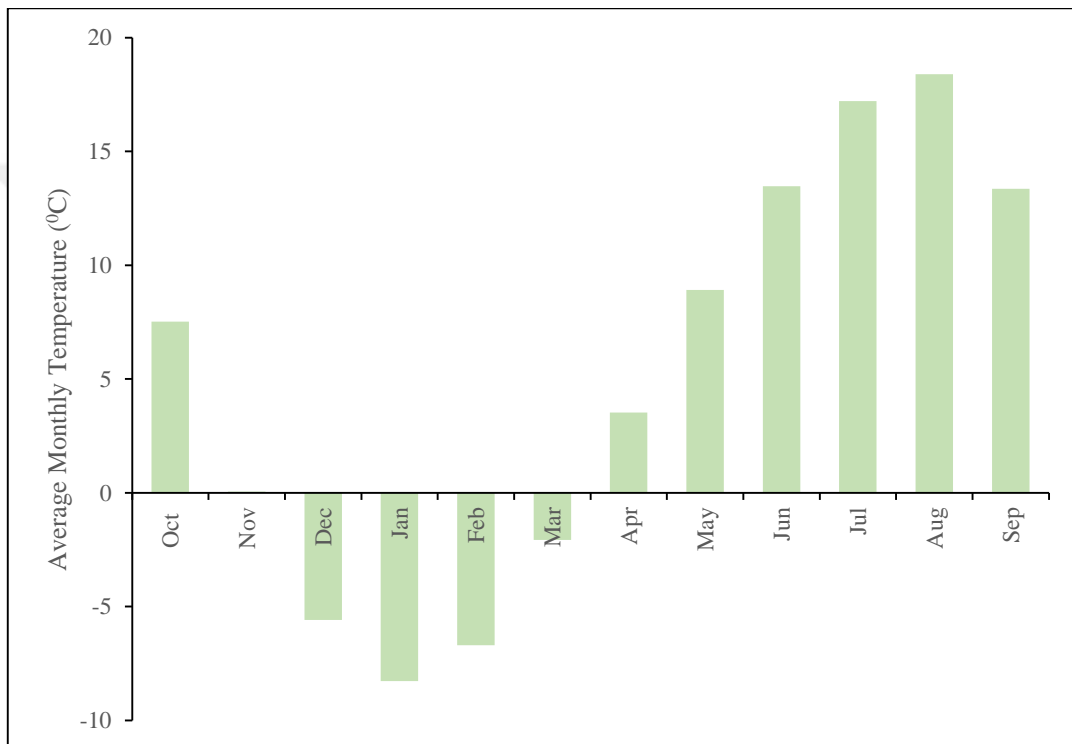


**Figure 3.9.** Average monthly temperature records for Karasu Basin (2002 – 2015).



**Figure 3.10.** Average annual temperature for Karasu Basin (2002 – 2015).

Figure 3.11 shows the hydrographs of water years with different classifications from the calibration (2004), validation (2012) and forecasting (2015) periods. As observed from the figure the snowmelt period, from March to July contributes the highest amount of flow. It contributes 60 – 70 % of the total annual flow. This makes modeling and forecasting of the streamflow during the snowmelt period essential for Karasu Basin.

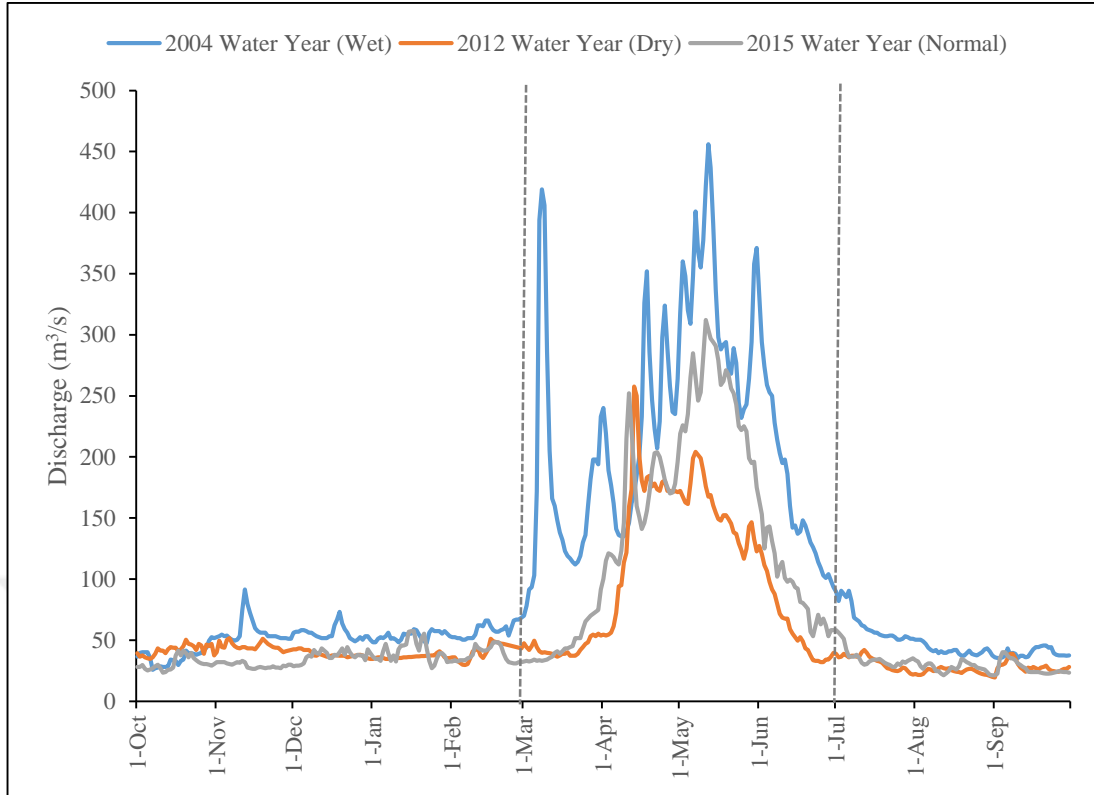


**Figure 3.11.** *Karasu Basin hydrographs for different water years.*

The hydrometeorological data are analyzed to classify the water years as dry, wet and normal. This classification is only done to interpret the model results accordingly. The analysis is carried out using the total precipitation, rainfall, snowfall, temperature and discharge as the main criteria.

To perform the classification the annual total precipitation, rainfall, snowfall, discharge and average temperatures are calculated as variables ( $x$ ) by using the Average ( $\bar{x}$ ) and Standard Deviation ( $\sigma$ ) of each data type for the last 14 years (2002 – 2015) and threshold values are calculated. A year is defined as wet, dry or normal according to the following approach. Three or more of the five variables were used to determine the condition of a year.

$$\text{Wet if } x > (\bar{x} + \sigma) \quad (3.1)$$

$$\text{Dry if } x < (\bar{x} - \sigma) \quad (3.2)$$

$$\text{Normal if } (\bar{x} - \sigma) \leq x \leq (\bar{x} + \sigma) \quad (3.3)$$

$x = f(Q,P,R,S,T)$ , where;

Q: Total and/or average discharge ( $m^3/s$ )

P: Total precipitation (mm)

R: Total rainfall (mm) (P when  $T > 0$  °C)

S: Total snow (mm) (P when  $T \leq 0$  °C)

T: Average temperature (°C)

Table 3.5 shows all years classifications for both calibration and validation periods for Karasu Basin.



**Table 3.5.** *Karasu Basin water year classification.*

Year	Total Precipitation (mm)		Rainfall (mm)		Snow (mm)		Total Discharge (m <sup>3</sup> /s)		Average Yearly Temp (°C)	Classification
2002	786.7	wet	485.3	normal	301.4	wet	28867.5	normal	3.2	normal
2003	614.8	normal	381.1	normal	233.7	normal	30151.8	normal	3.7	normal
2004	768.9	wet	389.3	normal	379.6	wet	39344.0	wet	4.0	wet
2005	739.6	normal	528.4	wet	211.2	normal	33643.4	normal	3.5	normal
2006	642.0	normal	379.6	normal	262.4	normal	37348.0	normal	4.6	normal
2007	714.5	normal	486.3	normal	228.2	normal	31155.9	normal	3.2	normal
2008	712.2	normal	504.1	normal	211.7	normal	26974.5	normal	4.3	normal
2009	540.6	normal	388.9	normal	151.7	normal	28437.9	normal	4.4	normal
2010	733.6	normal	513.4	wet	220.2	normal	38049.4	wet	7.2	wet
2011	547.9	normal	397.7	normal	150.2	normal	31838.1	normal	6.6	normal
2012	403.0	dry	278.2	dry	124.8	normal	21242.8	dry	4.2	dry
2013	377.6	dry	232.3	dry	145.3	normal	25433.5	normal	5.6	normal
2014	243.8	dry	167.9	dry	76.0	dry	14529.8	dry	5.17	dry
2015	516.9	normal	479.9	normal	62.8	dry	25048.9	normal	5.33	normal
AVE	595.9		400.9		197.1		29433.3		4.64	
STDEV	165.6		110.6		86.2		6758.9		1.20	

### 3.3. Numerical Weather Predictions

While the present conditions can be observed from the measuring stations, atmospheric models provide Numerical Weather Prediction (NWP) data for the future conditions. The process by which the current observed conditions of weather is used to forecast its future conditions of up to a several days referred to as NWP. The General Directorate of Meteorology (MGM) in Turkey is the governmental institute responsible to provide the weather forecasts.

Numerical Weather Prediction data can be classified as probabilistic and deterministic based on the prediction processes. Probabilistic process provides several possible predictions and the deterministic process provides a single prediction. In this study, the Weather Research and Forecasting (WRF) model data is selected as deterministic NWP to be implemented into the model for runoff forecasting.

The WRF model, formally known as the Mesoscale Model 5 (MM5) up until the end of 2012, is a fully compressible and non-hydrostatic terrain-following sigma-coordinate model designed to predict mesoscale atmospheric circulation. The model was developed to generate finer resolution forecast products both spatially and temporally by Pennsylvania State University/National Center for Atmospheric Research (<http://www2.mmm.ucar.edu/mm5/>).

In this study, the WRF average daily temperature and the total daily precipitation are calculated from the hourly data with the spatial resolution of 4 km and 6 – 24 hourly time projections. The data are used as inputs to HEC-HMS for streamflow forecasting during the 2015 water years for Karasu Basin. The linear bias correction is applied to improve the consistency of the WRF data with the ground observation data. This is done by deriving a linear relation between the WRF data and ground data for the past years. No correction is applied to the rainfall because of its high inconsistency. WRF temperature and precipitation data sets are used to forecast Karasu Basin streamflow for 2015 (Figure 3.12 to 3.15).



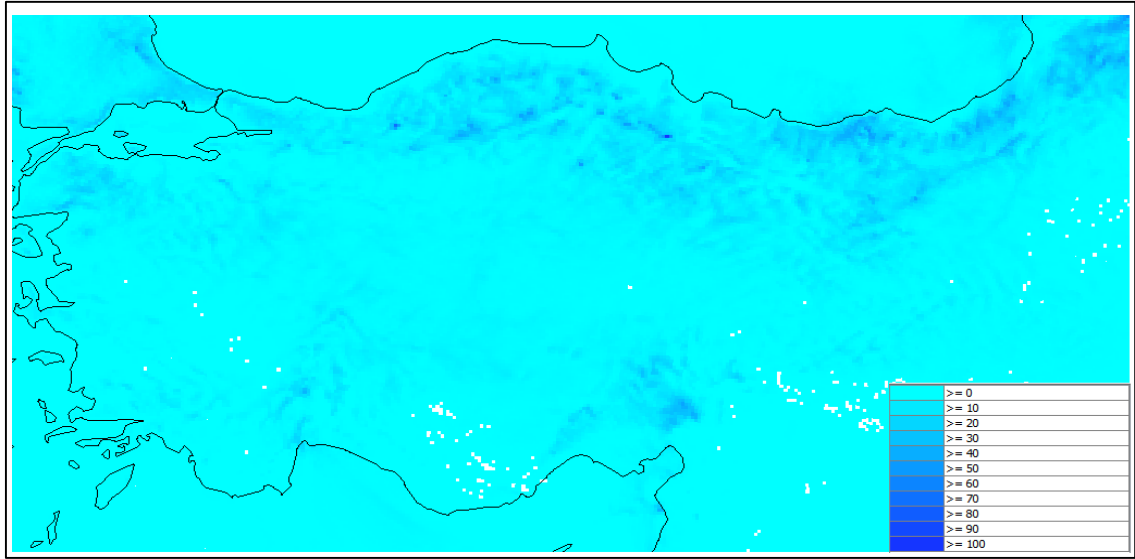


**Figure 3.12.** *WRF precipitation data in Turkey for 06 June 2013.*

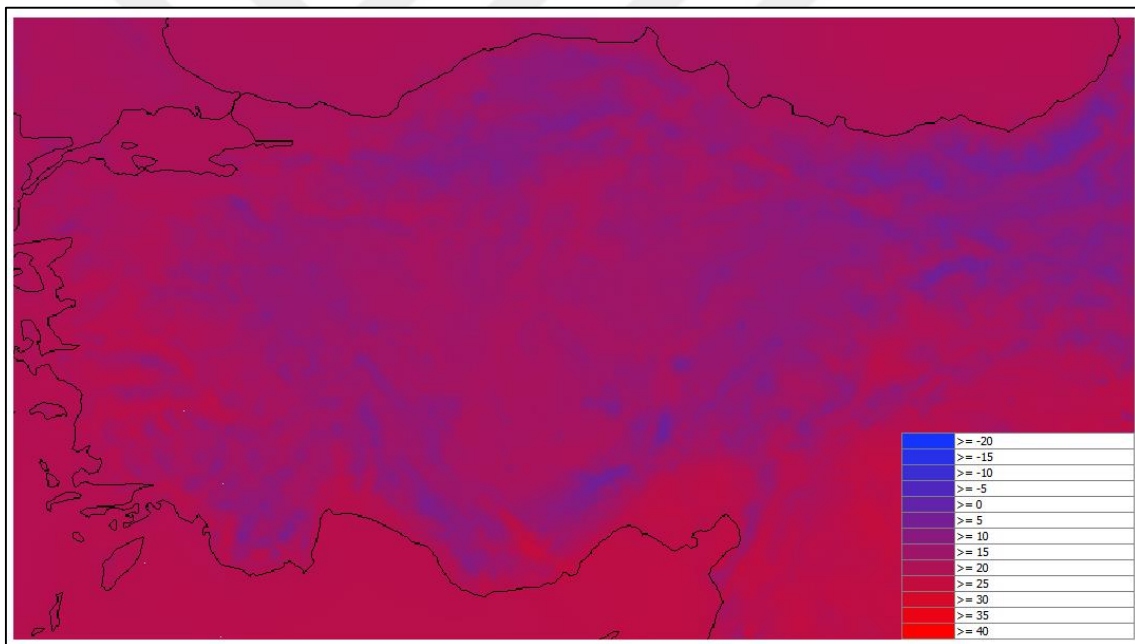


**Figure 3.13.** *WRF temperature data in Turkey for 06 June 2013.*

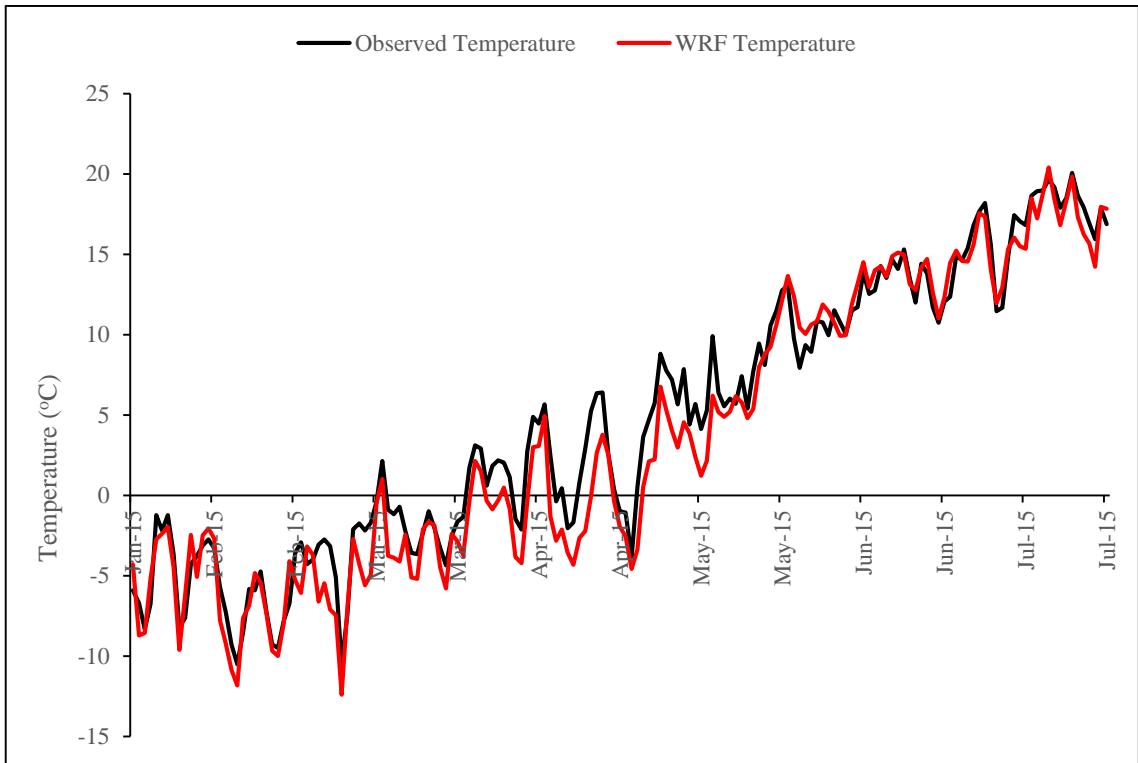


**Figure 3.14.** Observed and WRF temperature data for Karasu Basin, 2015.

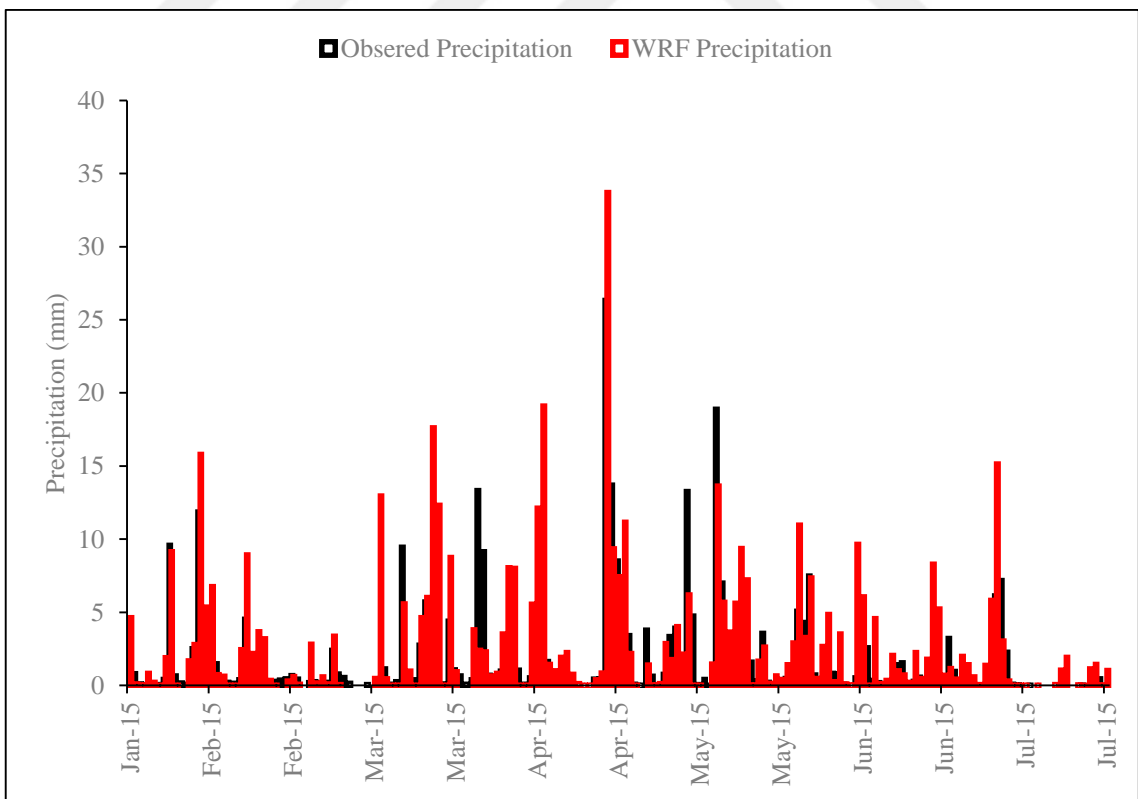


**Figure 3.15.** Observed and WRF precipitation data for Karasu Basin, 2015.

### 3.4. Satellite Products

#### 3.4.1. Soil moisture product

Continuous hydrological modeling applications span long time intervals covering wet and dry periods. The Soil Moisture (SM) conditions as state variables are therefore significant to continuous modeling. The recent advancements in remote sensing applications in hydrology, have contributed to the better understanding of SM. There are various satellite soil moisture products in the literature, in this study, SM product of Satellite Application Facility on Support to Operational Hydrology and Water Management (H-SAF) established by the Exploitation of Meteorological Satellites (EUMETSAT) is used.

The product H14 (<http://hsaf.meteoam.it>) which contains the root-zone soil moisture profile index is used to validate the simulated soil moisture results by HEC-HMS. The surface observation soil moisture assimilation system has the spatial resolution of 25 km, 36 hour timeliness and spreads down to 2.89 m towards the roots region below the surface. It provides four layer estimates with thicknesses of 0-7 cm, 7-28 cm, 28-100 cm, 100-289 cm (Figure 3.16 and 3.17.).

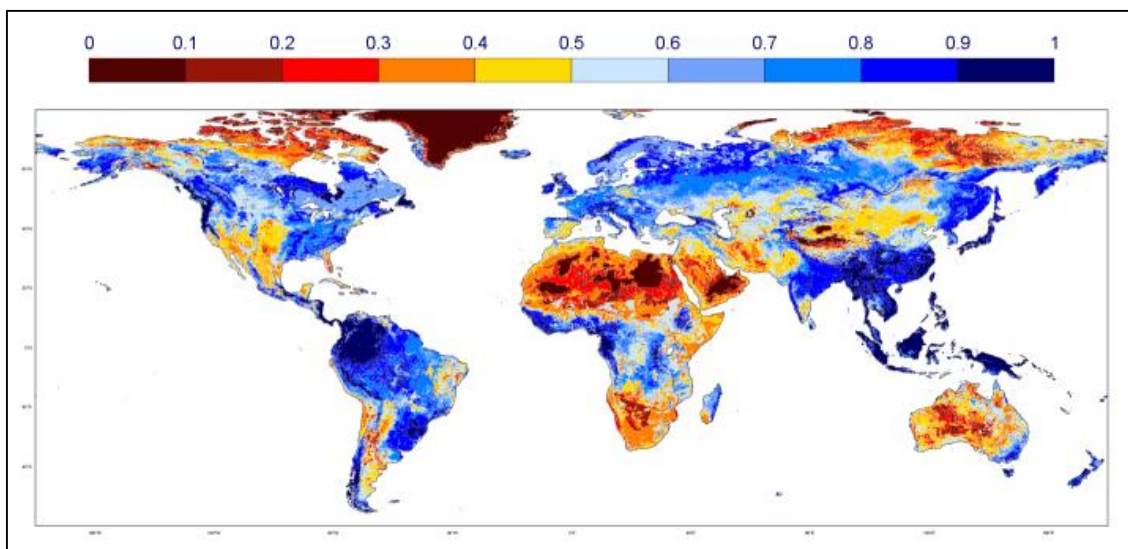


**Figure 3.16.** Global H-14 Soil Moisture data for 23 December 2016

(<http://hsaf.meteoam.it/soil-moisture.php>).

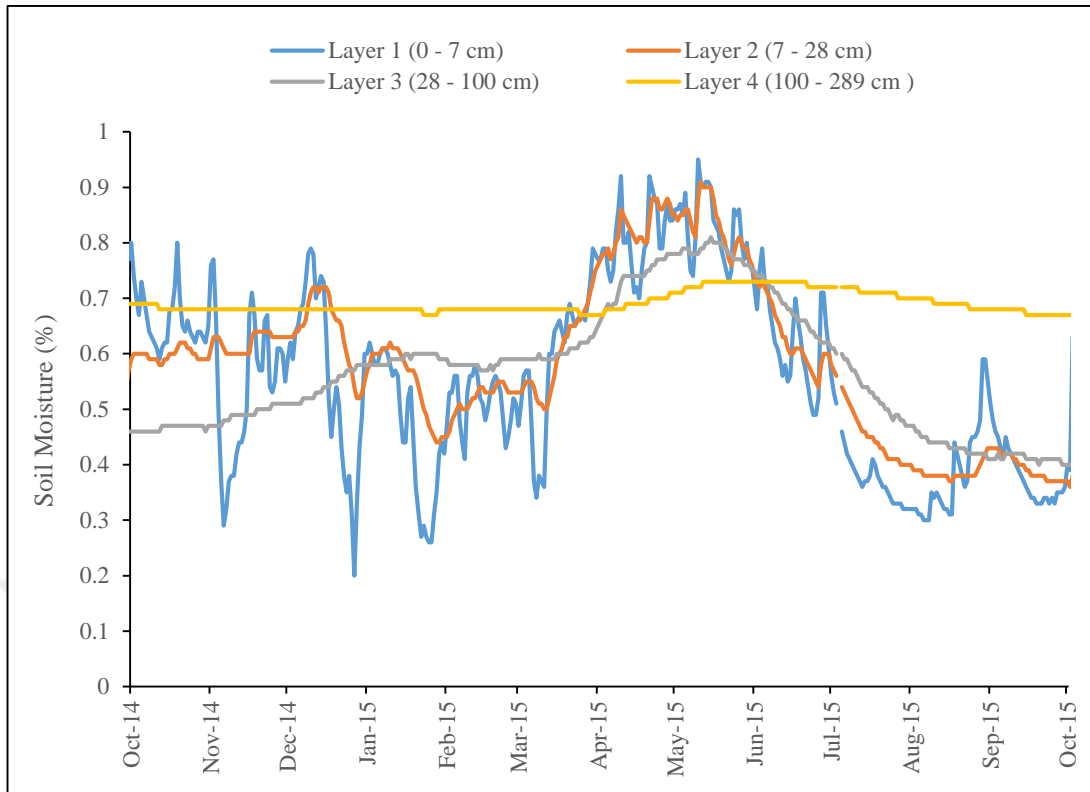


**Figure 3.17.** *H-14 Soil Moisture data for Karasu Basin, 2015.*

### 3.4.2. Snow cover product

Moderate Resolution Imaging Spectroradiometer (MODIS) is an imaging spectroradiometer which uses a cross-track scan mirror collecting optics, and a set of individual detector elements to provide imagery of the Earth's surface and clouds in 36 discrete, narrow spectral bands from approximately 0.4 to 14.4 $\mu$ m (Barnes et al., 1998). The 500 m resolution MODIS Snow Covered Area (SCA) product is used to validate the simulated Snow Water Equivalent in this study. The average Snow Depletion Curve and SCA are presented in Figure 3.18.

A combination of three filtering processes are employed to filter cloud cover. The spatial, temporal and elevation filters. In spatial filtering, Terra and Aqua images are combined to allow for a clearer surface view. Then the combination of imagery is employed in temporal filtering by going back in time. Finally in elevations filters, it is assumed that cloudy cells below the land elevation line are land and cells above the snow elevation line are snow (Şorman and Yamankurt, 2011).

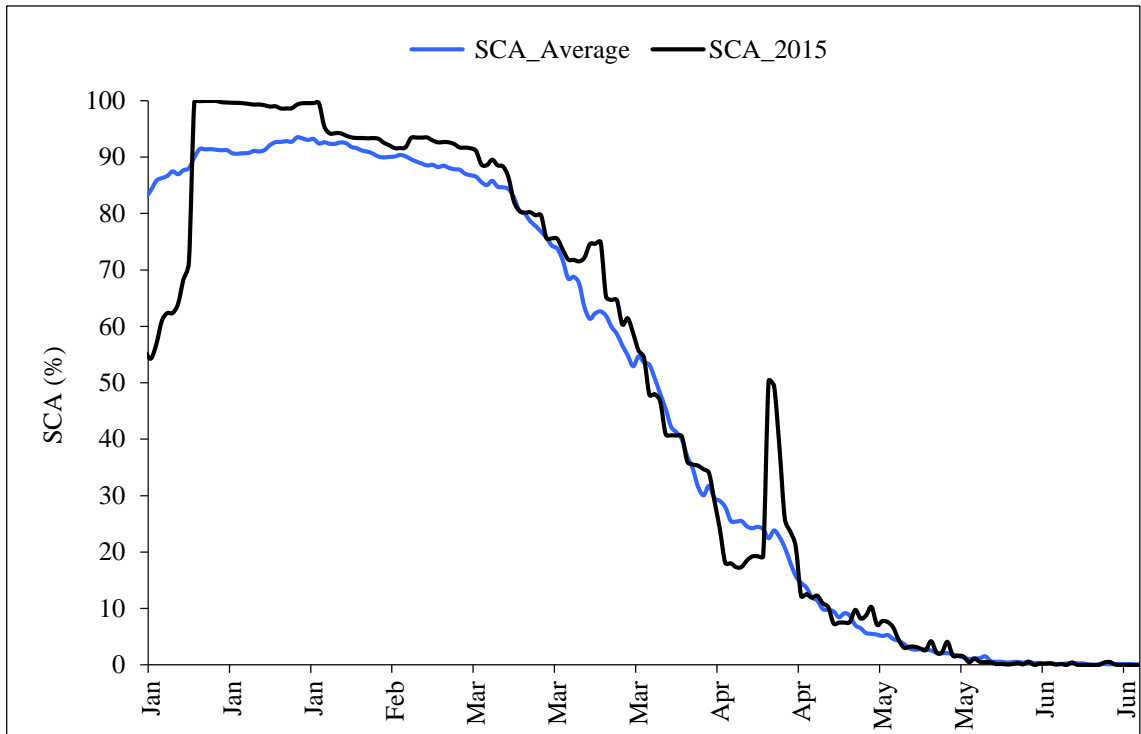


**Figure 3.18.** Snow depletion curves for Karasu Basin.

## 4. HYDROLOGICAL MODEL

### 4.1. Hydrological Model Description

The ever increasing world population has mounted pressure on water supply making both the availability and reliability of fresh water a critical issue. Nature is a complex phenomenon as it presents both unpredictable and abrupt changes in behavior. Modeling nature therefore has proven to be complex despite all the recent advancement in technology. Hydrological modeling refers to the calculation of the watershed's rainfall-runoff relationship in accordance with the watershed physical characteristics (ASCE 2000; Kumar et al., 2005).

Hydrological models are built for several reasons amongst which include the understanding of the watershed's behavioral analysis to meet water demands, flood control system and hydropower generation based on both current and future hydrological trends. Hydrological modeling is a key to understand the hydrological process of any watershed (Figure 4.1). Due to the limitations presented by the laboratory based modeling, the computerization of the models has since advanced to become popular modeling platforms (Xu, 2002).

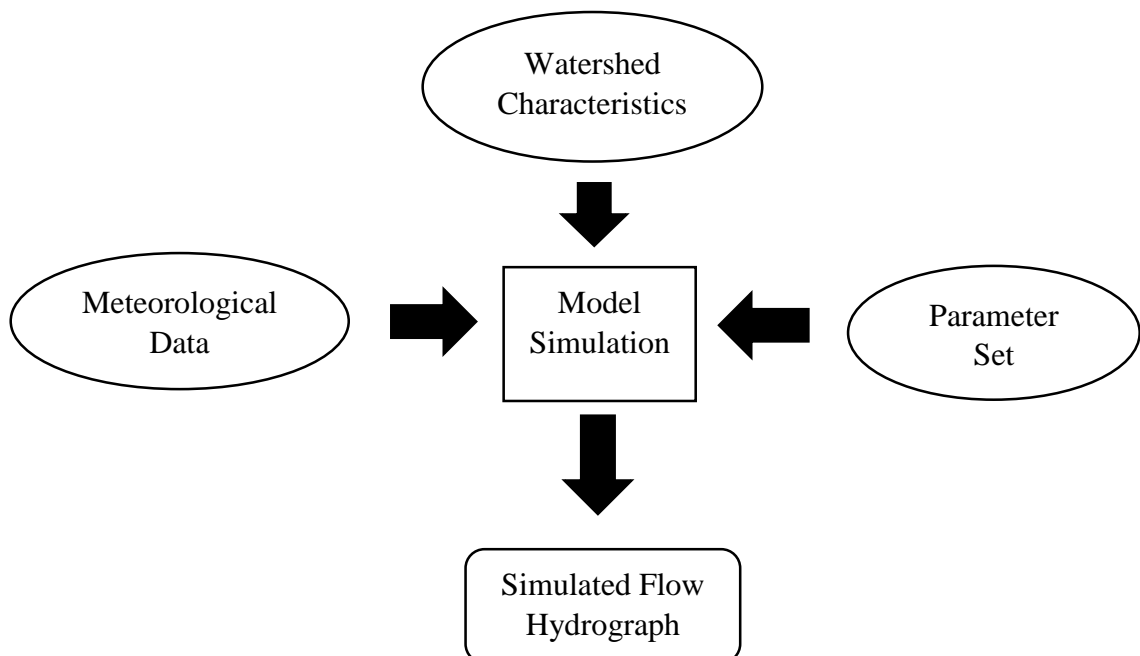


**Figure 4.1.** *Computational process of a hydrologic model.*

The Hydrologic Engineering Center's Hydrologic Modeling System (HEC-HMS) Version 4.1 (USACE, 2015) developed by the US Army Corps of Engineers (USACE), is a public software designed for both event-based and continuous rainfall-runoff simulation of dendritic watersheds (Figure 4.2). After the introduction of the Soil Moisture Accounting component (SMA) and geospatial capabilities, the model became widely used as an adaptable modeling tool for complex watersheds (Scharffenberg, 2008).

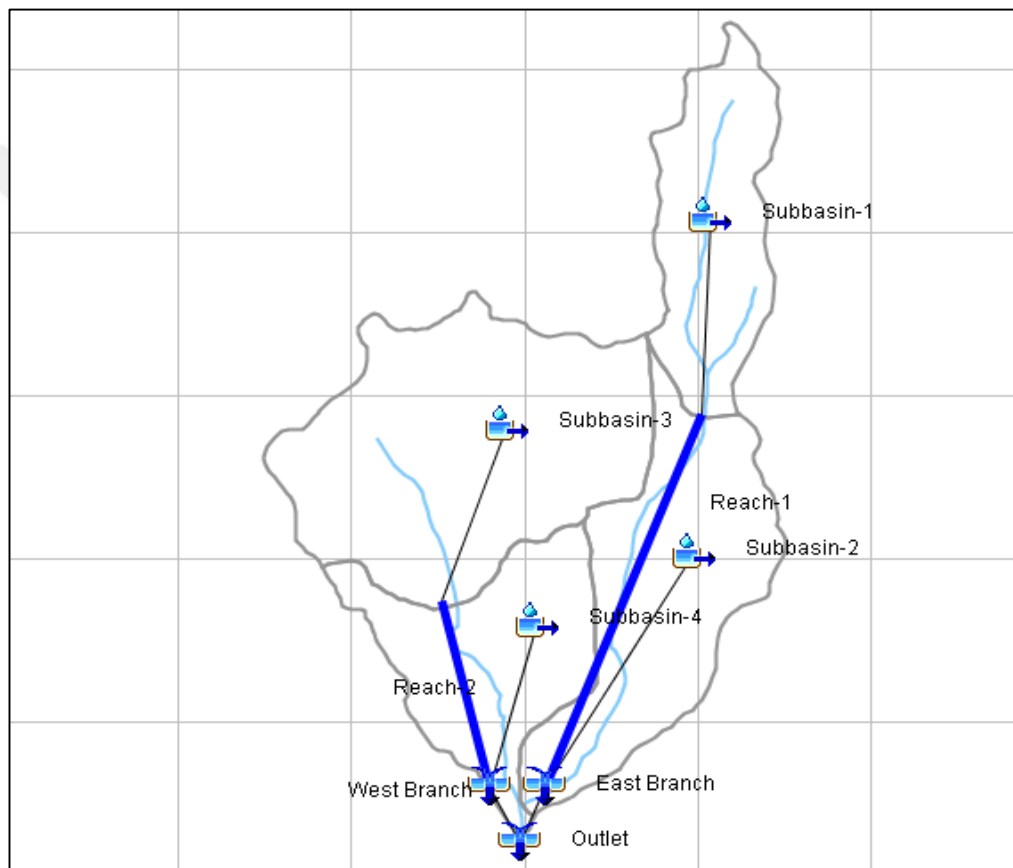


**Figure 4.2.** HEC-HMS basin model schematic (USACE, 2015).

The development of the current version of HEC-HMS dates back to the first version of HEC-1 developed in 1968. HEC-1 provided an all-inclusive hydrological cycle description integrating surface runoff, infiltration, channel routing, precipitation, reservoir simulation and baseflow. The Data Storage System (DSS) designed for time-series storage and retrieval was connected to the HEC-1 in the 1980's (Scharffenberg and Pak 2009).

Despite the impressive success of the HEC-1 it could only model and simulate a single storm event occurring in a medium size watershed. The desire to model larger watersheds and the introduction of continuous simulation led to the development of HEC-HMS. The HEC-HMS version 1.0 was comprised of several HEC-1 features such as the precipitation, transform, loss rate, baseflow, reservoirs and channel routing. The agreement with ESRI resulted in the development of HEC-GeoHMS, a component using Geographic Information Systems (GIS) to extract a watershed model from Digital Elevation Model (Scharffenberg and Pak 2009).

The development of Soil Moisture Accounting (SMA) a multi-layer loss rate method, and an average monthly evapotranspiration method resulted in the continuous simulation capabilities. These developments were incorporated in HEC-HMS version 2.0. The development of a snowmelt module in the form of 'Temperature Index' into the meteorologic model resulted in HEC-HMS version 3.0 (Scharffenberg and Pak 2009).

Further development works focusing on several capabilities including the sediment model capabilities, basin model zones and forecasting alternatives were incorporated in the version 4.0. The forecasting alternative component of the HEC-HMS version 4.1 is used for streamflow forecasting in this study.

#### **4.2. Hydrological Model Structure**

Continuous modeling comprises of a much longer time window covering both the wet and the dry periods. This time period can range from a few months to several years depending on the modeling scope. The event-based modeling on the other hand has a much smaller simulation time beginning just before the storm and ending with the storm. The simulation period can be a few hours to a few days depending on the watershed area. The main differences between these modeling approaches are the groundwater percolation and the potential evapotranspiration. They can be disregarded for event-based simulation but these are crucial for a continuous simulation as they define the process through which the soil dries (Scharffenberg, 2008).

Models are classified with respect to several criteria. The two most often used classification methods are the description of the physical processes and spatial description of catchment processes. Hydrological models may be stated as conceptual and physically based according to the first criterion and they may be stated as lumped and distributed in



regard to the second criterion (Figure 4.3). In this respect, two typical model types are lumped conceptual and the distributed physically based ones. In lumped models watersheds are considered to be a homogeneous one unit that can be characterized with a few variables and parameters. All the parameters impacting the rainfall-runoff process are spatially averaged across the watershed.

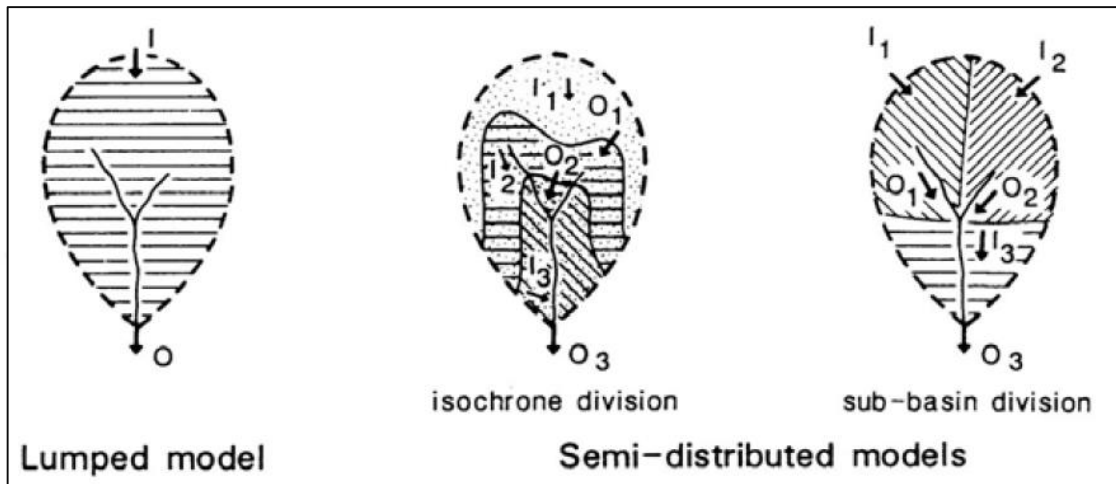


**Figure 4.3.** *Spatial characterization on rainfall-runoff models (Jones, 1997).*

Lumped model system takes a uniformity assumption over rainfall distribution across the watershed both temporally and spatially. The uniformity is also assumed for the land use, vegetation cover and the soil types. However, all these parameters may vary significantly across the watershed. Parameters are then averaged to create the uniform conditions across the basin with the lumped model.

The availability of high resolution data and the improved capabilities of the Geographic Information Systems (GIS) have made distributed modeling an active area of research. A watershed can be divided into a number of subcatchments where the hydrologic parameters may vary from one subcatchment to another. In such a case, lumped models may be labeled as “semi distributed” (Meselhe, 2009).

Distributed models represent the spatial variability of the parameters to analyze the rainfall-runoff process of a watershed. These parameters may include the vegetation cover, soil types, the watershed’s topography and geology. Distributed models also account for the spatial variability of the meteorological conditions of the drainage basin (Refsgaard, 1997).

HEC-HMS provides multiple ways to simulate the rainfall-runoff processes within a watershed that support both the distributed parameter based models and the lumped parameter-based models (Agrawal, 2005).

The model has three main components as basin model, meteorological model and control section. In a basin model, methods (loss, transform, baseflow) are defined to simulate hydrographs. There are various options for each of these methods. According to the purpose of application, data availability, special conditions of a catchment, one of these options is selected in the application. In a meteorological component, variables are defined for precipitation, temperature and discharge in relation with time series data sets. Data can be stored within the Data Storage System (DSS) for easy retrieval. Control component defines the start and end times for a desired simulation period.

#### **4.2.1. Loss method**

Infiltration plays a major role in the surface runoff simulation and is modeled by the loss methods in HEC-HMS. The infiltration rate affects both the peak discharge and the volume of a hydrograph and it is a function of time. Loss methods provide simulations that can be applied on the flood estimation designs as well as streamflow forecasting. The available loss method options in HEC-HMS model are Deficit and Constant, Exponential, Green and Ampt, Gridded Deficit and Constant, Gridded Green and Ampt, Gridded SCS Curve Number, Gridded Soil Moisture Accounting, Initial and Constant, SCS Curve Number, Smith Parlange, and Soil Moisture Accounting (SMA).

In most of the conceptual hydrologic models, the majority of the loss methods were empirical and have no clear sense of the physical infiltration process due to the lack of measurements. By taking into consideration the physical process occurring within the continuous simulation run, the infiltration methods have been improved. Soil Moisture Accounting (SMA) process incorporates important elements of the hydrologic cycle to simulate infiltration. These include the canopy interception, surface storage, soil infiltration, soil percolation and baseflow.

SMA has five storage zones (buckets) to simulate the losses, as shown in Figure 4.4. The initial conditions of each storage zone as the percentage of the zone's full capacity, the transfer rates such as percolation rates and infiltration are essential to run the simulation of the movement of water through the zones (Fleming and Neary, 2004).

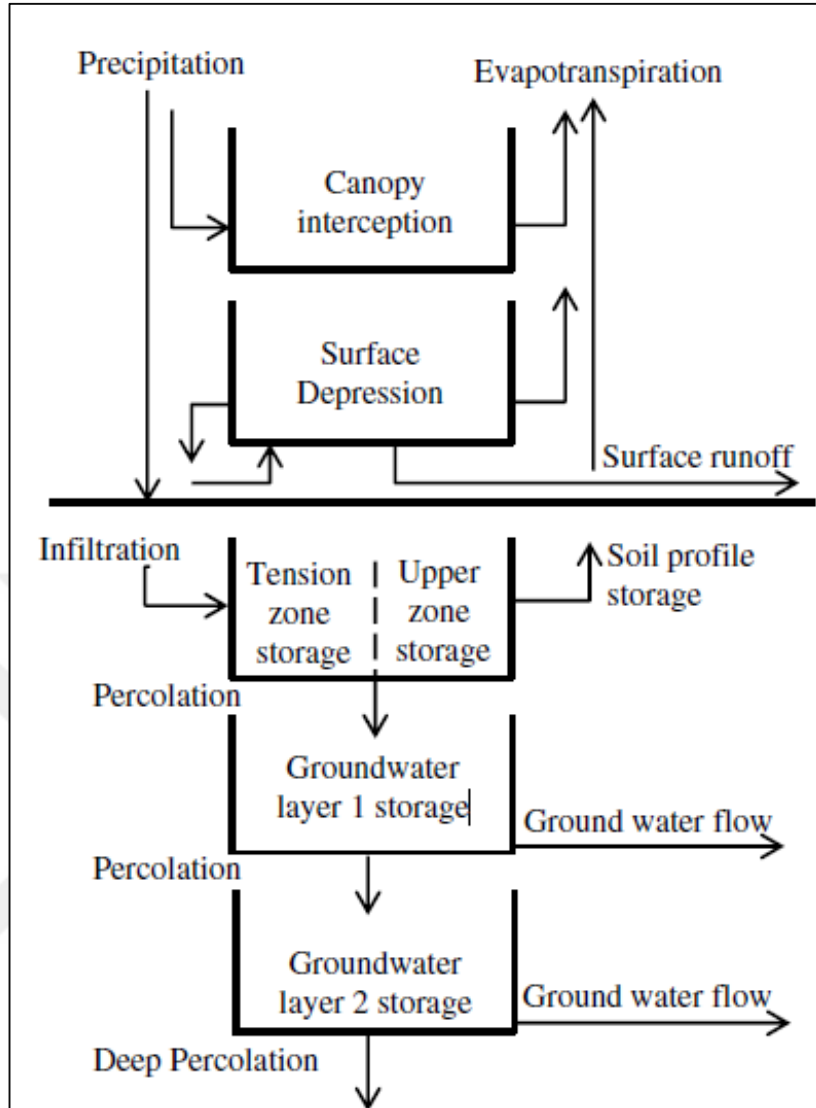


**Figure 4.4.** HEC-HMS schematic diagram for the SMA (USACE, 2015).

SMA calculates the water movement into, in between and out of the storage layers. This movement can take various forms such as, precipitation, surface runoff, evapotranspiration, infiltration, percolation and groundwater flow. The SMA equations were extracted from the HEC-HMS Technical Reference Manual (USACE, 2015) and summarized below (Equation 4.1 -4.6).

$$PotSoilInfil = MaxSoilInfil - \frac{CurrSoilStore}{MaxSoilStore} MaxSoilInfil \quad (4.1)$$

$$PotSoilPerc = MaxSoilPerc \left( \frac{CurSoilStore}{MaxSoilStore} \right) \times \left( 1 - \frac{CurGwStore}{MaxGwStore} \right) \quad (4.2)$$

$$PotGwPerc = MaxGwPerc \left( \frac{CurGw1Store}{MaxGw1Store} \right) \times \left( 1 - \frac{CurGw1Store}{MaxGw2Store} \right) \quad (4.3)$$

$$GwFlow_{t+1} = \frac{AcSoilPerc + CurGw_iStore - PotGw_iPerc - \frac{1}{2} GwFlow_t \times Time\ Step}{RoutGw_iStore + \frac{1}{2} Time\ Step} \quad (4.4)$$

$$GwVolume = \frac{1}{2} (GwFlow_{t+1} + GwFlow_t) \times Time\ Step \quad (4.5)$$

$$ActEvapSoil = PotEvapSoil \times f(CurSoilStore, MaxTenStore) \quad (4.6)$$

At any interval during a simulation, the volume of infiltration is a function of time and SMA computes the potential infiltration with Equation 4.1. Where, *MaxSoilInfil* is the maximum infiltration rate in millimeters (mm). *CurSoilStore* is the percentage (%) of volume in the soil storage at the beginning of the time step. *MaxSoilStore* is the maximum volume of the soil storage in millimeters (mm).

SMA computes the percolation rate between the soil-profile storage and the Groundwater 1 layer with Equation 4.2 and computes the percolation from Groundwater 1 to Groundwater 2 with Equation 4.3. Where, *PotSoilPerc* is the potential soil percolation rate in millimeters per hour (mm/hr), *MaxSoilPerc* is the maximum percolation rate in millimeters per hour (mm/hr). *CurSoilStore* is the calculated soil storage at the beginning of the time step in millimeters (mm), *CurGwStore* is the calculated groundwater storage for the Groundwater 1 layer in millimeters (mm) and *MaxGwStore* is the maximum ground water storage in millimeters (mm). *MaxGwPerc* is the maximum Groundwater 1 percolation rate in millimeters per hour (mm/hr). *CurGwStore* in millimeters (mm) is the calculated Groundwater storage for the groundwater 2 layer and *MaxGw2Store* is the maximum Groundwater storage for layer 2.

The Groundwater flow is the total flow volume from each Groundwater layer at the end of an interval. The Groundwater flow rate and Groundwater volume released by the watershed are computed with Equation 4.4 and 4.5. Where, *GwFlow<sub>t</sub>* and *GwFlow<sub>t+1</sub>* are the groundwater flow rates at the beginning of the time interval *t* and *t+1*, respectively. *ActSoilPerc* is the actual percolation from the soil profile to the Groundwater layer. *PotGw<sub>i</sub>Perc* is the potential percolation from Groundwater layer *i*. *RoutGw<sub>i</sub>Store* is the Groundwater flow routing coefficient from Groundwater storage *i*.

When potential EvapoTranspiration (ET) is drawn from the tension zone, the actual ET is a percentage of the potential, computed by Equation 4.6 where, *ActEvapSoil* is the

calculated ET from soil storage. *PotEvapSoil* is the calculated maximum potential ET. *MaxTenStore* is maximum tension storage in millimeters (mm).

Therefore, the Soil Moisture Accounting algorithm has 14 parameters to simulate the movement through the soil (Figure 4.5). The first three parameters (Soil, Groundwater 1 and Groundwater 2) represent only the initial conditions, the next four parameters (Max infiltration, imperviousness, soil storage and tension storage) simulate the changes in state conditions of the soil moisture. The last seven parameters (Soil Percolation, GW1 Storage, GW1 Percolation GW1 Coefficient, GW2 Storage, GW2 Percolation and GW2 Coefficient) represent the movement of the water through the second and third layers of the soil.

The water that percolates beyond the third layers represented by the GW2 percolation and it is referred as ‘deep percolation’ since the water will not join the baseflow while the rest of the water within the second and third levels is expected to join the baseflow (USACE, 2015).

The screenshot shows a software interface for editing parameters. At the top, there are tabs: 'Subbasin' (selected), 'Loss', 'Transform', 'Baseflow', and 'Options'. Below the tabs, the following information is displayed:

- Basin Name: Basin1**
- Element Name: Serindere**

A list of 14 parameters is shown, each with a red asterisk and a text input field containing a numerical value:

*Soil (%)	20
*Groundwater 1 (%)	10
*Groundwater 2 (%)	10
*Max Infiltration (MM/HR)	4
*Impervious (%)	0
*Soil Storage (MM)	50
*Tension Storage (MM)	40
*Soil Percolation (MM/HR)	1.0
*GW 1 Storage (MM)	40
*GW 1 Percolation (MM/HR)	0.9
*GW 1 Coefficient (HR)	300
*GW 2 Storage (MM)	40
*GW 2 Percolation (MM/HR)	0.8
*GW 2 Coefficient (HR)	200

**Figure 4.5.** Component editor for SMA (USACE, 2015)

#### 4.2.2. Transform method

Storm event may result in excess precipitation and surface flow depending on the storm duration and intensity. The movement of the surface flow through the basin is mainly influenced by two processes, the attenuation and translation. Translation refers to the downward flow under the influence of gravity through the watershed. Attenuation on the other hand refers to forces opposing the flow such as channel storage and friction force (Melching, 1997). Figure 4.6 demonstrates the transform process, the excess precipitation is transformed into a hydrograph.

In HEC-HMS the calculations of the actual surface runoff resulting from the observed precipitation are performed by the transform method (USACE, 2015). HEC-HMS provides the user with several transform methods, these methods include amongst others Clark, Snyder, SCS unit hydrograph and user-specified unit hydrographs.

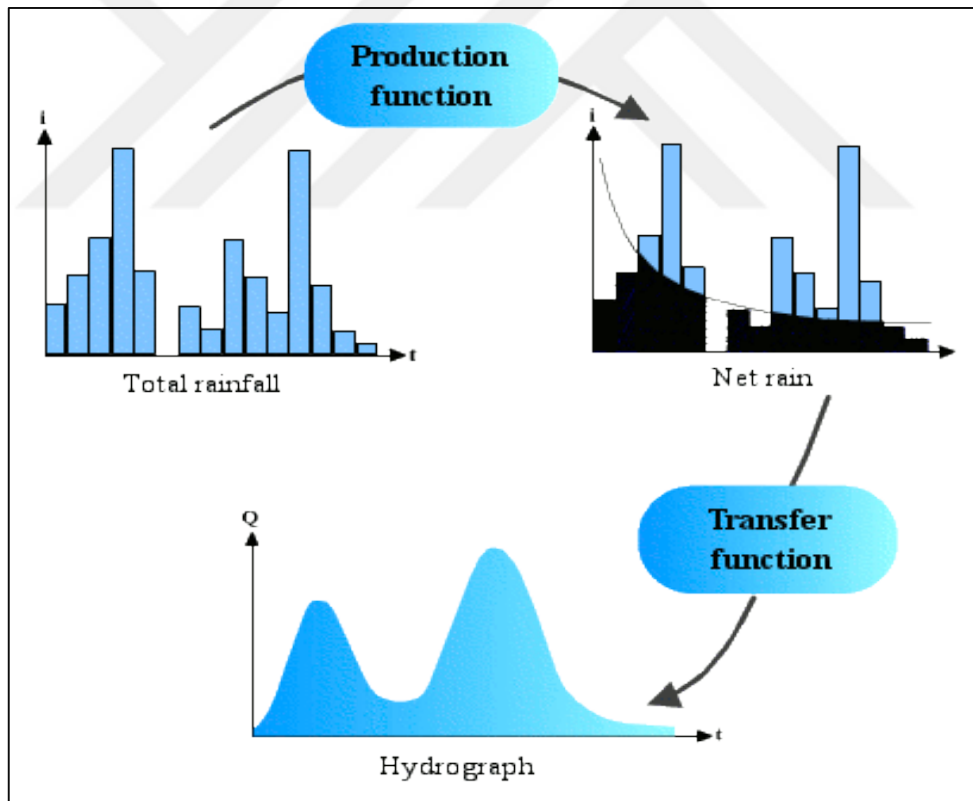


**Figure 4.6.** Transformation of excess precipitation into a hydrograph (Musy, 2001).

Clark (1945) stated that the movement of flow across the watershed can be explained with a time-area curve. This demonstrates a curve for the part of the watershed area contributing flow to the watershed outlet as a function of time from the beginning of

the effective precipitation. The watershed's time of concentration bounds the time-area curve in time. The Clark unit hydrograph computes two process, the translation and attenuation. Clark unit hydrograph in HEC-HMS makes use of the time of concentration ( $T_c$ ) representing the translation and the storage coefficient representing the attenuation to calculate the conversion (Figure 4.7).

**Figure 4.7.** Component editor for Clark unit hydrograph (USACE, 2015).

To calculate the translation, the translational unit hydrograph is calculated as;

$$U = Q_S - Q_{SL} \quad (4.7)$$

$$Q_S = A_c i_e \quad (4.8)$$

$$A_c = 1.414A \left( \frac{t}{T_c} \right)^{1.5} \quad \text{for } 0 \leq \frac{t}{T_c} \leq 0.5 \quad (4.9)$$

$$A_c = A \left( 1 - 1.414 \left( 1 - \frac{t}{T_c} \right)^{1.5} \right) \quad \text{for } 0.5 \leq \frac{t}{T_c} \leq 1.0 \quad (4.10)$$

Where  $Q_S$  and  $Q_{SL}$  are the ordinates of the S-curve and lagged S-curve, respectively.  $A_c$  is the cumulative area contributing to the runoff at the basin's outlet and  $i_e$  is the intensity of the effective rainfall. To account for the storage effect, the linear reservoir with a storage constant  $K$  is used to route the  $U$  hydrograph. The ordinates of hydrograph are linked by;

$$(Q_u)_j = (Q_u)_{j-1} + C_R [U_{j-1} + U_j - 2(Q_u)_{j-1}] \quad (4.11)$$

$$C_R = \frac{\Delta t}{2K + \Delta t} \quad (4.12)$$

### 4.2.3. Baseflow method

The portion of the precipitation percolates until the water table. Upon reaching the water table, it moves laterally till rejoining the streamflow. In comparison with the surface runoff, baseflow is a lot slower and has no effect on flood peaks caused by a storm event (Singh, 1988). HEC-HMS provides users with several baseflow methods which include constant baseflow, recession and linear reservoir methods.

Constant baseflow method assumes the constant monthly value and can vary from month to month. Linear reservoir is best suited for application in collaboration with SMA. The HEC-HMS linear reservoir represents movement of water through two groundwater layers. The initial conditions refer to the amount of groundwater flow at the beginning of the simulation runs. The linear reservoir *Component Editor* for the HEC-HMS is represented in Figure 4.8. Groundwater storage coefficient refers to the time constant of each layer and it gives a sense of the response time of the subbasin. The flow in Groundwater 1 and 2 layers is routed by the reservoirs.

Basin Name: Basin1	
Element Name: Serindere	
Initial Type:	Discharge
*GW 1 Initial (M3/S)	0.3
*GW 1 Coefficient:	800
GW 1 Reservoirs:	1
GW 2 Initial (M3/S)	0.1
GW 2 Coefficient:	500
GW 2 Reservoirs:	1

Figure 4.8. Component editor for linear reservoir (USACE, 2015).

### 4.2.4. Temperature index method

Accuracy of snowmelt predictions in snow-dominated basins is a crucial step towards efficient management of flood warning systems and flood protection structures. Temperature index is used to simulate the snowmelt and computes the meltrate actively based on the snowpack's current and past conditions. Temperature index attributes the energy change on a snow surface solely by the air temperature. Its computation of



snowmelt using the average daily air temperatures is advantageous as the temperature is an easily measured meteorological variable (Sensoy, 2005; Anderson, 2006). Therefore, even though the radiation is another important factor in snowmelt calculations, it is not considered in this application.

The degree-day method is a widely used temperature index approach. It equates the daily total melt to the difference in temperature, the base temperature and the daily mean temperature multiplied by a coefficient (Equation 4.13).

$$M = a(T - T_c) \quad (4.13)$$

Where;

$M$  is the snowmelt (mm/day)

$a$  is the degree-day coefficient (mm/degree-day °C)

$T$  is the mean daily air temperature (°C)

$T_c$  is the base temperature (°C)

HEC-HMS employs the temperature index together with paired data component (Figure 4.9).

Temperature Index	
<b>Met Name: Met</b>	
*PX Temperature (C)	0
*Base Temperature (C)	1
*Wet Meltrate (MM/DEG C-DAY)	4
Rain Rate Limit (MM/DAY)	3
ATI-Meltrate Coefficient:	0.95
*ATI-Meltrate Function:	Table 1
Meltrate Pattern:	--None--
Cold Limit (MM/DAY)	0
ATI-Coldrate Coefficient:	0
ATI-Coldrate Function:	--None--
Water Capacity (%)	5
Groundmelt Method:	Constant Value
Groundmelt (MM/DAY)	0.5

**Figure 4.9.** Component editor for the temperature index (USACE, 2015)

PX Temperature is a threshold used to determine whether precipitation falls as rainfall or snowfall and Base Temperature is the threshold used to determine above which temperature snowmelt starts. Wet Meltrate refers to the melting rate when the rainfall rate is greater than the rain rate limit, Rain Rate Limit sets the lower bound of rain rate over which there will be rain on snow effect and ATI-Meltrate Coefficient calculates the meltrate from the current meltrate index.

Cold Limit accounts for the rapid changes undergone by the snowpack during high precipitation rates, ATI-Coldrate Coefficient updates the antecedent cold content from one time interval to the next and Water Capacity representing the amount of accumulated melted water before runoff. Groundmelt refers to the snowmelt rate resulting from the heating ground.

Antecedent temperature index (ATI) melt rate function states the meltrate for the antecedent temperature index (Fazel, 2014). This is done by applying the degree-day adjustments in a tabular form in HEC-HMS (Table 4.1).

**Table 4.1.** Component editor for ATI meltrate function, (USACE, 2015).

Paired Data Table Graph	
ATI (DEG C-DAY)	Meltrate (MM/DEG C-DAY)
0.0	2.0
100.0	3.0
200.0	3.0
300.0	4.0

#### 4.2.5. Start-state condition

Hydrological and meteorological models employ numerous mathematical equations and functions comprising state variables. State variables indicate the conditions of the system by the end of a simulation time interval. The state variable in the soil moisture accounting method is the moisture conditions of all the soil layers at the end of a simulation run (USACE, 2015).

Start-states component in HEC-HMS has two main applications, the real-time forecasting and the breaking of long simulations into several shorter periods. During a simulation run, the state variables undergo a change as a result of the changes in the

dynamics of the mathematical equations and the boundary conditions governing the method. The state variables explain the conditions which experience a change during a simulation run, for example soil moisture, snow water equivalent and initial baseflow. Saved states store the values of the basin model's variable at a specific time during an earlier simulation run (Cunderlik and Simonovic, 2004).

The state variables should therefore be stated at the beginning of the simulation run as the initial conditions. To be employed in any subsequent simulation run it has to be saved at the end of the current simulation run (Figure 4.10).

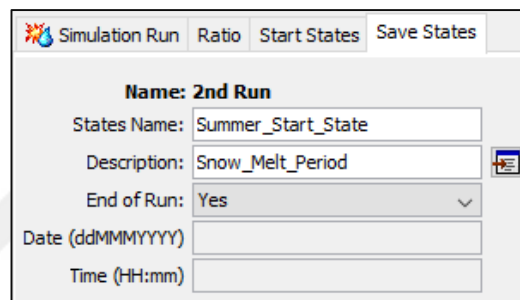


**Figure 4.10.** Component editor for saved state (USACE, 2015).

#### 4.2.6. Runoff forecast module

To forecast the streamflow, the watershed's recent hydrologic and meteorologic conditions as well as the future conditions are of fundamental importance. On the other hand, the quality and quantity of the forecast data directly affects the accuracy and precision of the streamflow forecasts (Uysal et al., 2016; USACE, 2015; Çoşkun, 2016).

HEC-HMS applies the forecast alternative component (Figure 4.11) to forecast the streamflow. The forecast alternatives are composed of a meteorological model, basin model and the time control to compute the results. The configurations for the basin parameters such as the loss, baseflow and the transform methods are also included within the forecast alternative. The forecast simulation is started at least 24 hours before the desired end time. The simulation results from the start time to the forecast time is referred to as the 'look back period'. In the absence of the meteorological data, the simulation of future streamflow conditions is done based on the prediction data. This simulation period is referred to as the 'forecast'.

Name: Alternative 1	
Description:	<input type="text"/>
DSS File:	C:\Users\Daniel\Desktop\Kara:
Basin Model:	Basin_1
Meteorologic Model:	Met_1
*Start Date (ddMMMYYYY)	01Oct2014
*Start Time (HH:mm)	00:00
*Forecast Date (ddMMMYYYY)	12Jul2015
*Forecast Time (HH:mm)	00:00
*End Date (ddMMMYYYY)	15Jul2015
*End Time (HH:mm)	00:00
Time Interval:	1 Day
Loss Rate Config:	Configuration 1
Transform Config:	Configuration 1
Baseflow Config:	Configuration 1
Routing Config:	--None Selected--

**Figure 4.11.** *Component editor for forecast alternative (USACE, 2015).*

The streamflow simulation is almost never perfect as both the quality and accuracy of the computed results depend on the quality and quantity of the prediction data, the knowledge of the watershed conditions and model uncertainties. The forecast blending uses the observed flow to systematically adjust the simulated streamflow. To perform the streamflow adjustment, the blending method calculates the difference between the observed and simulated streamflow. Starting from the forecast time to the end time, the blending applies a correction. The calculated difference is then added to the streamflow simulated for the forecast period (USACE, 2015).

HEC-HMS employs three different blending methods in accordance with the user's preference, namely the Step, Taper and None. As the name implies, the 'none' option applies no correction to the forecast simulation. The 'step' option employs a constant adjustment to the computed forecast streamflow simulation from the forecast time to the end time. The difference between the observed streamflow and the computed streamflow is added to the computed streamflow starting from the forecast time till the end time.

The 'taper' option employs a declining adjustment to the computed forecast streamflow after the forecast time. The initial difference between the observed streamflow and the computed streamflow is added to the computed streamflow at forecast time and decreased linearly across the taper duration.



## **5. MODEL APPLICATION AND RESULTS**

This chapter discusses the hydrologic model application and the results obtained in each step of the study. The study employed the Hydrologic Engineering Center's Hydrologic Modeling System (HEC-HMS) Version 4.1 developed by the U.S. Army Corps of Engineers (USACE) in 2015 (USACE, 2015). The study is presented basically in three steps; model parameter estimation, results and streamflow forecasting. The hydro-meteorological data of the last fourteen years (2002 to 2015) provided by the State Hydraulic Works (DSI) and General Directorate of Meteorology (MGM) are used in HEC-HMS model. The calibration and validation periods are selected to be seven years each, (2002 to 2008) and (2009 to 2015) respectively. The streamflow forecasting is done for the 2015 water year using Numerical Weather Prediction data.

### **5.1. Model Parameter Estimation**

Model calibration is the rigorous process of adjusting the model parameters until the simulated streamflows match the observed historical streamflows. This section explains the model parameter calibration process of the HEC-HMS model.

HEC-HMS is a hydrologic model designed to simulate the hydrological processes and compute runoff volume. It includes the hydrological processes such as infiltration, transformation and routing. To simulate infiltration, HEC-HMS provides eleven loss methods; Initial and Constant, Deficit and Constant, Exponential, Green Ampt, Soil Conservation Service (SCS) Curve Number, Soil Moisture Accounting (SMA), Gridded Deficit and Constant, Gridded Green and Ampt, Gridded SCS Curve Number and Gridded SMA. However, most of these loss methods are suitable for modeling only event simulations. SMA is selected in this study due to its consistency and good performance in continuous simulations compared with other methods, and also to make use of new satellite soil moisture products in the hydrovalidation analysis. On the other hand, SMA needs a large set of input parameters most of which need to be calibrated.

The canopy storage defines the precipitation interception by the vegetation. HEC-HMS offers three canopy methods, Dynamic, Gridded and Simple methods. However in this study, the canopy storage is not employed since the land use map of Karasu Basin covers mostly bare land and pastures.

The surface storage defines the water storage occurring in the surface depressions. Due to the large area of Karasu Basin, the surface storage effects are negligible. Therefore, even though several trials are done with this module, it is finally not used in the applications.

Furthermore, HEC-HMS uses various unit hydrograph methods for transformation of excess precipitation. The methods include the Clark unit hydrograph, Snyder unit hydrograph, SCS unit hydrograph, Kinematic wave, ModClark, user-specified S-Graph and user-specified unit hydrograph. Since the storage coefficient of Clark unit hydrograph applies linear reservoir, and SMA cooperates better with this method, Clark unit hydrograph is selected for the transformation method in this study.

A total of five baseflow methods; Bounded Recession, Constant Monthly, Linear Reservoir, Nonlinear Boussinesq and Recession are provided by HEC-HMS. Linear reservoir was selected for the main snowmelt season because of its better compatibility with SMA and constant baseflow approach was utilized for the low flow periods for a higher consistency.

Temperature index method is used for snowmelt calculations. Its parameters are calibrated using the previous experiences on snowmelt modeling with different conceptual hydrological models.

The combination of the automated optimization, manual calibration and sensitivity analysis were utilized as model estimation procedure in the study. The automated methods built in the model were not helpful in estimating a better parameter set with a consistent range. The methods are not suitable to detect a global optimum and there are a number of parameters that have to be estimated. The estimation generally stuck on the initial guess of the parameter optimization. Therefore, the manual trial and error and sensitivity analysis techniques were applied. A combination of event and continuous application is used commonly indicated by SMA and snowmelt component users in the literature. The calibration process first focused on the snowmelt period of each year, then the complete water year simulation and finally the entire calibration period. HEC-HMS offers two model performance criteria, Nash-Sutcliffe Efficiency (NSE) and Root Mean Square Error (RMSE), these are examined to determine the parameter set producing the

best model performance. In addition percent peak error and percent peak volume error were examined to assess the consistency of the observed and simulated hydrographs.

The two commonly used model performance assessment criteria in hydrology are applied to Karasu Basin streamflow simulations. Nash Sutcliffe Efficiency (NSE) and Root Mean Square Error (RMSE). NSE has the ranges of  $-\infty$  to 1,  $-\infty$  being the poor model performance and 1 as the perfect model performance. NSE is represented by Equation 5.1. RMSE (Equation 5.2) is used to assess the accuracy of the model performance. In addition, the percent peak is employed to assess the model's peak and volume accuracy (Equation 5.3 and 5.4).

$$NSE = 1 - \frac{\sum_{i=1}^N (O_i - P_i)^2}{\sum_{i=1}^N (O_i - \bar{O})^2} \quad (5.1)$$

$$RMSE = \sqrt{\frac{\sum_{i=1}^N (O_i - P_i)^2}{N}} \quad (5.2)$$

$$\% \text{ Error Volume} = \left( \frac{\text{Simulated Volume} - \text{Observed Volume}}{\text{Observed Volume}} \right) \times 100 \quad (5.3)$$

$$\% \text{ Error Peak} = \left( \frac{\text{Simulated Peak} - \text{Observed Peak}}{\text{Observed Peak}} \right) \times 100 \quad (5.4)$$

Where;  $O$  is the observed data,  $\bar{O}$  is the mean for the whole evaluation period.  $P$  is the estimated data and  $N$  is the total simulation period denoted in daily time steps.

Estimation of the model parameters are explained for each of the methods below.

### 5.1.1. Loss parameter estimation

The soil moisture component by SMA method rely on the precipitation to simulate the water movement through the soil profile and into the groundwater layers. SMA employs 14 parameters to simulate the surface runoff, the groundwater flow, the losses as a result of deep percolation and evapotranspiration. Three of these parameters Soil (%), Groundwater 1 (%) and Groundwater 2 (%) represent the initial moisture conditions of the soil. The initial conditions of the soil can be different for each application period as the dryness of the soil changes. Thus calibration of the initial parameters is then based on



the antecedent precipitation conditions preceding the model starting date for the simulation run accordingly.

Percentage of imperviousness is obtained from the land use map. Therefore, ten of SMA parameters are calibrated for the loss method. The initial parameter value ranges are defined using both HEC-HMS user's manual and previous studies done in the literature (Table 5.1).

**Table 5.1.** Range of SMA parameters used in HEC-HMS.

<b>Parameters</b>	<b>Parameter Range</b>
Max Infiltration (mm/hr)	0.01 to 20
Soil Storage (mm)	0 - 120
Tension Storage (mm)	0 - 75
Soil Percolation (mm/hr)	0.01 – 10
GW 1 Storage (mm)	0 - 75
GW 1 Percolation (mm/hr)	0.01 – 1.0
GW 1 Coefficient (hr)	100 - 1000
GW 2 Storage (mm)	0 - 75
GW 2 Percolation (mm/hr)	0.01 – 1.0
GW 2 Coefficient (hr)	100 - 1000

A sensitivity analysis is carried out to narrow the range of parameter values. The 2007 water year is selected to represent the sensitivity analysis since the model consistency for the simulated and observed discharges is higher in comparison with the other calibration years. The observed peak discharge and volume (in depth) of the hydrograph are 497.0 m<sup>3</sup>/s and 261.53 mm, respectively.

Max infiltration (mm/hr) sets the infiltration rate limit into the groundwater from the surface storage. Sensitivity analysis show that the maximum infiltration has an effective range of 1-5 mm/hr for Karasu Basin (Table 5.2). The calibrated parameter is determined to be 2 mm/hr through trial and error, which gives the best performance on the peak flows and runoff volumes for all the years.

**Table 5.2.** Sensitivity analysis for maximum infiltration, 2007.

<b>Max Infiltration (mm/hr)</b>	<b>Peak Discharge (m<sup>3</sup>/s)</b>	<b>Volume (mm)</b>	<b>RMSE (m<sup>3</sup>/s)</b>	<b>NSE</b>
0	901.1	785.18	225.8	-6.667
1	532.5	319.21	55.1	0.544
3	447.5	247.41	38.7	0.772
5	437.9	256.02	40.0	0.759

The total storage available within the soil layer is represented by the soil storage (mm). Sensitivity analysis show that the total storage has an effective range around 80-120 mm for Karasu Basin (Table 5.3). The calibrated parameter is determined to be 100 mm through trial and error.

**Table 5.3.** Sensitivity analysis for soil storage, 2007.

<b>Soil Storage (mm)</b>	<b>Peak Discharge (m<sup>3</sup>/s)</b>	<b>Volume (mm)</b>	<b>RMSE (m<sup>3</sup>/s)</b>	<b>NSE</b>
60	586.9	351.9	69.8	0.268
80	521.2	286.5	41.4	0.742
100	473.1	265.8	37.5	0.788
120	431.1	262.5	40.2	0.757

Tension storage (mm) is the volume of water in storage that doesn't drain under gravity effects. Tension storage should be less than the soil storage. Taking into consideration the initial values extracted from the literature and applying the optimization, trial and error analysis, the effective range for tension storage is determined to be 20-60 mm for Karasu Basin (Table 5.4). The calibrated parameter value for tension storage is determined as 50 mm concerning the model performance.

**Table 5.4.** Sensitivity analysis for tension storage, 2007.

<b>Tension Storage (mm)</b>	<b>Peak Discharge (m<sup>3</sup>/s)</b>	<b>Volume (mm)</b>	<b>RMSE (m<sup>3</sup>/s)</b>	<b>NSE</b>
0	364.1	263.0	50.5	0.617
20	397.4	266.5	46.2	0.679
40	450.7	267.4	39.7	0.763
60	507.1	280.4	39.3	0.767

The soil percolation (mm/hr) defines the water movement from the soil storage into Groundwater 1 storage. Sensitivity analysis on the soil percolation (mm/hr) applied with

the initial parameter ranges indicates that the soil percolation to have the effective range of 0.5-2 mm/hr (Table 5.5). At the end of trial and error procedure this parameter is determined as 0.6 mm/hr, this value has an important effect on the peak flows.

**Table 5.5.** *Sensitivity analysis of soil percolation, 2007.*

<b>Soil Percolation (mm/hr)</b>	<b>Peak Discharge (m<sup>3</sup>/s)</b>	<b>Volume (mm)</b>	<b>RMSE (m<sup>3</sup>/s)</b>	<b>NSE</b>
0	901.1	695.18	192.7	-4.581
0.5	490.2	273.63	38.3	0.779
1	443.6	260.27	38.1	0.781
2	406.4	255.34	39.9	0.761

The rest of the SMA parameters are calibrated with the same methodology. Groundwater 1 percolation (mm/hr) defines the percolation of water from Groundwater 1 storage to Groundwater 2 storage. Groundwater 2 percolation (mm/hr) defines the percolation of water from Groundwater 2 storage into deep percolation. Groundwater 1 and Groundwater 2 storage (mm) define the storage capacity of the upper and lower groundwater layers, respectively. The Groundwater 1 and Groundwater 2 coefficients (hr) are used as time lags for formation of lateral flow transformed from water in groundwater storage. Table 5.6 presents the calibrated and validated SMA parameter set for Karasu Basin. The minimum and maximum values for each parameter are also provided as a result of (2002 – 2015) period analysis.

**Table 5.6.** *Soil Moisture Accounting model parameter set for Karasu Basin.*

<b>Parameters</b>	<b>Value</b>	<b>Min.</b>	<b>Max.</b>
Max Infiltration (mm/hr)	2	1	4
Soil storage (mm)	100	60	120
Tension Storage (mm)	50	40	60
Soil Percolation (mm/hr)	0.6	0.3	1.2
GW 1 Storage (mm)	30	20	50
GW 1 Percolation (mm/hr)	0.4	0.2	1.2
GW 1 Coefficient (hr)	300	150	450
GW 2 Storage (mm)	40	20	50
GW 2 Percolation (mm/hr)	0.3	0.1	0.7
GW 2 Coefficient (hr)	400	200	600

### 5.1.2. Baseflow parameter estimation

The baseflow component explains the groundwater contribution to the total flow. Two baseflow methods are applied in this study, linear reservoir and constant monthly baseflow. Linear reservoir method uses six parameters to simulate the baseflow, GW 1 initial ( $\text{m}^3/\text{s}$ ) GW 1 coefficient, GW 1 reservoirs, GW 2 initial ( $\text{m}^3/\text{s}$ ) GW 2 coefficient and GW 2 reservoirs. The initial flow condition in the groundwater layers are represented by GW 1 ( $\text{m}^3/\text{s}$ ) and GW 2 ( $\text{m}^3/\text{s}$ ) and should be adjusted according to the preceding flow conditions at the beginning of the simulation.

The GW 1 and GW 2 coefficients are taken to be the same with the SMA Groundwater 1 and Groundwater 2 coefficients. This is because when linear reservoir baseflow method is applied in conjunction with the SMA loss method, it connects the infiltration to the lateral flow of the Groundwater 1 and Groundwater 2 soil layers (USACE, 2015).

The groundwater reservoirs are used for routing the baseflow through a number of reservoirs. Through trial and error procedure, GW 1 and GW 2 reservoirs are determined to be 1 in terms of model performance criteria. Table 5.7 presents the calibrated linear reservoir parameter set for Karasu basin.

**Table 5.7.** *Linear reservoir baseflow parameter set for Karasu Basin.*

Parameters	Value	Min.	Max.
GW 1 Initial ( $\text{m}^3/\text{s}$ )	30	20	50
GW 1 Coefficient	300	200	4000
GW 1 Reservoirs	1	1	3
GW 2 Initial ( $\text{m}^3/\text{s}$ )	40	10	30
GW 2 Coefficient	400	100	2000
GW 2 Reservoirs	1	1	3

The linear reservoir method produced peak discharges having a high consistency with the observed peak discharges. However, the method showed poor model performance while simulating the low flows. On the contrary, constant monthly baseflow method produced poor consistency during the snowmelt period but high model performance with the low flows. Therefore, a joint method application is chosen to better

simulate both low and high flows. A water year is divided into three seasons for joint simulation implementation. Pre-season (01 October – 01 March), snowmelt (01 March – 01 July) and post season (01 July – 01 October).

Peak discharges occurred during the snowmelt season in Karasu Basin. Therefore, the linear reservoir baseflow method is preferred to be used during snowmelt seasons. For the rest of the year, constant monthly baseflow method is applied. According to the observed low flows, the best values are assigned to each month of a year. The average values are then calculated for monthly discharges throughout the calibration period. Table 5.8 presents the calibrated constant monthly baseflow values for Karasu Basin.

**Table 5.8.** *Constant monthly baseflow parameter set.*

<b>Month</b>	<b>Baseflow (m<sup>3</sup>/s)</b>
Oct	40
Nov	45
Dec	50
Jan	50
Feb	50
Mar	-
Apr	-
May	-
Jun	-
Jul	45
Aug	40
Sep	40

### **5.1.3. Snowmelt Parameter Estimation**

Temperature index method within the snowmelt component, depends on the temperature values and degree day coefficient to simulate the melting of a snowpack. Seven of the temperature index model parameters are calibrated during snowmelt period. The initial parameter ranges are defined using HEC-HMS user's manual and the previous studies in the literature (Table 5.9).

**Table 5.9.** *Temperature index parameter ranges.*

<b>Parameters</b>	<b>Range</b>
PX Temperature (°C)	-2 – (2)
Base Temperature (°C)	-2 – (2)
Wet Meltrate (mm/deg C-day)	1 – 5
Rain Rate Limit (mm/day)	1 – 5
ATI-Meltrate Coefficient	0 – 1
Water Capacity (%)	0 – 10
Groundmelt (mm/day)	0 – 1

The first two parameters define the temperature thresholds. The PX temperature (°C) is a temperature threshold which differentiates precipitation falling as snow and as rainfall. Base temperature (°C) defines the limit at which snowmelt begins, no snowmelt occurs when the air temperature is below the base temperature (USACE, 2015).

Wet meltrate (mm/deg °C-day) defines the snowmelt as a result of rain falling on the snowpack. The rain rate limit (mm/day) differentiates dry melt from wet melt. Water capacity (%) representing the amount of accumulated melted water before runoff. Groundmelt (mm/day) represents melt as a result of the heated ground.

The majority of the streamflow volume occurs as a result of snowmelt during the snowmelt period (01 March – 01 July). To calibrate the temperature index parameters, an event-based model approach is examined during the snowmelt period. To accommodate the amount of snow from the preceding snowfall period, the observed Snow Water Equivalent (SWE) values are used as initial inputs at the beginning of each event.

The SWE values are provided for the mean elevation zone at the beginning each event (snowmelt period) and distributed to the other zones with adjustment coefficients (Table 5.10). Observed SWE values through in situ and AWOS observations at Güzelyayla AWOS (2065 m) are assigned to Zone C. The average adjustment coefficients are determined for several years in calibration period and applied uniformly across all years. Table 5.10 presents the adjustment coefficients for SWE in Karasu Basin.

**Table 5.10.** *Adjustment coefficients for Snow Water Equivalent (SWE) distribution in Karasu Basin.*

<b>Zones</b>	<b>Mean Elevation</b>	<b>Area (%)</b>	<b>Adjustment Coefficient</b>
Zone A	1355	10.64	0.5
Zone B	1732	31.70	0.7
Zone C	2098	33.80	1.0
Zone D	2485	22.26	1.3
Zone E	2993	1.60	1.3

The calibration of 2002 snowmelt period is shown in Figure 5.1. The simulation has Nash Sutcliffe Efficiency (NSE) of 0.852 and the Root Mean Square Error (RMSE) of 26.6 m<sup>3</sup>/s. Figure 5.2 presents the event-based model application results for the whole 2002 to 2007 snowmelt periods. The results are determined to be satisfactory with respect to the model performance criteria for the snowmelt throughout the calibration period. Finally, temperature index parameter set is obtained as in Table 5.11.

**Table 5.11.** *Temperature index parameter set for Karasu Basin.*

<b>Parameters</b>	<b>Value</b>	<b>Min.</b>	<b>Max</b>
PX Temperature (°C)	0	-2	2
Base Temperature (°C)	-1	-2	2
Wet Meltrate (mm/deg c-day)	4	2	6
Rain Rate Limit (mm/day)	3	1	5
ATI-Meltrate Coefficient	0.95	0.85	1
Water Capacity (%)	5	2	10
Groundmelt (mm/day)	0.5	0.1	1

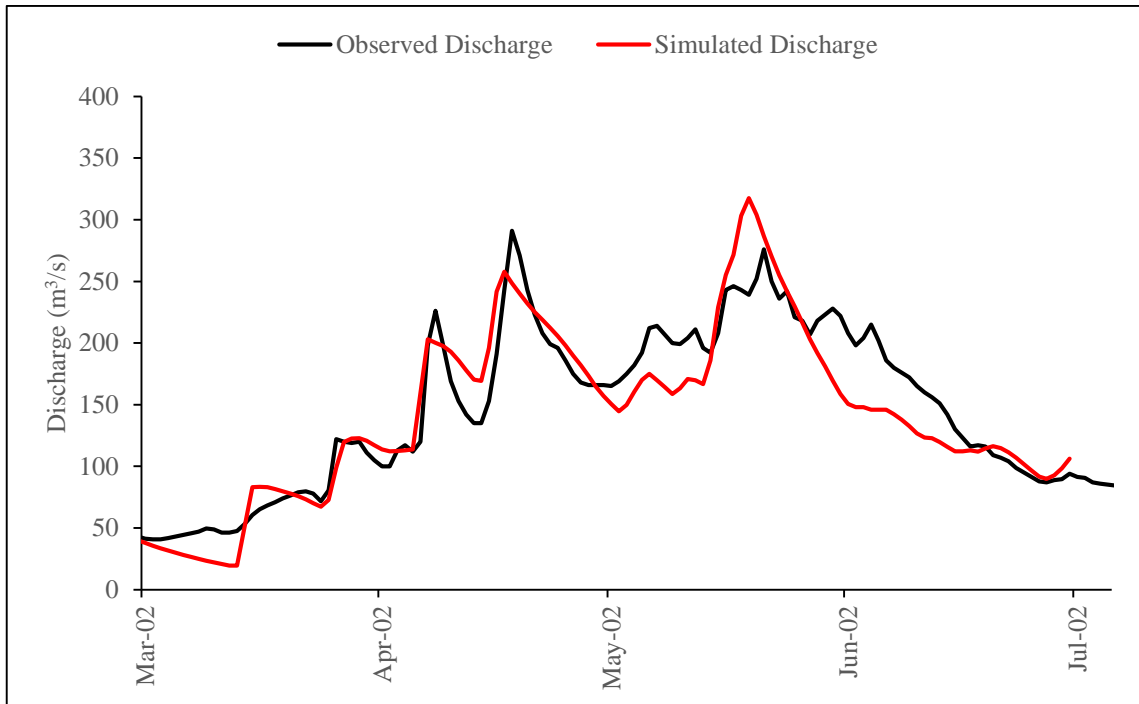


**Figure 5.1.** Event based simulation of 2002 snowmelt period.



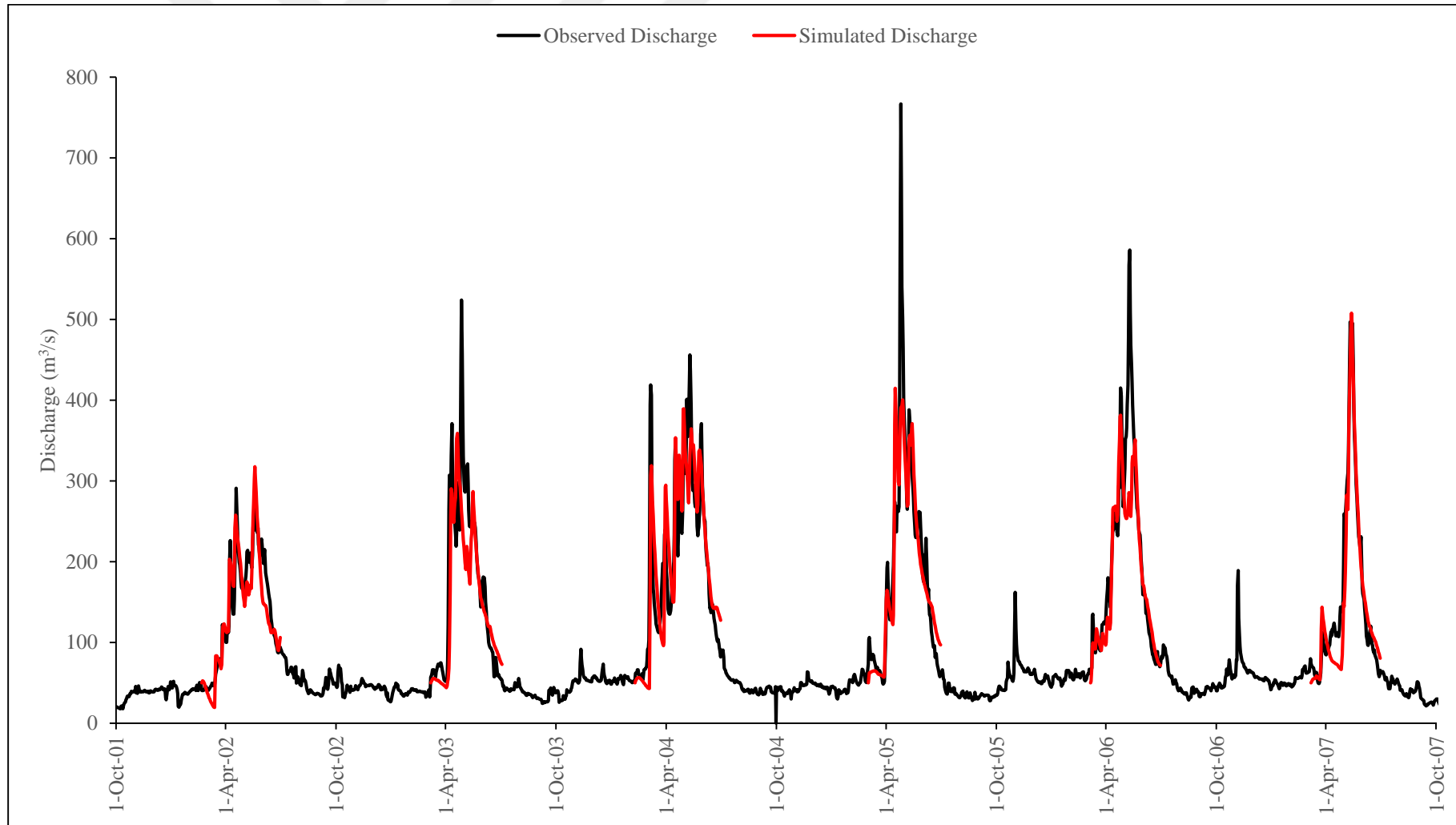


**Figure 5.2.** Observed and event based simulated hydrographs for Karasu Basin (2002 – 2007).

#### 5.1.4. Transform parameter estimation

Clark unit hydrograph employs two parameters to transform excess precipitation to direct runoff. The time of concentration (hr) defines the time required for water to flow from the furthest point in a watershed to the outlet of the watershed. Storage coefficient (hr) is used to account for the storage effects.

In regard to the topographic analysis, several equations can be used to calculate time of concentration ( $T_c$ ). From the calculations  $T_c$  is determined to be in between 12 - 18 hours. However, because of the large watershed area it is observed that this parameter is not very sensitive on the results. The storage coefficient is determined based on the trial and error procedure. The parameter values are shown in Table 5.12.

**Table 5.12.** Clark unit hydrograph parameter set for Karasu Basin.

Parameters	Range
Time of Concentration (hr)	12
Storage Coefficient (hr)	250

## 5.2. Model Results

In this section the results obtained through the calibration and validation are provided with graphical representations and statistical scores. The results are discussed in three headings as, discharge, snow water equivalent and soil moisture.

### 5.2.1. Discharge

Accuracy in modeling streamflow discharges is essential to various hydrologic applications including design of hydraulic structures, flood simulation, forecasting and optimal operation of water resources. HEC-HMS, as a rainfall/snowmelt-runoff model is used to simulate and forecast Karasu Basin streamflow applying the estimated parameters. Two continuous simulation approaches are utilized as conventional simulation and start-state simulation, where conventional (or former) simulation indicates lumped period application with one method of solution for baseflow, transformation, infiltration etc. and the start-state (or later) simulation indicates multi period implementation with various methods.

The total period (2002 – 2015) is divided into two seven year periods for calibration and validation according to the previous experience on other model applications where the split showed the best performance in this basin. The model calibration is carried out for the first period (2002 – 2008) and the validation is done in the subsequent period (2009 – 2015).

The amount and form (rainfall or snow) of precipitation is significant to modeling discharge. Being a snow-dominated watershed, snowmelt contributes approximately 60-70 % of Karasu Basin's runoff volume during spring and early summer months. HEC-HMS employs the loss, transform, baseflow and temperature index components to simulate the discharge. However this provides a large set of input parameters that require calibration which makes it a complex modeling procedure. The snowmelt period (01 March – 01 July) was therefore selected to be modeled first due its high contribution to the discharge as explained in section 5.1.3. Then continuous model application is carried out in yearly basis.

Following the consistent snowmelt calibration, the conventional modeling approach is employed for the whole year discharge simulations. The use of the initial SWE is eliminated as the conventional approach covered the snowfall, snowmelt and summer periods. As shown in Figure 5.3 only for the year 2002, the conventional method even though resulted in high consistency while modeling high flows resulting from snowmelt, the model presents unsatisfactory performance during low flows. The conventional simulation yielded NSE of 0.755 and RMSE of 31.59 m<sup>3</sup>/s for 2002 (Table 5.13).

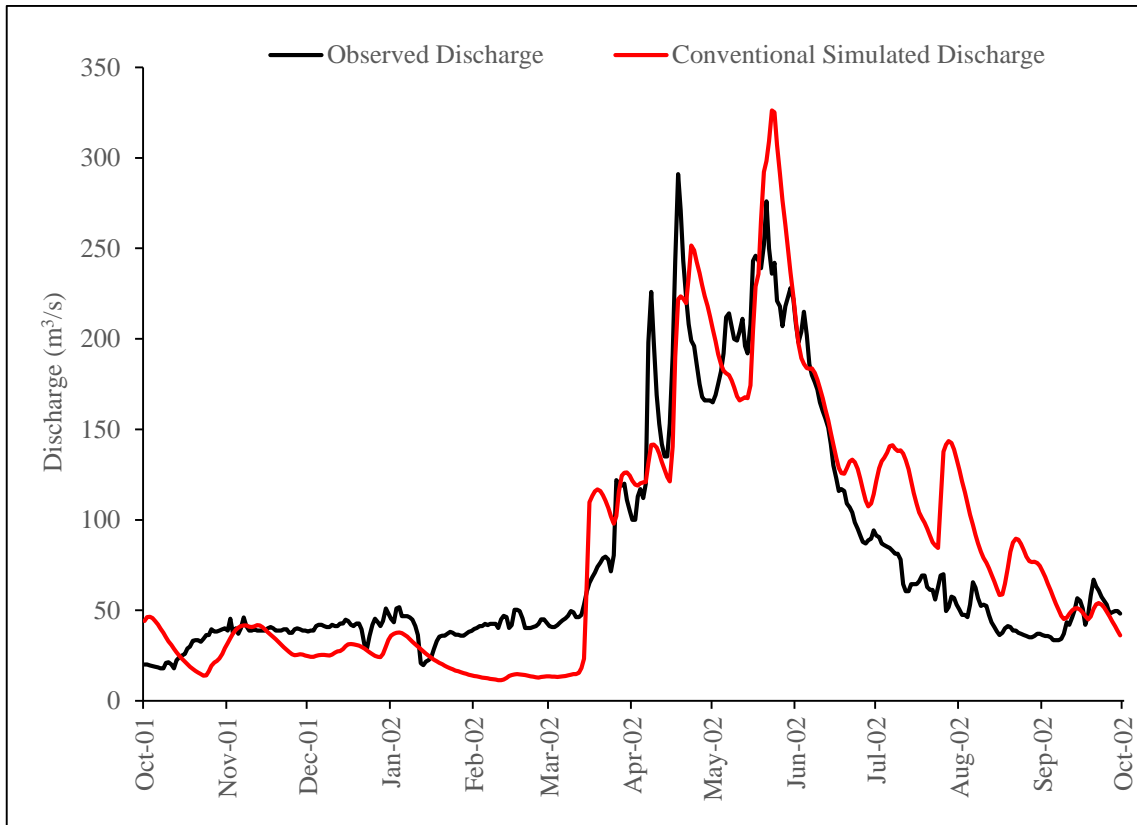


**Figure 5.3.** Observed and conventional simulated hydrographs for Karasu Basin, 2002.

To improve the low flow consistency, the start-state modeling option of the model is utilized. The start-state allowed to use different methods for different periods. The model state conditions (Soil moisture, SWE, etc.) are stored at the end of each simulation period and applied as initial values in a subsequent simulation period (Figure 5.4.). This permits the use of several parameter sets while running a continuous simulation. Due to the relatively constant observed low flows in Karasu Basin, only the baseflow parameter set is adjusted seasonally using constant monthly method instead of linear reservoir method in this study (Section 5.1.2). The conventional simulation yielded NSE of 0.895 and RMSE of  $19.87 \text{ m}^3/\text{s}$  for 2002 (Table 5.13). The application results are available in appendices for the rest of the calibration and validation periods.

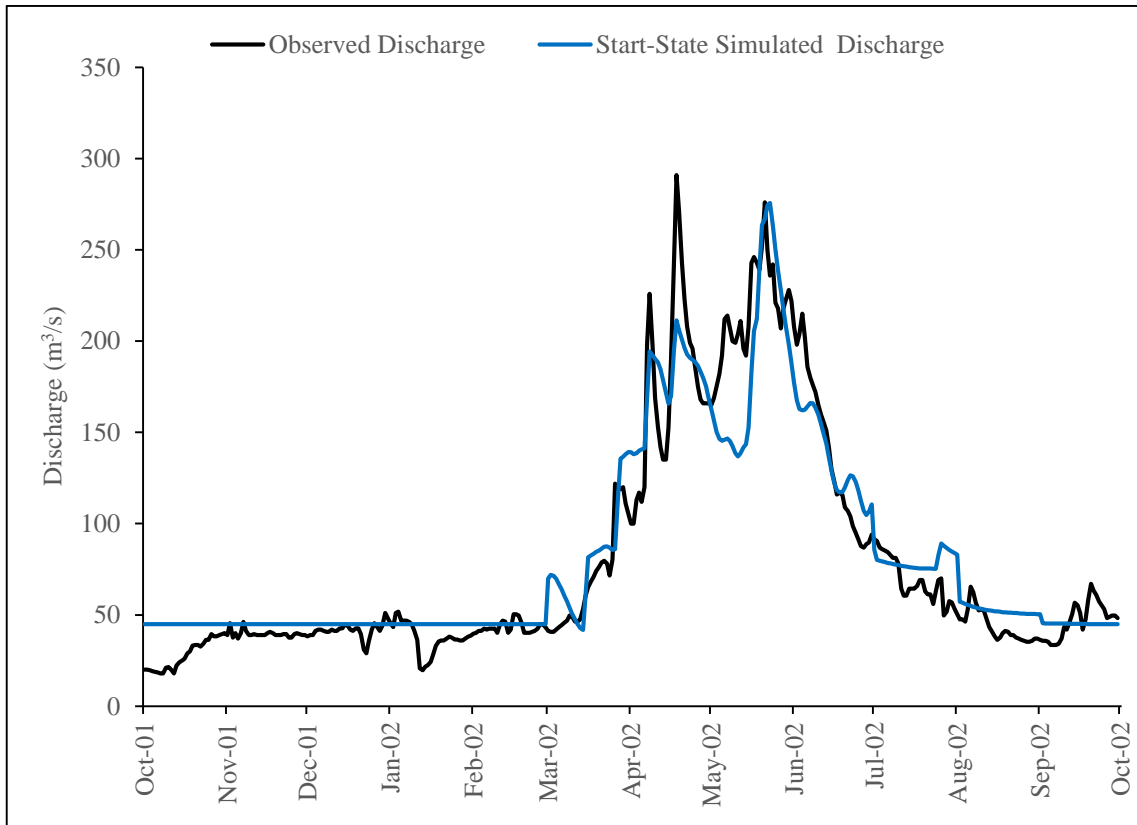


**Figure 5.4.** *Observed and start-state simulated hydrographs for Karasu Basin, 2002.*

The conventional and start-state modelling approaches are applied to both the calibration and validation periods. Validation is the measure of the calibrated parameter set reliability and accuracy. As it can be seen from Figures 5.5 and 5.6, a significant increase in the model performance can be observed in the application of start-state hydrologic modeling which is higher than that of the conventional hydrologic modeling application. The hydrographs for the calibration and validation periods are presented in Figure 5.5 - 5.6 and Figure 5.7 - 5.8, respectively.

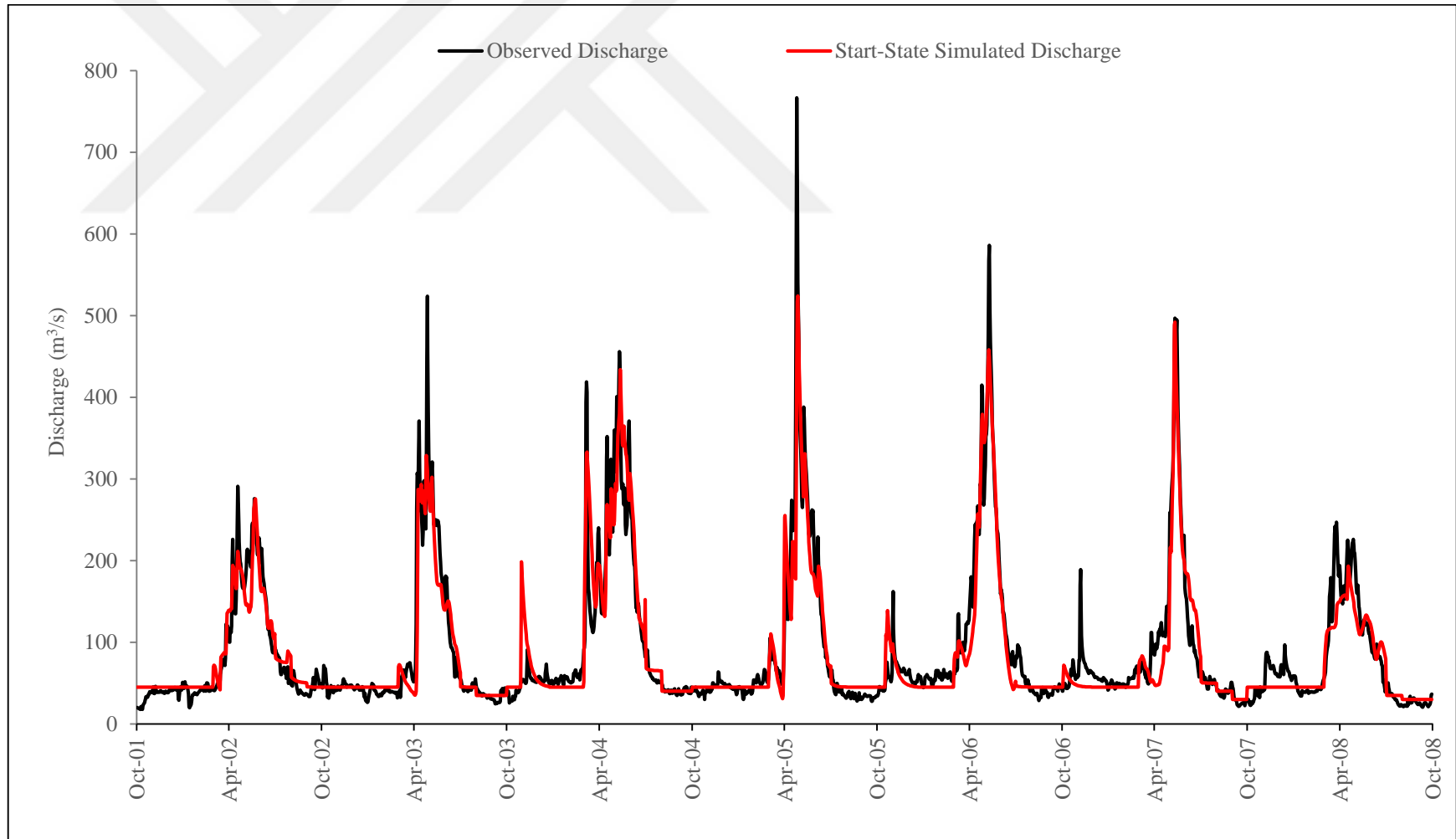


**Figure 5.5.** Observed and Start-State simulated hydrographs for Karasu Basin, calibration period.

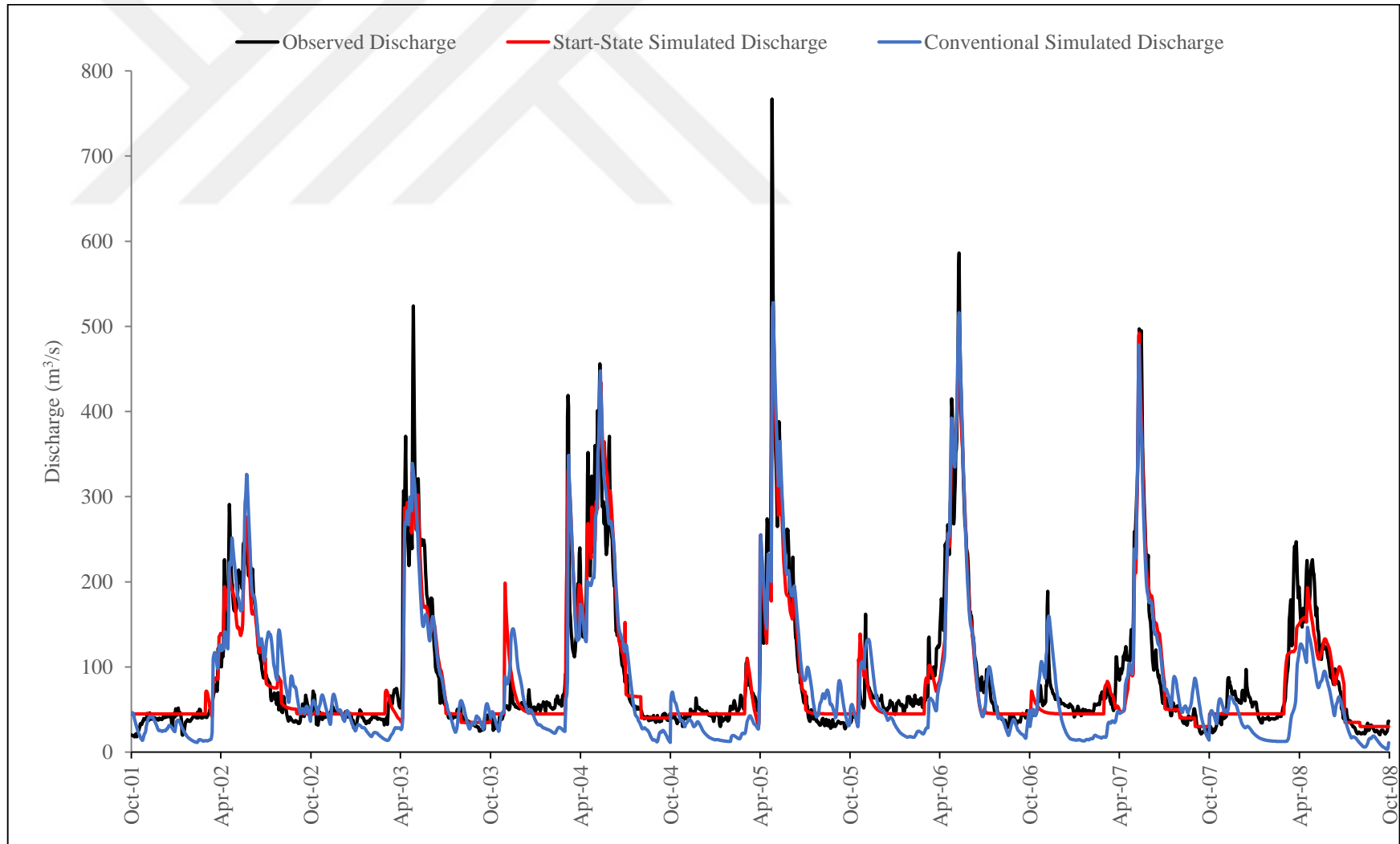


**Figure 5.6.** Observed, Start-State and Conventional simulated hydrographs for Karasu Basin, calibration period.

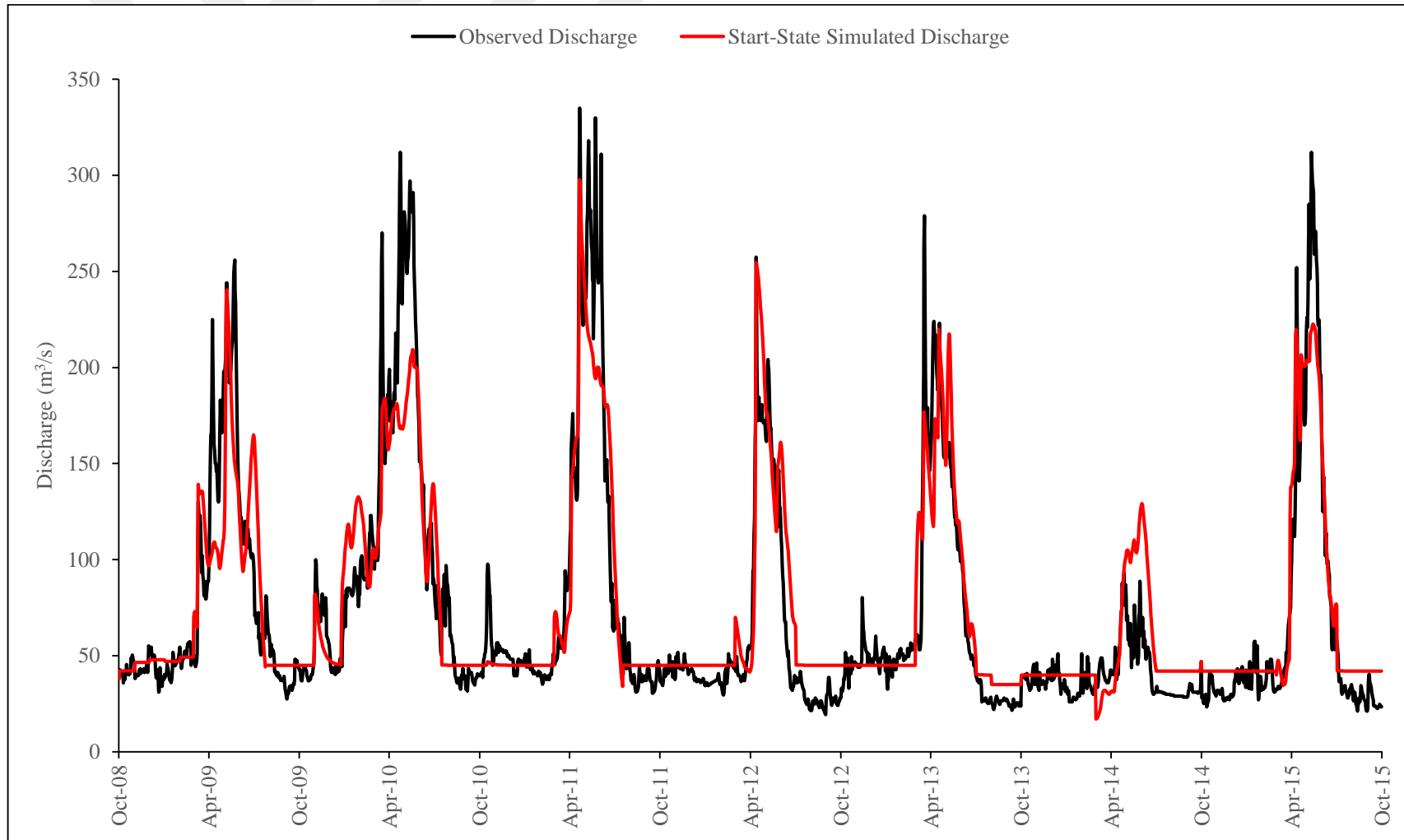


**Figure 5.7.** Observed and Start-State simulated hydrograph for Karasu Basin, validation period.



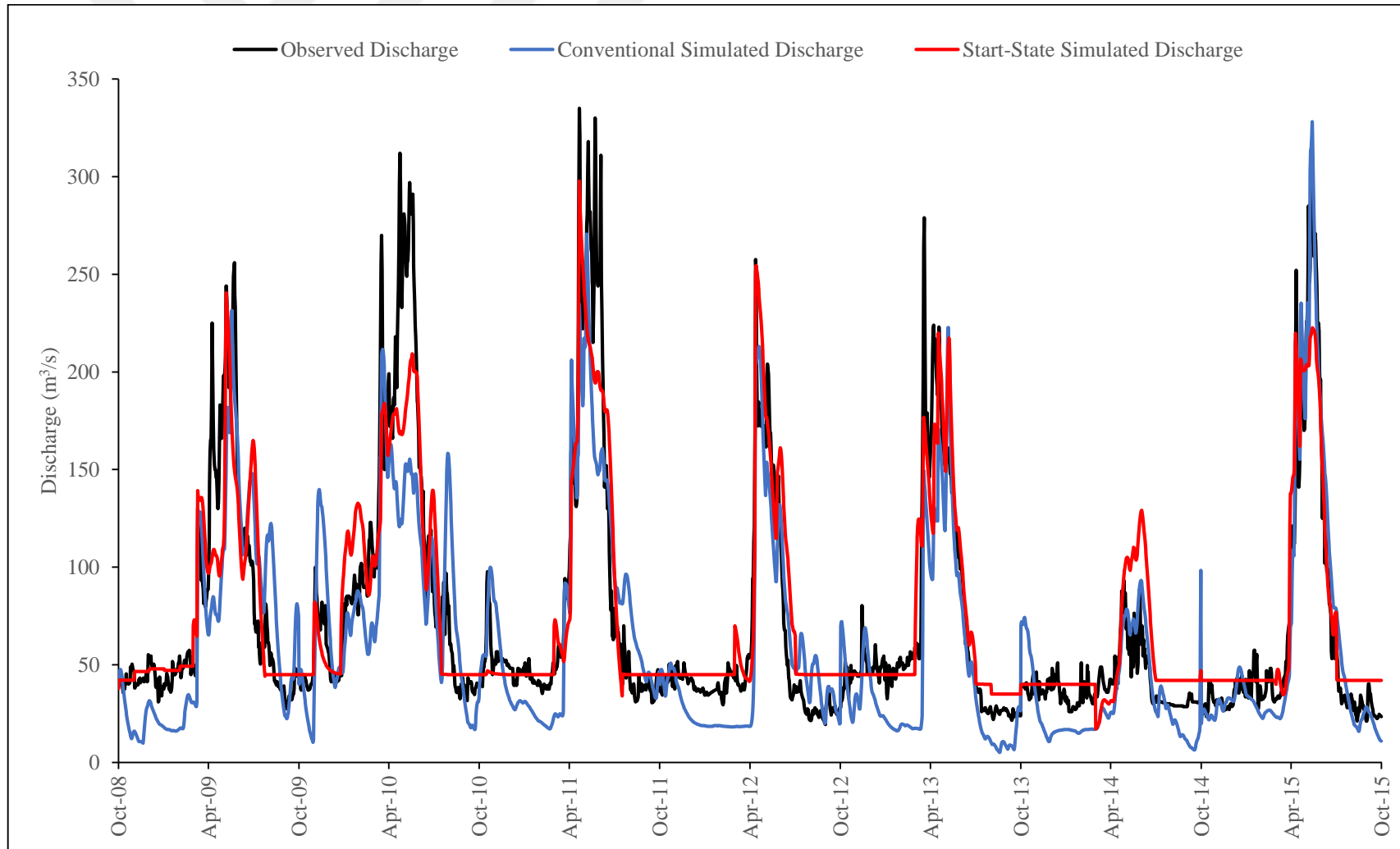


**Figure 5.8.** Observed, Start-State and Conventional simulated hydrograph for Karasu Basin, validation period.

**Table 5.13.** *Model performance assessment for Karasu Basin.*

Year	Conventional Simulation				Start-State Simulation			
	NSE	RMSE (m <sup>3</sup> /s)	% Peak	% Volume	NSE	RMSE (m <sup>3</sup> /s)	% Peak Error	% Volume Error
2002	0.76	31.59	-14.5	-5.1	0.90	19.87	27.4	-0.4
2003	0.85	33.36	35.9	25.4	0.89	29.47	54.4	0.6
2004	0.78	45.93	1.8	8.7	0.84	38.40	4.8	-5.6
2005	0.85	40.93	31.2	3.9	0.88	35.59	31.6	-0.4
2006	0.90	31.01	11.9	12.0	0.93	26.01	21.8	-0.1
2007	0.83	33.71	3.7	7.5	0.89	27.59	1.6	4.6
2008	0.32	46.65	48.9	30.2	0.76	25.56	36.4	11.5
2009	0.55	37.03	9.6	-24.1	0.64	29.40	7.9	3.0
2010	0.50	50.88	51.5	-20.7	0.75	34.49	33.5	3.0
2011	0.77	36.97	29.9	9.4	0.89	27.30	11.1	-0.7
2012	0.78	22.19	17.7	-28.0	0.74	22.14	1.2	-17.2
2013	0.64	32.76	42.9	12.2	0.80	21.66	36.6	7.3
2014	-0.93	18.06	16.1	-1.1	-1.96	20.96	-11.4	-38.1
2015	0.95	16.12	25.5	-22.1	0.92	20.07	28.8	-13.4
Calibration	0.81	38.12			0.88	29.52		
Validation	0.67	32.68			0.82	25.65		

As it can be observed from Figure 5.5 to 5.8 and Table 3.5, the calibration period (2002-2008) has the high observed average precipitation of 711.3 mm and high average discharges of 32.5 m<sup>3</sup>/s. On the other hand, the validation period (2009-2015) has relatively lower observed average precipitation and average discharge of 480.5 mm and 26.4 m<sup>3</sup>/s, respectively.

The model performance presented in Table 5.13 shows an improvement in the Nash Sutcliffe Efficiency (NSE) and Root Mean Square Error (RMSE) for both the calibration (0.81 to 0.88, 38.1 to 29.5 m<sup>3</sup>/s) and validation (0.67 to 0.82, 32.7 to 25.7 m<sup>3</sup>/s) periods, with the utilization of the start-state modeling approach.

Despite having high observed precipitation, 2008 experienced an early rapid snowmelt because of rainfall on snowmelt effect with an observed high rainfall (505 mm) and low snowfall (211.7 mm). This resulted in a rather poor modeling performance of 0.32 NSE and 46.7 m<sup>3</sup>/s RMSE for conventional simulations and 0.764 NSE and 35.6 m<sup>3</sup>/s RMSE for start-state simulation.

The 2014 water year experienced significantly low flows and it can be seen in the poor NSE of -0.93 for conventional and -1.94 for start-state simulations. 2014 water year experienced the lowest total precipitation for all the model years with 243.83 mm which is below the average precipitation of 595.86 mm for the period. Therefore 2014 is classified as a dry water year and low flow outlier.

The comparison of the observed and simulated peak discharges, the observed and simulated volumes are also employed to assess the model performance, the best consistency being 0%. The peak discharges in Karasu Basin occur on average between the end of April and early May. The conventional simulation resulted in relatively high peak consistency for the calibration period but relatively poor consistency during the validation period. Start-state simulation on the other hand showed high volume consistency for the whole simulation period and relatively high peak consistency for the validation period as can be seen in Table 5.13.

From the application of both the conventional and start-state simulations on the Karasu Basin, it can be observed that the conventional simulation has a high peak consistency for the years with high total precipitation. On the other hand, the start-state simulation is determined to have the high volume consistency for years with high and low

precipitation, also high peak consistency for years with low precipitation. The start-state application therefore can be preferred for the overall study period.

### 5.2.2. Snow water equivalent

The improved accuracy of modeling and forecasting in snow dominated watersheds is significant for flood control and water resources management. Snow Water Equivalent (SWE) and Snow Covered Area (SCA) are very important variables in snowmelt modeling. SWE refers to the widely used method of measuring the snowpack's water content. HEC-HMS calculates basin's average SWE and provides the results in times-series format.

Since it is difficult to provide continuous time series of SWE measurements in such a data scarce region, to check the consistency of the simulated SWE, the comparisons are made with the SCA in the sense of contingency detection. The SCA is derived using satellite snow products and presented as a percentage value on a snow depletion curve. Even though the model SWE and SCA are of different dimensions, the comparison can be done because both are concurrent variables in existence. The satellite SCA and start-state simulated SWE are presented in Figure 5.9.

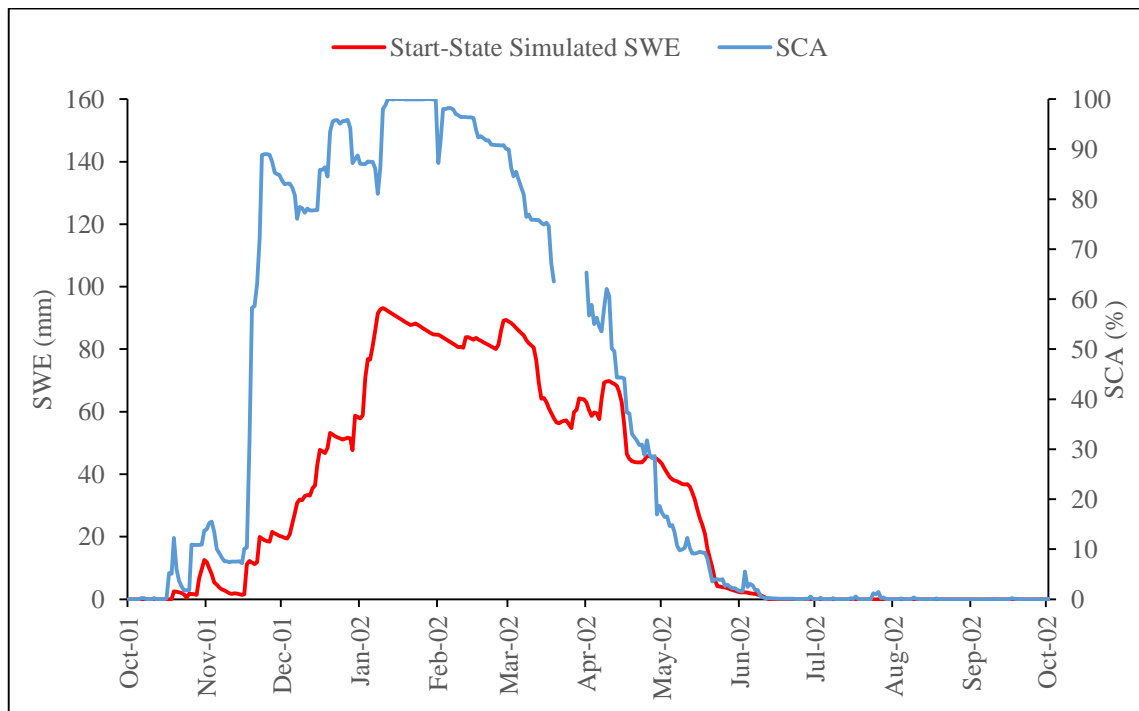


**Figure 5.9.** Snow Depletion Curve and Start-State simulated SWE for Karasu Basin, 2002.

The consistency of the SWE and SCA is assessed by a contingency analysis with four criteria when both SWE and SCA are present in the basin, both absent and one is present in the absence of the other for the calibration and validation periods (Table 5.14). The assessment showed consistent results between the simulated SWE and the satellite SCA. The time series of simulated snowfall and snowmelt periods are analyzed using SCA data of MODIS. Two thresholds are used to account for snow in satellite data as SCA is greater than zero or 3% (to minimize the effect of patchy or shallow snow conditions).

The results can also be observed from Figure 5.10 and 5.11 for the calibration period and Figure 5.12 and 5.13 for the validation period. There is a high consistency in the trends of SWE and SCA. The results were therefore considered to be satisfactory.

**Table 5.14 (a).** *The consistency analysis of simulated SWE and satellite derived SCA (>0) for Karasu Basin.*

SCA (%)	SWE (mm)	Number of days in Calibration	Consistency (%) in Calibration	Number of days in Validation	Consistency (%) in Validation
>0	>0	1538	60	1601	63
>0	0	511	20	484	19
0	>0	2	0	2	0
0	0	492	19	468	18
<b>Total</b>		2543	79	2555	81

**Table 5.14 (b).** *The consistency analysis of simulated SWE and satellite derived SCA (>3) for Karasu Basin.*

SCA (%)	SWE (mm)	Number of days in Calibration	Consistency (%) in Calibration	Number of days in Validation	Consistency (%) in Validation
>3	>0	1409	55	1334	52
>3	0	33	1	12	0
0	>0	131	5	269	11
0	0	970	38	940	37
<b>Total</b>		2543	94	2555	89

Accuracy (AC) has a range of 0 to 1 with one being the perfect score, it shows the fraction correct forecasts (Equation 5.5). Bias score (BIAS) has a perfect score of 1, it shows the comparison of the observed ‘yes’ events and the forecasted ‘yes’ events

(Equation 5.6). False alarm ratio (FAR) has a range of 0 to 1 and a perfect score of 0, it shows the fraction of forecasted ‘yes’ events that did not occur (Equation 5.7). Success ratio (SR) has a range of 0 to 1 and a perfect score of 1, it shows the fraction of ‘yes’ events correctly observed (Equation 5.8). The contingency results are shown in Table 5.15 and 5.16.

$$AC = \frac{\text{hits} + \text{correct negatives}}{\text{total}} \quad (5.5)$$

$$BIAS = \frac{\text{hits} + \text{false alarms}}{\text{hits} + \text{misses}} \quad (5.6)$$

$$FAR = \frac{\text{false alarms}}{\text{hits} + \text{false alarms}} \quad (5.7)$$

$$SR = \frac{\text{hits}}{\text{hits} + \text{false alarms}} \quad (5.8)$$

**Table 5.15 (a).** *Model performance for snow state.*

Calibration	Number of days		Observed		
			Yes	No	Total
Model	Yes		1538	2	1540
	No		511	492	1003
	Total		2049	494	2543
Validation			Yes	No	Total
	Model	Yes	1601	2	1603
		No	484	468	952
		Total	2085	470	2555

**Table 5.16 (b).** *Model performance for snow state.*

	Calibration		Validation	
SCA (%)	>0	>3	>0	>3
Accuracy	0.80	0.94	0.81	0.89
Bias score	0.75	1.07	0.77	1.19
False Alarm Ratio	0.00	0.09	0.00	0.17
Success ratio	1.00	0.91	1.00	0.83

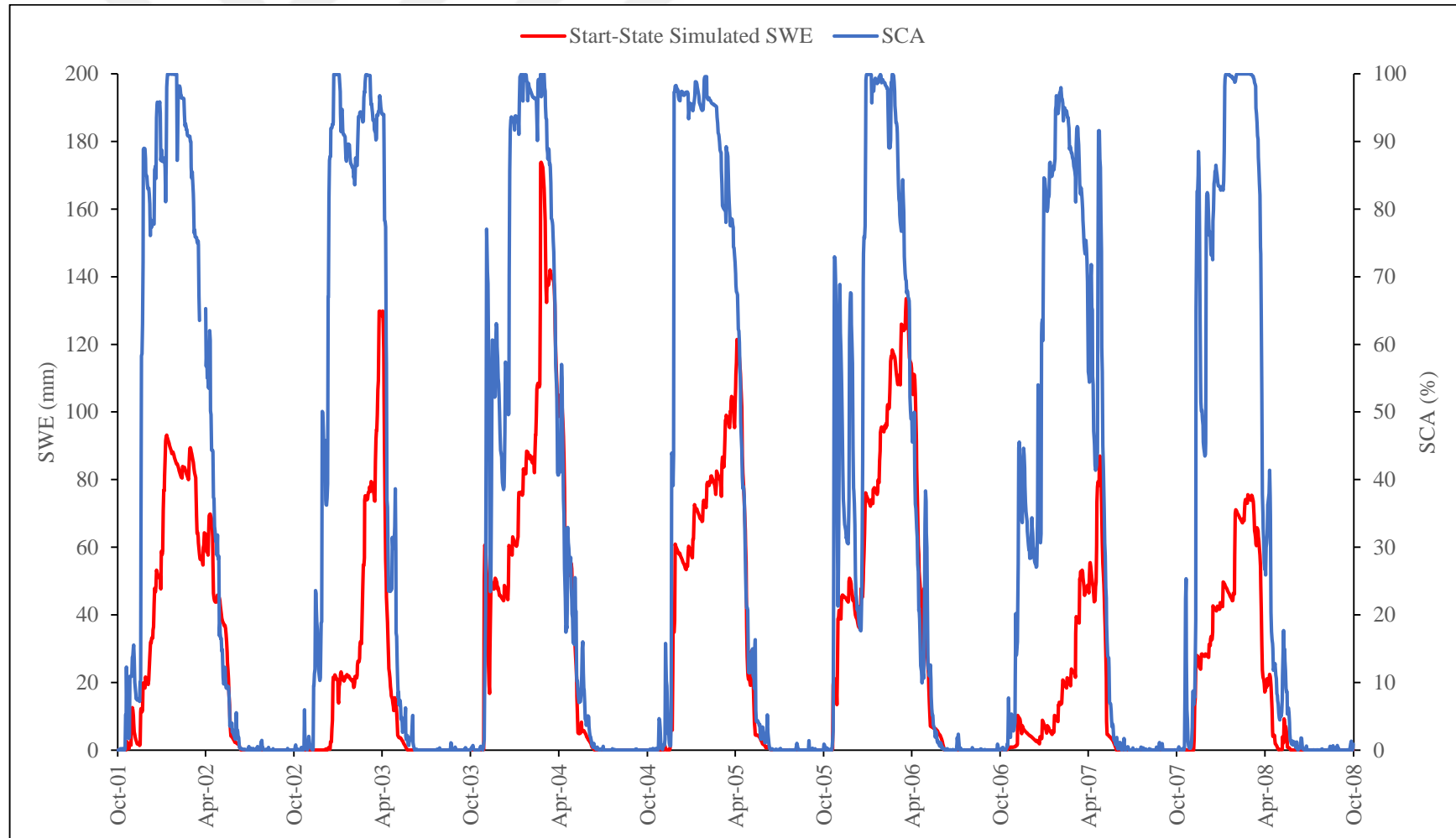


**Figure 5.10.** Start-State simulated SWE and Snow Depletion Curve for Karasu Basin, calibration period.

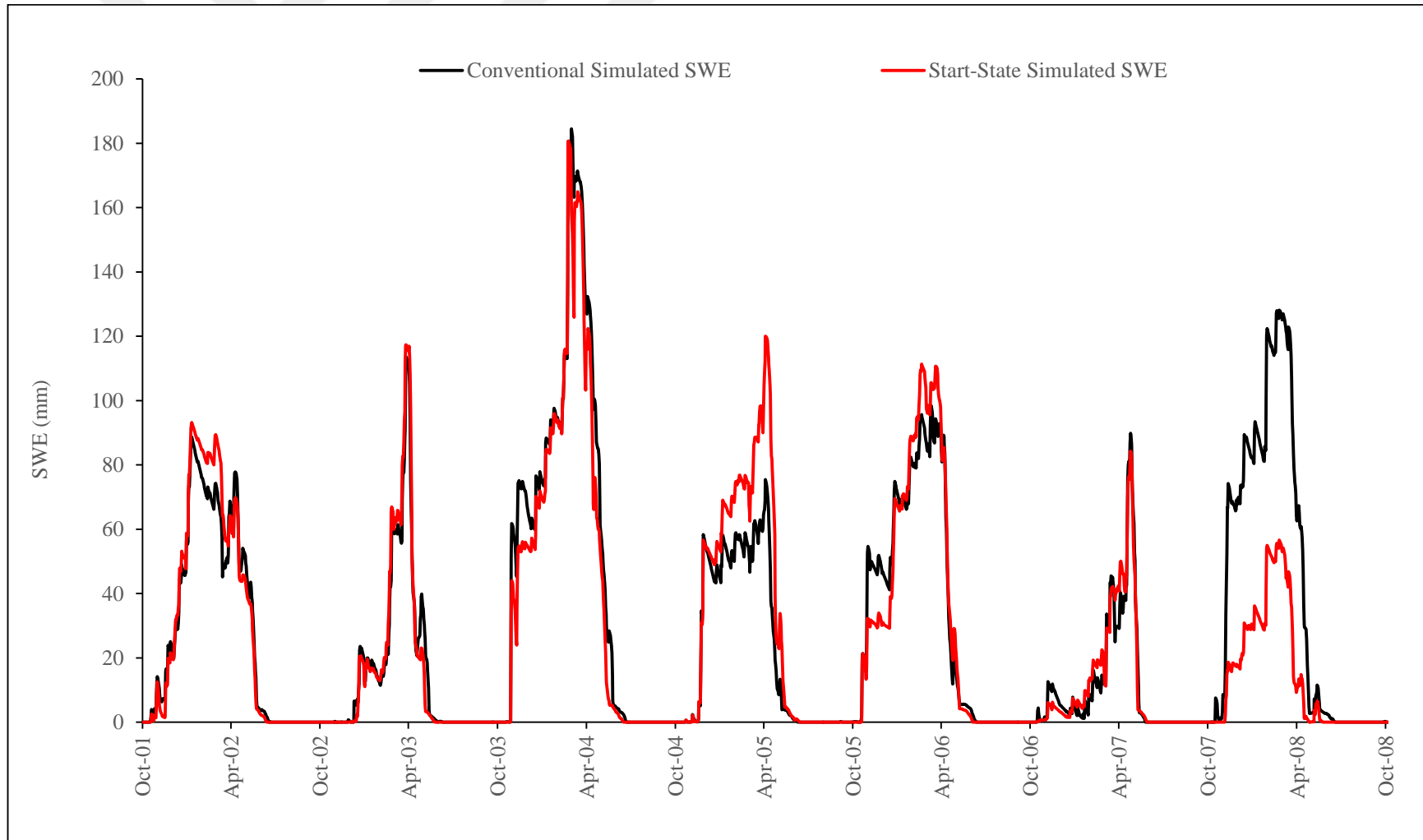


**Figure 5.11.** Conventional and Start-State simulated SWE for Karasu Basin, calibration period.



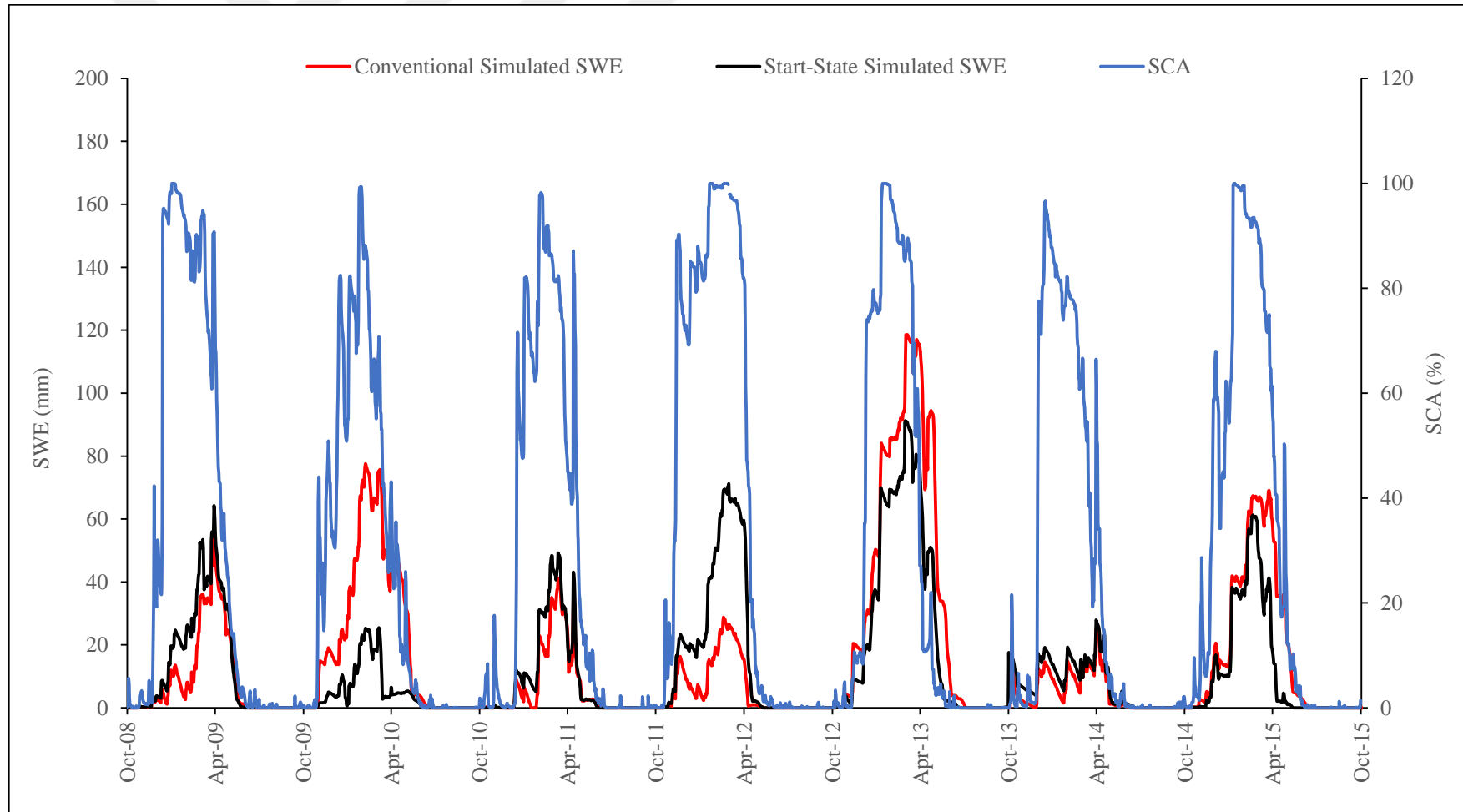


**Figure 5.12.** Start-State simulated SWE and Snow Depletion Curve for Karasu Basin, validation period.

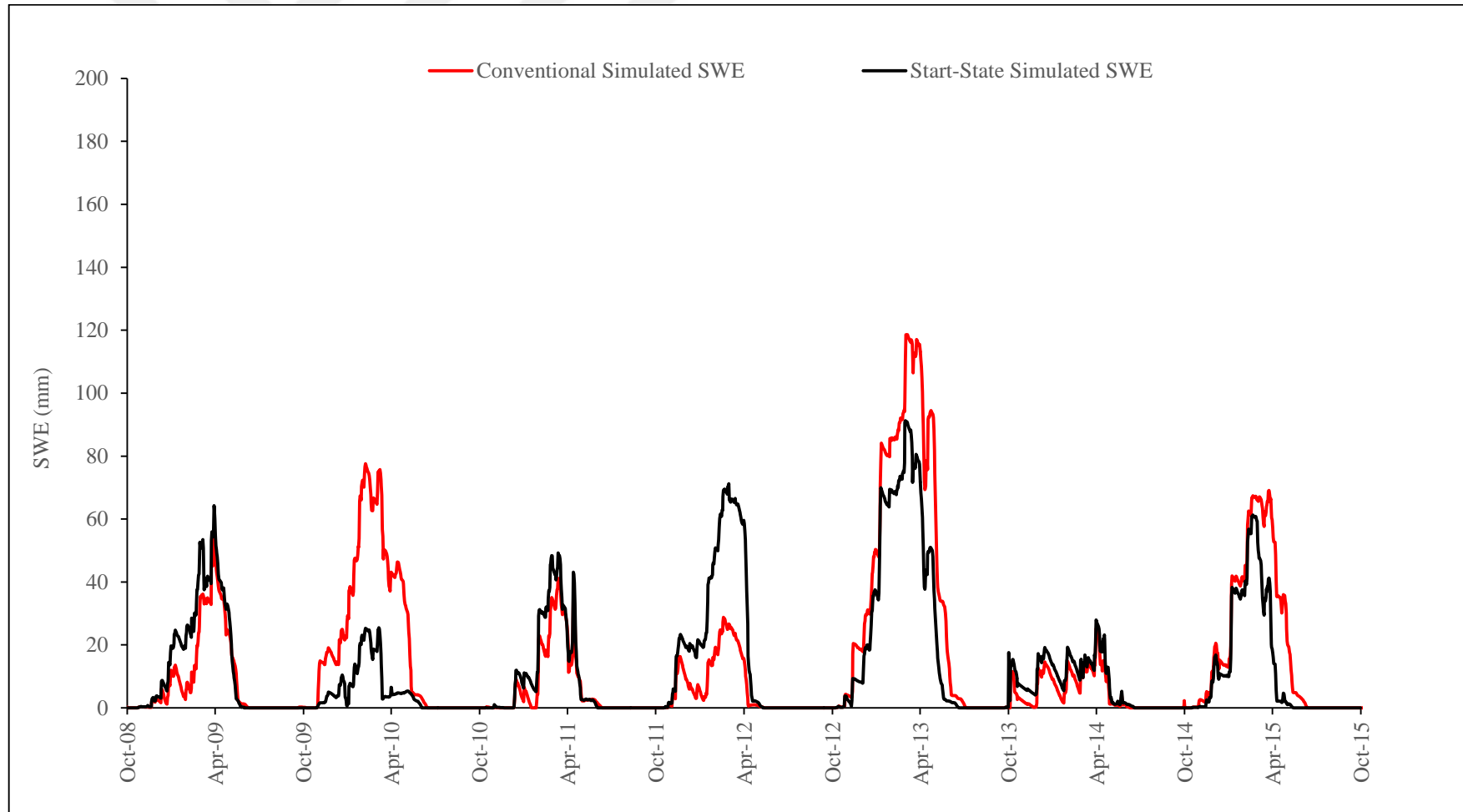


**Figure 5.13.** Conventional and Start-State simulated SWE for Karasu Basin, validation period.

### 5.2.3. Soil moisture

The Soil Moisture (SM) represents the amount of water in the soil at a particular time. In continuous model simulations, soil moisture is particularly important because it differentiates the dry and wet periods. Dry periods show the periods with very little to no soil moisture, these periods result in high precipitation losses and less surface runoff in a storm event. Wet periods represent the periods with soil moisture, these periods result in less precipitation losses and more surface runoff in a storm event. Therefore, the soil moisture is important to understand the dynamics of precipitation losses and surface runoff formation. HEC-HMS calculates the SM and it provides the results in time-series format.

In this study, satellite soil moisture product (H14) of HSAF project is used to evaluate the consistency of the HEC-HMS (Start-State) simulated soil moisture results for the period of 2013 – 2015. The H-SAF H14 satellite product determines the soil moisture in four depth-layers, Layer 1 (0-7 cm), Layer 2 (7-21 cm), Layer 3 (21-72 cm) and Layer 4 (100-189 cm). The results are provided as relative soil moisture values in between 0-1. On the other hand, HEC-HMS does not apply the depth-layer to calculate the soil moisture but provides the result as soil storage, Groundwater 1 and Groundwater 2 storage.

The weighted average is applied to determine the overall average soil moisture both for the satellite product and HEC-HMS simulation results in each day for the whole basin. Then, a normalization (Equation 5.9) is performed in order to make the comparisons in the same scale in a consistency analysis. Several trials are undertaken to determine the combinations of weight coefficients to establish the best representative regression between the observed and modelled soil moisture values. Due to inconsistencies in satellite soil moisture data during snow cover, masking is employed to eliminate the snow covered periods from the time series analysis by establishing a threshold of the snow covered area percentage (SCA). Four thresholds are tested for 1 %, 5 %, 10 % and 20 % and 5 % is selected for masking (Table 5.16).

$$x_{new} = \frac{x_i - x_{min}}{x_{max} - x_{min}} \quad (5.9)$$

**Table 5.16.** *Pearson R performance results for Karasu Basin.*

	<b>SCA Mask (%)</b>	<b>H-14 level weight coefficients</b>	<b>HMS layer weight coefficients</b>	<b>2013</b>	<b>2014</b>	<b>2015</b>
Model 1	>5	2,1,0,0	1,1,1	0.78	0.88	0.78
Model 2	>5	1,0,0,0	1,1,1	0.82	0.86	0.78
Model 3	>5	2,1,0,0	2,1,1	0.83	0.87	0.75
Model 4	>5	1,1,0,0	4,1,1	0.87	0.84	0.66
Model 5	>5	5,3,2,0	1,1,1	0.73	0.89	0.68
Model 6	<5	1,2,7,0	1,1,1	0.69	0.79	0.69
Model 7	>20	1,0,0,0	1,1,1	0.69	0.83	0.84
Model 8	>20	2,1,0,0	1,1,1	0.71	0.84	0.85

Several models are tested to account for different weight coefficients of satellite data and simulated soil layers. A summary of the analysis is given in Table 5.16. Model 6 includes the weights calculated in regard to the level depths for H14 product. The Model 2 determined to have satisfactory results with respect to all analysis years and is selected for the linear regression and consistency evaluation. The results are provided both as the series and linear regression graphs presented in Figure 5.14 to 5.19. As it can be observed from the graphs, the periods with snow are eliminated and the evaluated results demonstrated relatively high consistency between the normalized soil moisture of simulation (HEC-HMS) and observation (H14).

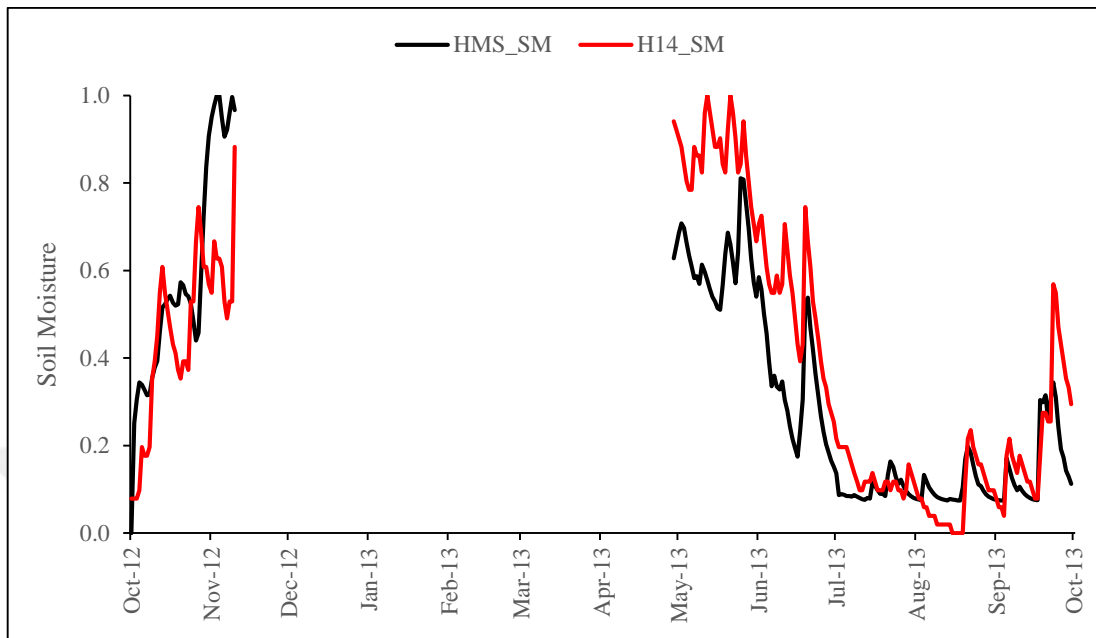


**Figure 5.14.** Simulated and satellite based soil moisture for Karasu Basin, 2013.

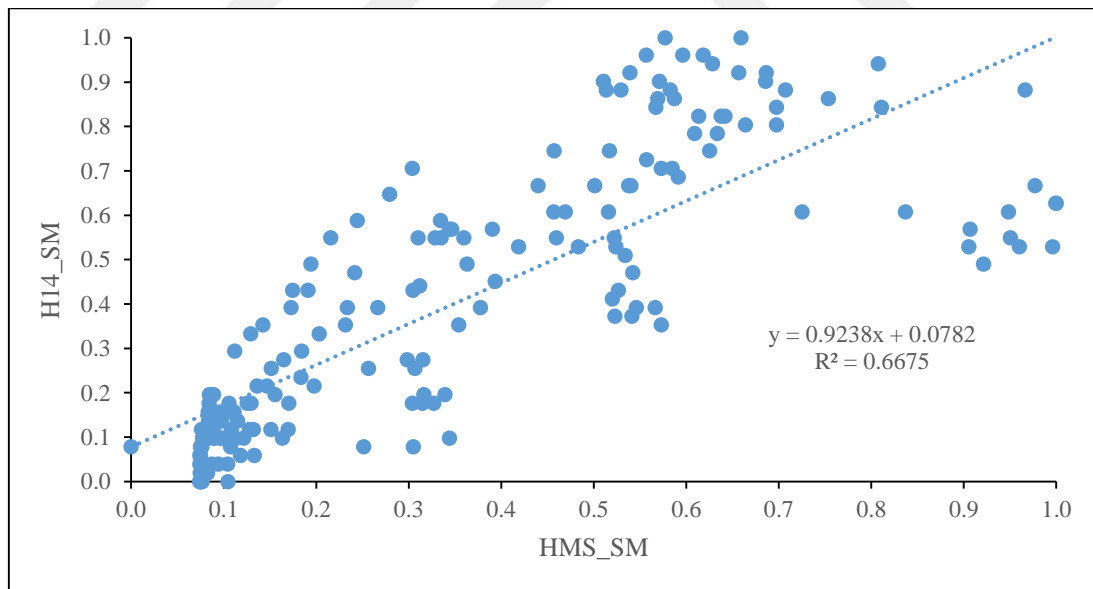


**Figure 5.15.** Linear regression of soil moisture for Karasu Basin, 2013.

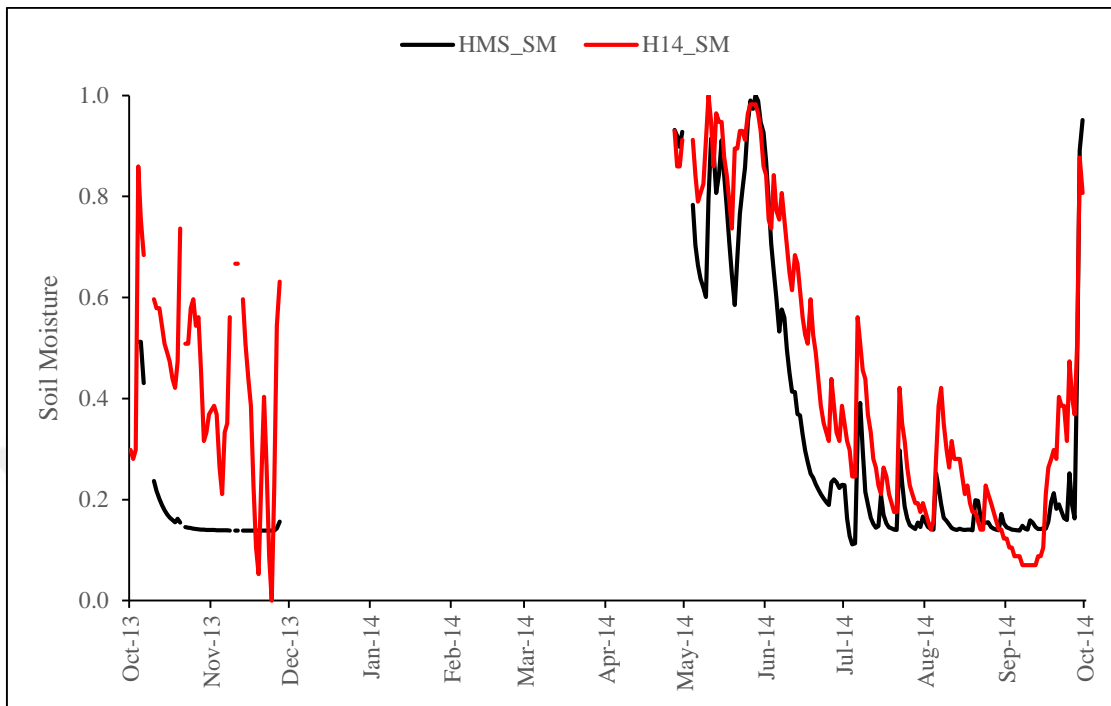


**Figure 5.16.** Simulated and satellite based soil moisture for Karasu Basin, 2014.

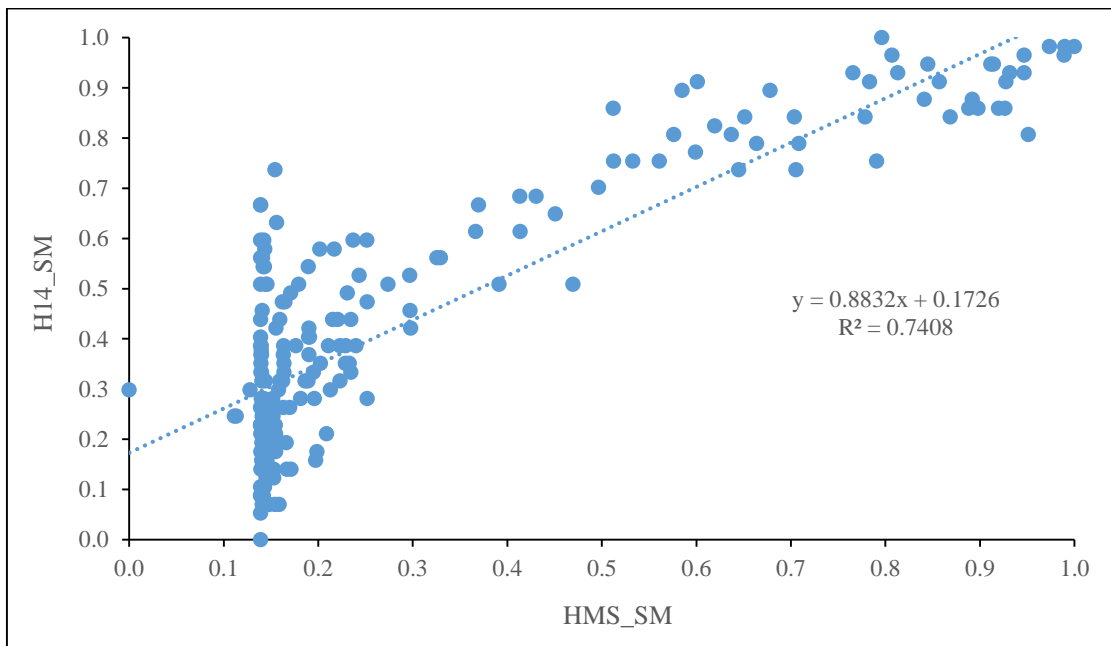


**Figure 5.17.** Linear regression of soil moisture for Karasu Basin, 2014 (Dry water year).

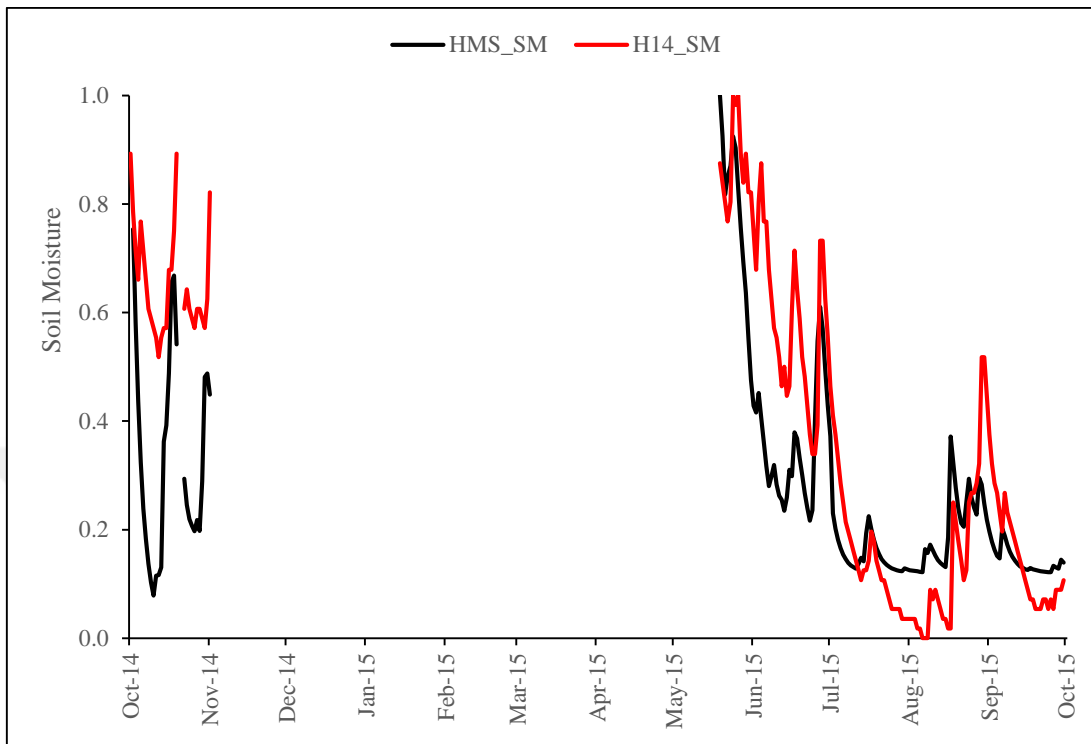


**Figure 5.18.** Simulated and satellite based soil moisture for Karasu Basin, 2015.

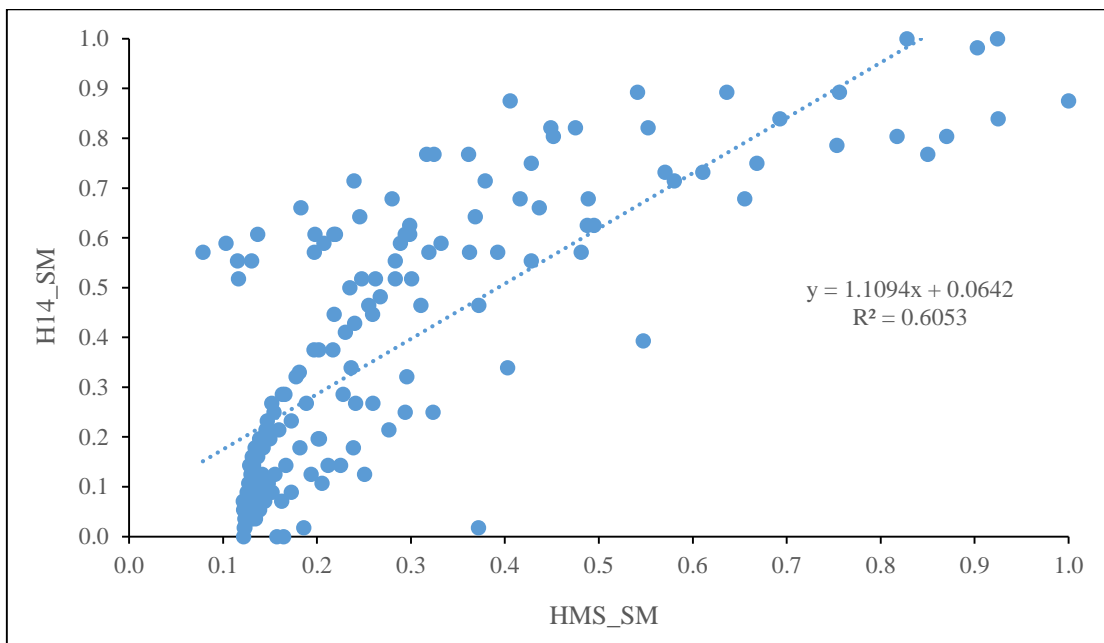


**Figure 5.19.** Linear regression of soil moisture for Karasu Basin, 2015.

### 5.3. Streamflow Forecasting

Deterministic streamflow forecasting is applied to Karasu Basin in this study. To perform streamflow forecasting for Karasu Basin, the HEC-HMS version 4.1 forecasting module is used. First the forecasting period is selected to be that of the snowmelt period because of its large contribution to the total streamflow. The forecast is run for the period starting 01 March to 01 July 2015. Two forecasting approaches are utilized with two different input data sets, the first approach is done using the observed precipitation and temperature data to forecast streamflow. The second approach is using the Numerical Weather Prediction data set. The forecasting is updated with three and five days from the Forecast date to the End date and the results compared in Figure 5.20. Table 5.17 shows the model performances of several forecast runs. The model simulation results and runoff forecasts with 3 and 5 days update using the forecast and observed data are presented. Also 5 days forecast without the application of corrections component is presented. The model performance is high both for the simulation and forecasting. NSE and RMSE shows a similar model performance for 3 or 5 days updated forecasting. On the other hand, corrections improve the model's ability to better forecast the runoff values.

**Table 5.17.** *Forecast model performance with different data sets.*

<b>Forecast Approach</b>	<b>NSE</b>	<b>RMSE (m<sup>3</sup>/s)</b>
5 Days with Observed Data	0.943	19.92
5 Days with Forecast Data	0.933	21.35
5 Days without Corrections	0.774	39.34
3 Days with Observed Data	0.944	19.60
3 Days with Forecast Data	0.938	20.64
Simulated Flow	0.918	23.73



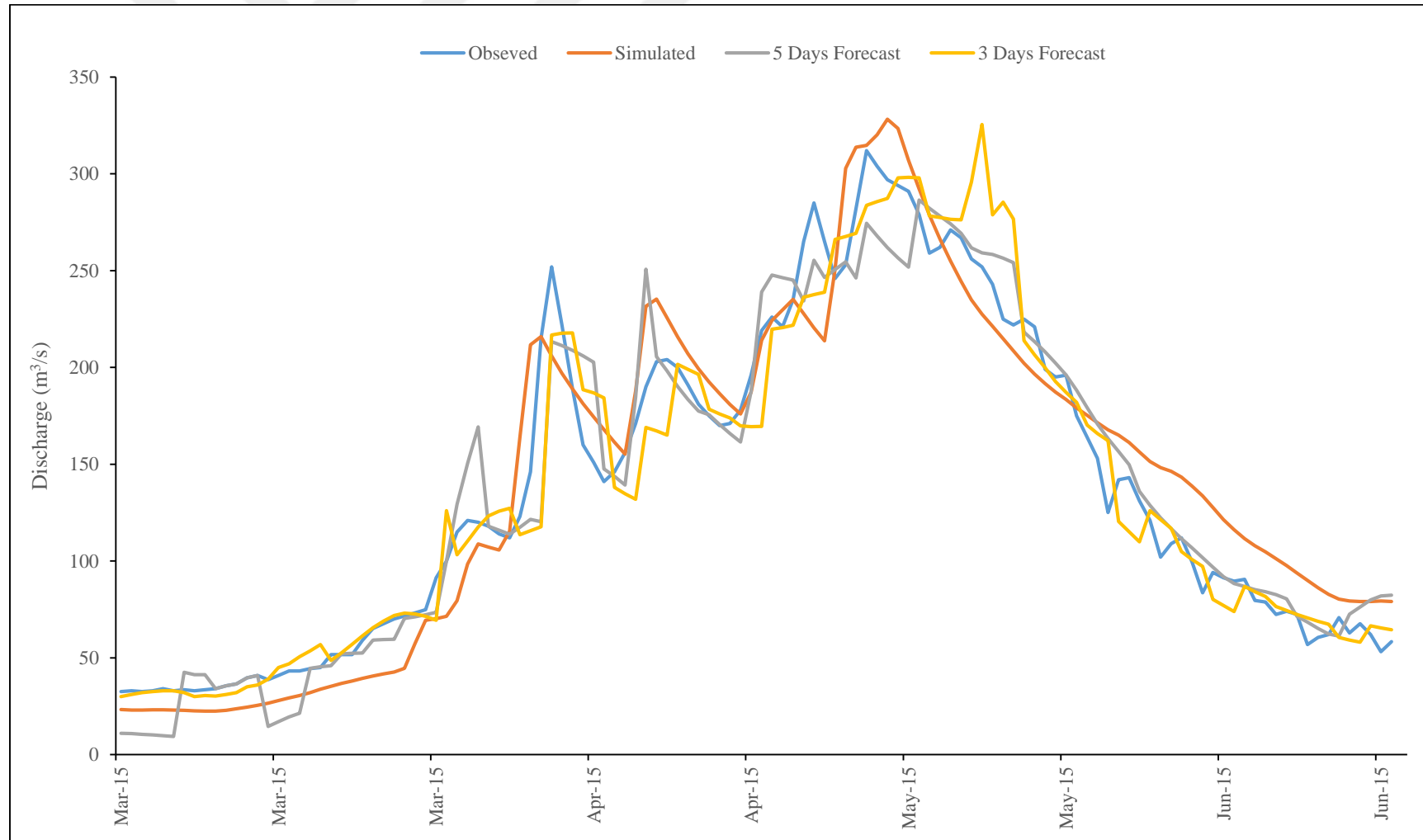


**Figure 5.20.** Runoff forecasting with observed and Numerical Weather Prediction data for Karasu Basin, 2015.

## 6. CONCLUSION AND RECOMMENDATIONS

Accurate snowmelt modeling in snow dominated mountainous watersheds is crucial to streamflow forecasting. Streamflow forecasting applied through hydrological models is important not only for estimating future streamflow conditions but also water resources management and early flood warning systems. Snowmelt modeling is particularly important for the Karasu Basin as it contributes the majority (60 – 70 %) of the total discharge.

HEC-HMS is selected for hydrological model application. The model parameters are calibrated and validated, and then the model is employed to forecast streamflows in Karasu Basin. The continuous hydrologic modeling is carried out with soil moisture accounting and snow component through two different modeling approaches, as conventional and start-state.

Continuous hydrologic modeling with soil moisture accounting in HEC-HMS which is becoming more popular recently due to the developments in soil moisture monitoring, is implemented using daily total precipitation and daily average temperature values for the last fourteen years (2002-2015) as input to the model. The main advantage of a continuous hydrologic modeling is that it spans long time intervals accounting for both wet and dry periods. The modeling period is divided into calibration (2002-2008) and validation (2009-2015) parts. The streamflow forecasting is done for the 2015 water year snowmelt period (March-June).

Three modeling approaches are utilized to calibrate and validate the model parameters, event based and continuous modeling with conventional and start-state options. In each modeling approach, soil moisture accounting, Clark unit hydrograph and linear reservoir methods are employed to model the loss, transform and baseflow, respectively. The event based application is handled for the snowmelt period (01March-01July) using the observed Snow Water Equivalent (SWE) values as initial states.

The conventional approach specifies the lumped period application while the start-state approach defines the multi period application with different methods. To the best of our knowledge, this study is one of the first to apply HEC-HCMS Soil Moisture Accounting (SMA) method in Turkey using satellite data to evaluate the model performance in terms of internal states of snow water equivalent and soil moisture, and

also to use the numerical weather predictions data with the forecast component of HEC-HMS (Version 4.1).

The conventional hydrologic modeling is done for the complete water year (01 October - 30 September) as one period. The approach resulted in the Nash Sutcliffe Efficiency (NSE) and Root Mean Square Error (RMSE) of 0.81 and 38.12 m<sup>3</sup>/s for calibration and 0.67 and 32.68 m<sup>3</sup>/s for validation, respectively. The model showed high peak runoff consistency with the observed flows for the calibration but rather poor peak runoff consistency for the validation period. The assessment of the modeled runoff with the observed ones are inferior during low flow periods.

The continuous start-state hydrologic modeling approach is employed mainly to tackle the poor low flow consistencies and to improve the model performance. The approach utilizes the state conditions to ensure continuity between simulations. Only the baseflow method is changed, the linear reservoir and constant monthly methods are applied interchangeably. The approach showed an overall improved model performance with the NSE and RMSE of 0.88 and 29.52 m<sup>3</sup>/s for calibration, 0.82 and 25.65 m<sup>3</sup>/s for validation, respectively. In general, start-state hydrologic modeling approach presents better results than the conventional hydrologic modeling. One reason for these is that start-state improved the low flow consistency by implementing the constant monthly baseflow method, this improved the model performance on the volume consistency resulting in improved NSE.

The evaluation of the model state variables is done with the usage of satellite products. Validation of SWE as a state variable using the observed ground data is challenging due to the limited number of observations. The satellite snow covered area (SCA) is therefore used as it is a significant tool for monitoring snow extend over large areas. Since SWE is an output of HEC-HMS, the Moderate Resolution Imaging Spectroradiometer (MODIS) snow covered area is used to evaluate SWE consistency. The results showed that the SWE-SCA (hits and correct negatives are in total) accuracy is 94 % and 92 % for calibration and validation, respectively.

Evaluation of the simulated soil moisture consistency is done with Satellite Application Facility on Support to Operational Hydrology and Water Management (H-SAF) H14 root zone soil moisture index satellite product. The first evaluations indicates

that satellite based observations and modelled state results for soil moisture to have satisfactory Pearson  $R$  around 0.80-0.85.

The streamflow forecasting is applied for the period between March and June during 2015 water year using the Numerical Weather Prediction (NWP) data of Weather Research and Forecast (WRF) model. The WRF data is updated through the correlation between the observed and forecast temperature data for a bias correction and applied in the forecast module. According to the results, the forecasting produced a model NSE and RMSE performances of 0.92 and 22.66 m<sup>3</sup>/s, respectively.

In conclusion, this study demonstrates the application of continuous hydrologic modeling approaches with different methods to improve the runoff estimation performance in terms of NSE, RMSE, percent peak and volume errors. It also shows the implementation of the conventional hydrologic modeling approach to model the peak discharges and the start-state hydrologic modeling approach to model the low flows in order to improve the consistency of runoff.

This modeling study sets precedence over the other modeling approaches in the pilot basin since it includes SMA, also it implements different data sources to validate the results which is proven to be advantageous. Furthermore, the study is the first for HEC-HMS soil moisture and H14 root zone soil moisture index satellite product comparison.

The model can be further used for the distributed model applications with the use of gridded precipitation and temperature inputs as well as gridded parameter sets. Also the model can be used with canopy storage especially in watersheds with dense vegetation cover and broad leaves. The study also demonstrated that different modelling approaches have a positive impact on hydrological modeling and streamflow forecasting which can be applied for efficient management of water resources in a study area.

In situ soil moisture and snow measurements could improve on the soil moisture and SWE validations respectively. On the other hand, the assessment of simulated snow water equivalent by satellite observations would add value to this study. Using spatial coverage of satellite observations via data assimilation will improve runoff estimation ability of models.

## REFERENCES

- Abudu, S., King, J. P. & Bawazir A. S. (2011). *Forecasting Monthly Streamflow of Spring-Summer Runoff Season in Rio Grande Headwaters Basin Using Stochastic Hybrid Modeling Approach*. Journal of Hydrologic Engineering, 16(4): 384-390.
- Agrawal, A. (2005). *Prepro2004: A data model with pre-and-post processor for HEC-HMS*. Master of Science thesis. Texas A&M University.
- Akkol, B. (2016). *Improving runoff prediction by data assimilation in HBV hydrological model for upper Euphrates basin*. Master of Science thesis. Eskişehir: Anadolu University.
- Alverado, R., Schwanenberg, D., Krahe, P., Lisniak, D., Şensoy, A., Şorman, A. A., & Akkol, B. (2016). *Moving horizon estimation for assimilating H-SAF remote sensing data into the HBV hydrological model*. Advances in Water Resources, 92, 248-257.
- Anderson, E. (2006). *Snow accumulation and ablation model – SNOW-17*. National Weather Service (NWS), Silver Spring, MD.
- Anderson, M. L., Chen, Z.Q., Kavvas M. L., & Feldman, A. (2002). *Coupling HEC-HMS with Atmospheric Models for Prediction of Watershed Runoff*. Journal of Hydrologic Engineering, 7(4): 312-318.
- ASCE (2000). Task Committee on Application of Artificial Neural Networks in Hydrology. *Artificial neural networks in hydrology. I: preliminary concepts*. ASCE J Hydrol Eng 5(2):115–123
- Aytemiz, L., & Kodaman, T. (2006). *Sınıraşan Sular Kullanımı ve Türkiye-Suriye İlişkileri*. TMMOB Su Politikaları Kongresi, 21-23.
- Barnes, W. L., Pagano, T. S., & Salomonson, V. V. (1998), *Prelaunch characteristics on the moderate resolution imaging spectroradiometer (MODIS) on EOS-AM1*, IEEE Transactions on Geoscience and Remote Sensing, 36, 1088–1100.
- Bashar, K. E. & Zaki, A. F. (2010). *SMA Based Continuous Hydrologic Simulation of the Blue Nile*. UNESCO Chair in Water Resources.

- Beşer, Ö. (2002). *The use of SSM/I for snow mapping over the eastern part of Turkey*. Master of Science Thesis. Ankara: Middle East Technical University.
- Chen, Z.R.Q., Kavvas, M.L., Ohara, N., Anderson, M.L. & Yoon, J. (2011). *Coupled regional hydroclimate model and its application on the Tigris-Euphrates basin*. Journal of Hydrologic Engineering, 16(12), 1059-1070.
- Chow, V.T., Maidment, D.R. & Mays, L.W. (1988). *Applied Hydrology*. McGraw-Hill Book Company.
- Chu, X & Steinman, A. (2009). *Event and Continuous Hydrologic Modeling with HEC-HMS*. Journal of Irrigation and Drainage Engineering 0733-9437, 1-119.
- Clark, C.O. (1945). *Storage and the unit hydrograph: Transactions*. American Society of Civil Engineers, 110, 1419-1488.
- Çoşkun, C. (2016). *Comparative analysis of various satellite products through hydrological modeling*. Master of Science thesis. Eskişehir: Anadolu University.
- Cunderlik, J. M. & Simonovic, S. P. (2004). *Calibration, Verification and Sensitivity analysis of the HEC-HMS Hydrologic Model*. CFCAS project: Assessment of Water Resources Risk and Vulnerability to Changing Climatic Conditions Project Report IV.
- De Silva M.M.G.T., Weerakoon, S. B. & Herath, S. (2014). *Modeling of Event and Continuous Flow Hydrographs with HEC-HMS: Case Study in the Kelani River Basin, Sri Lanka*. Journal of Hydrologic Engineering, 19(4): 800-806.
- Ertuş M. C. (2014). *Dağlık Fırat Havzasında Ensemble Tahmin Sistemine Dayalı Hidrolojik Modelleme*. Master of Science thesis. Eskişehir: Anadolu University.
- Fazel, K., Scharffenberg, W. A., & Fabián, A. B. (2014). *Assessment of the Melt Rate Function in a Temperature Index Snow Model Using Observed Data*. Journal of Hydrologic Engineering, 19(7): 1275-1282.
- Fleming, M. & Neary, V. (2004). *Continuous hydrologic modeling study with the Hydrologic modeling system*. Journal of Hydrologic Engineering, 9(3), 175-183.

- Garen, C. D., Johnson, L. G. & Hanson, L. C. (1994). *Mean Areal Precipitation for daily hydrologic modeling in mountainous regions*. Water Resources Bulletin, 30, 481–491.
- Gözel, E. (2011). *Yukari Firat Havzasında kar suyu potansiyelinin dönemsel ve akımların günlük modellenmesi*. Master of Science Thesis. Eskişehir: Anadolu University.
- Gyawali, R. & Watkins, D. W. (2013). *Continuous Hydrologic Modeling of Snow-Affected Watersheds in the Great Lakes Basin Using HEC-HMS*. Journal of Hydrologic Engineering, 18(1): 29-39.
- Johansson, B., Caves, R., Ferguson, R., & Turpin, O. (2001). *Using remote sensing data to update the simulated snow pack of the HBV runoff model*. IAHS Publication, 595-597.
- Jones, J.A.A. (1997). *Global Hydrology*, Pearson Education Limited, Edinburgh Gate, Harlow, England.
- Jónsdóttir, J. F., & Þórarinnsson, J. S. (2004). *Comparison of HBV models, driven with weather station data and with MM5 meteorological model data*. Reykjavík, National Energy Authority, Report ISBN 9979-68-147-0. OS-2004/017, 17pp.
- Jones, J.A.A., (1997). *Global Hydrology*, Pearson Education Limited, Edinburgh Gate, Harlow, England.
- Kaya, I. (1999). *Application of snowmelt runoff model using remote sensing and GIS*. Master of Science Thesis. Ankara: Middle East Technical University.
- Kumar, A. R., Sudheer K. P., Jain S. K. & Agarwal P. K. (2005). *Rainfall-runoff modeling using artificial neural networks: comparison of network types*. Hydrological Processes, 19:1277–1291
- Kunstmann, H. & Stadler, C. (2005). *High resolution distributed atmospheric-hydrological modelling for Alpine catchments*. Journal of Hydrology, 314(1), 105-124.
- Lastoria, B. (2008). *Hydrological processes on the land surface: A survey of modelling approaches*, 21 -23.

- Melching, C. S. (1997). *Equations for estimating synthetic unit-hydrograph parameter values for small watersheds in Lake County, Illinois*. Open-File Report 96-474.
- Meselhe E. A., Habib E. H., Oche O. C., & Gautam S. (2009). *Sensitivity of Conceptual and Physically Based Hydrologic Models to Temporal and Spatial Rainfall Sampling*. *Journal of Hydrology*, 14(7): 711-720.
- Mulvaney, T. J. (1850). *On the use of self-registering rain and flood gauges*. *Trans. Inst. Civ. Eng. Ireland*, 4(2): 1-8.
- Musy, A. (2001). *E-drologie*. Ecole Polytechnique Fédérale, Lausanne, Suisse.
- Ohara, N., Kavvas, M. L., Anderson, M. L., Chen, Z. R. Q., & Yoon, J. (2011). *Water balance study for the Tigris-Euphrates river basin*. *Journal of Hydrologic Engineering*, 16(12), 1071-1082.
- Olivera, F. (2001). *Extracting Hydrologic Information from Spatial Data for HMS Modeling*. *Journal of Hydrologic Engineering*, 6(6): 524-530.
- Ponce, V. M. (1989). *Engineering Hydrology*, Prentice-Hall, Englewood Cliffs, N.J.
- Ramakrishnan D., Bandyopadhyay, K. A., & Kusuma, N. (2009). *SCS-CN and GIS-based approach for identifying potential water harvesting sites in the Kali Watershed, Mahi River Basin, India*. *Journal of Earth System Science*, 118 (4): 355-368.
- Refsgaard, C. J., & Jesper, K. (1996). *Operational Validation and Intercomparison of Different Types of Hydrological Models*. *Water Resources Research*, 32(7), 2189-2202.
- Refsgaard, C. J. (1997). *Parameterization, Calibration, and Validation of Distributed Hydrological Models*. *Journal of Hydrology*, 198, pp. 69-97.
- Scharffenberg, B. (2008). *Introduction to HEC-HMS. Watershed modeling with HEC-HMS*. California Water and Engineering Forum, Sacramento, CA.
- Scharffenberg, W., & Pak, J. H. (2009). *History of the HEC-Hydrologic Modeling System (HEC-HMS)*. *Water for Future*, 42(11).



- Şensoy, A. (2000). *Spatially distributed hydrologic modeling approach using geographic information systems*. Master of Science Thesis. Ankara: Middle East Technical University.
- Şensoy, A. (2005). *Physically based point snowmelt modeling and its distribution in Upper Euphrates Basin*. Doctoral dissertation. Ankara: Middle East Technical University.
- Şensoy, A., Uysal, G. and Şorman, A. A. (2016). *Developing a decision support framework for real-time flood management using integrated models*. Journal of Flood Risk Management, DOI: 10(1111),12280.
- Sherman, L.K., (1932). *Streamflow from rainfall by the unit-graph method*. Engineering News Record, 108: 501-505.
- Singh, V. P. (1988). *Hydrologic Systems – Rainfall-Runoff Modeling* (Volume 1). Prentice Hall, Englewood Cliffs, New Jersey.
- Şorman, A. A., (2005). *Use of satellite observed seasonal snow cover in hydrological modeling and snowmelt runoff prediction in upper Euphrates basin, Turkey*. Doctoral Dissertation. Ankara: Middle East Technical University.
- Şorman, A. A., Şensoy, A., Tekeli, A. E., Şorman, A. Ü., & Akyürek, Z. (2009). *Modelling and forecasting snowmelt runoff process using the HBV model in the eastern part of Turkey*. Hydrological Processes, 23(7), 1031-1040.
- Şorman, A.A., Yamankurt, E., 2011. *Modified satellite products on snow covered area in upper Euphrates basin, Turkey*. Geophysics Research Abstract. 13. EGU2011-7887.
- Tekeli, A. E. (2000). *Integration of remote sensing and geographic information systems on snow hydrology modeling*. Master of Science Thesis. Ankara: Middle East Technical University.
- Tekeli, A. E. (2005). *Operational Hydrological Forecasting of Snowmelt Runoff by Remote Sensing and Geographic Information Systems Integration*. Doctoral Dissertation. Ankara: Middle East Technical University.

- Tekeli, A. E., Akyürek, Z., Şorman, A. A., Şensoy, A., & Şorman, A. Ü. (2005). *Using MODIS snow cover maps in modeling snowmelt runoff process in the eastern part of Turkey*. *Remote Sensing of Environment*, 97(2), 216-230.
- Tekeli, A. E., Şensoy, A., Şorman, A., Akyürek, Z., & Şorman, Ü. (2006). *Accuracy assessment of MODIS daily snow albedo retrievals with in situ measurements in Karasu basin, Turkey*. *Hydrological Processes*, 20(4), 705-721.
- TÜBİTAK (108Y161) (2008 – 2011), *Yukarı Fırat Havzasında, arazi ölçümleri, uydu teknolojileri, hava tahmin verileri ve hidrolojik modeller kullanılarak, kar potansiyelinin dönemsel ve akımların günlük tahmini*, Anadolu Üniversitesi, Eskişehir
- TÜBİTAK (113Y075) (2013 – 2016), *Dağlık Fırat ve Seyhan Havzalarında EPS ve Uydu Verileri ile Operasyonel Hidrolojik Tahmin Sisteminin Geliştirilmesi*, Anadolu Üniversitesi, Eskişehir
- USACE (2015). *Hydrologic Modeling System (HEC-HMS) User's Manual*. Davis, California.
- Uysal, G., Şensoy, A. Ş., Şorman, A. A. (20016). *Improving daily streamflow forecasts in mountainous Upper Euphrates basin by multi-layer perceptron model with satellite snow products*. *Journal of Hydrology*. 543(B), 630-650.
- Uzunoğlu, E. (1999). *Application of the SLURP model using remote sensing and geographic information systems*. Master of Science Thesis. Ankara: Middle East Technical University.
- Xu, C. (2002). *Textbook of Hydrologic Models (Lärobok i Avrinningsmodeller)*, 1-8.
- Yamankurt, E., (2010). *Harmanlanan uydu görüntülerinin karla kaplı alanlar üzerindeki etkisi ve Türkiye'nin Yukarı Fırat Havzası'nda dönemsel kar potansiyelinin modellenmesi*. Master of Science Thesis. Eskişehir: Anadolu University.
- Yener, M. K. (2006). *Semi-distributed hydrologic modeling studies in Yuvacik basin*. Master of Science Thesis. Ankara: Middle East Technical University.

Yilmaz, A., Imteaz, M., and Ogwuda, O. (2012). *Accuracy of HEC-HMS and LBRM models in simulating snow runoffs in Upper Euphrates Basin*. Journal of Hydrologic Engineering, 17(2), 342–347.

Zhao, Q., Liu, Z., Ye1, B., Qin, Y., Wei, Z., & Fang, S. (2009). *A snowmelt runoff forecasting model coupling WRF and DHSVM*. Hydrology and Earth System Sciences, 13, 1897–1906.

<https://earthexplorer.usgs.gov/> (searched in 2016)

<http://hsaf.meteoam.it/> (searched in 2016)

[http://www.cost.eu/COST\\_Actions/essem/ES1404](http://www.cost.eu/COST_Actions/essem/ES1404) (Searched in 2016)

<http://www.eea.europa.eu/> (Searched in 2016)

<http://www2.mmm.ucar.edu/mm5/> (Searched in 2016)

<http://hsaf.meteoam.it/description-sm-das-2.php> (searched in 2016)

<http://hsaf.meteoam.it/> (searched in 2016)

<http://hsaf.meteoam.it/soil-moisture.php> (searched in 2016)

**APPENDIX A. Yearly Observed, Conventional and Start-State Hydrographs for Karasu Basin, 2002-2015.**

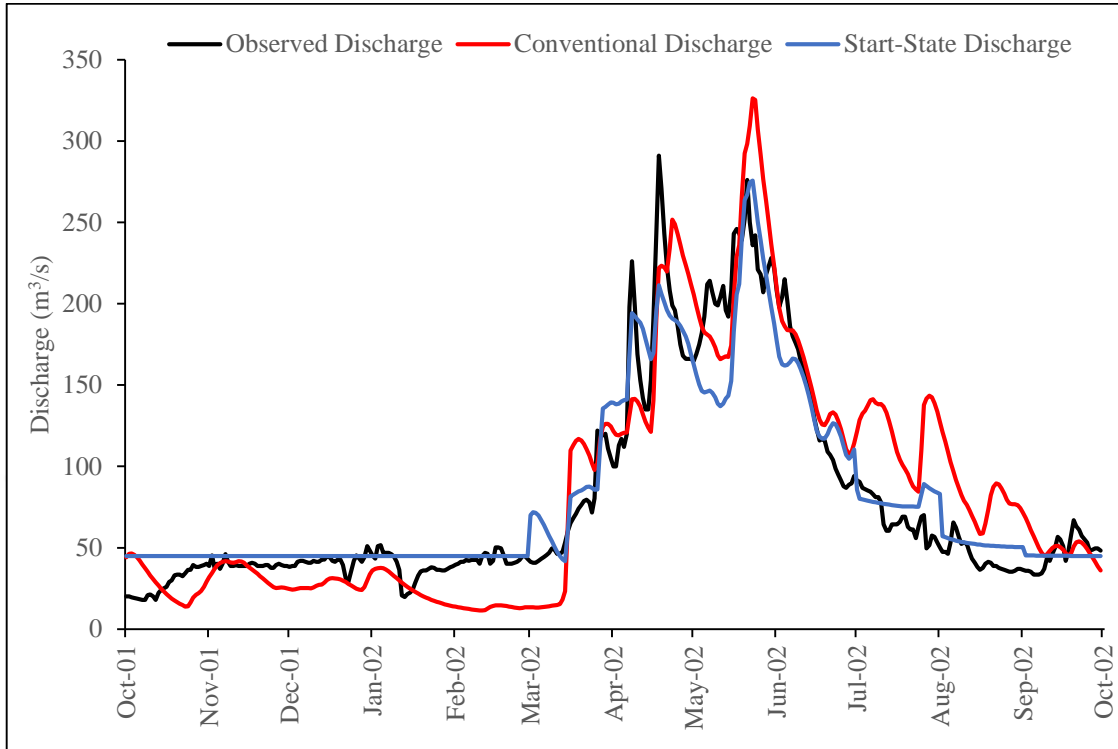


**Figure A.1.** Observed and simulated flows for Karasu Basin, 2002.

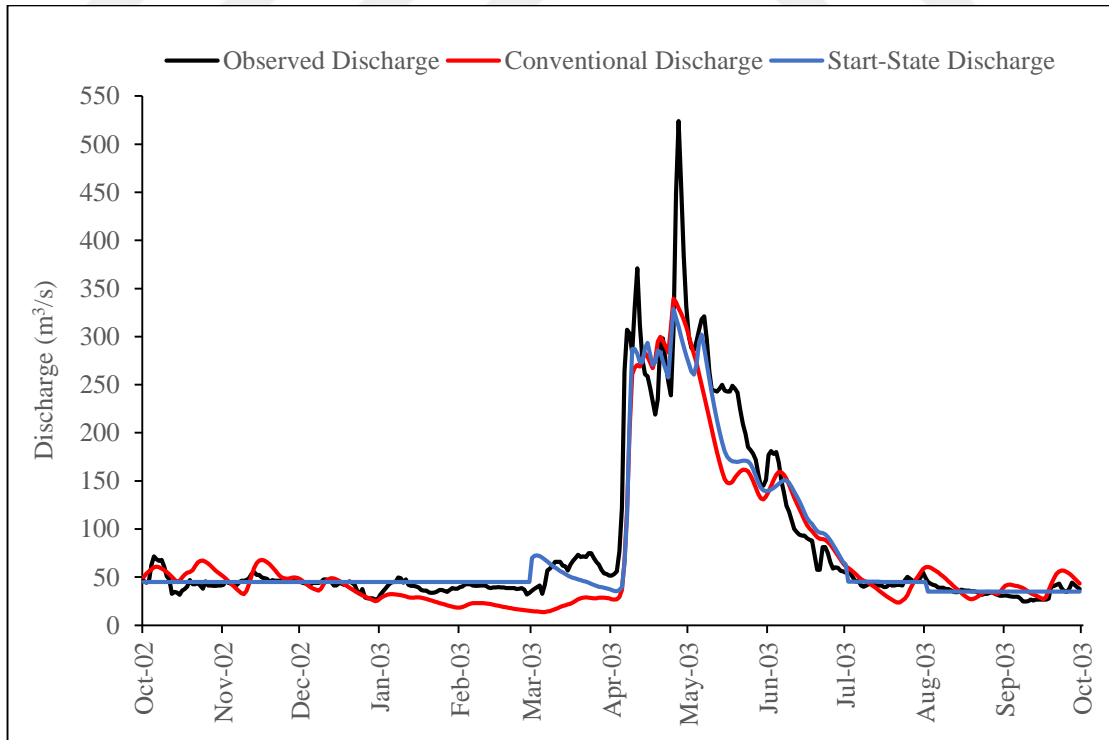


**Figure A.2.** Observed and simulated flows for Karasu Basin, 2003.

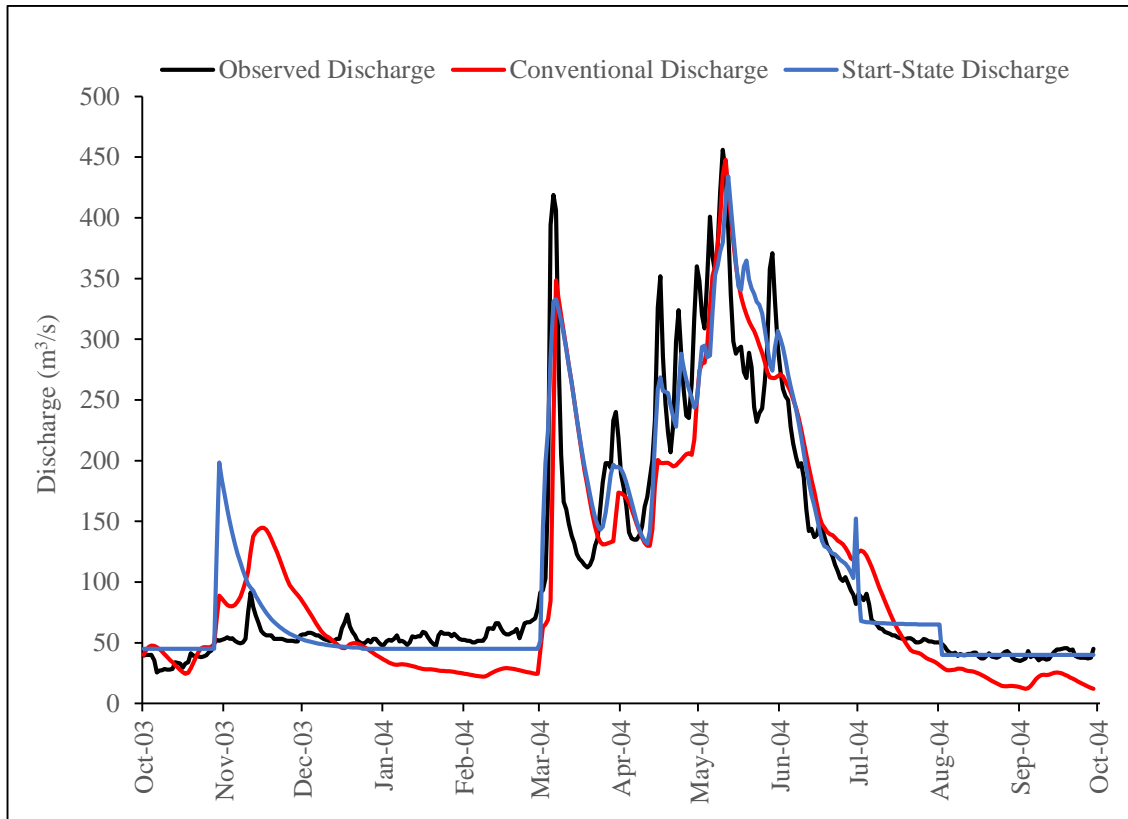


**Figure A.3.** Observed and simulated flows for Karasu Basin, 2004.

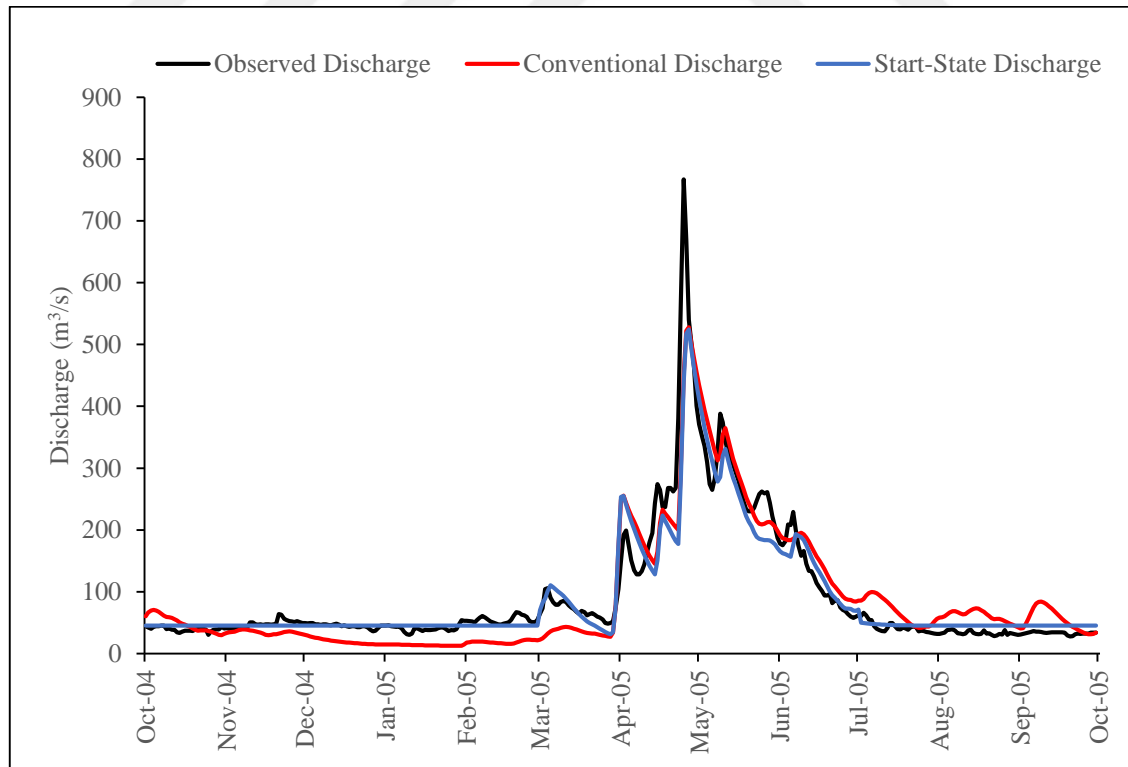


**Figure A.4.** Observed and simulated flows for Karasu Basin, 2005.

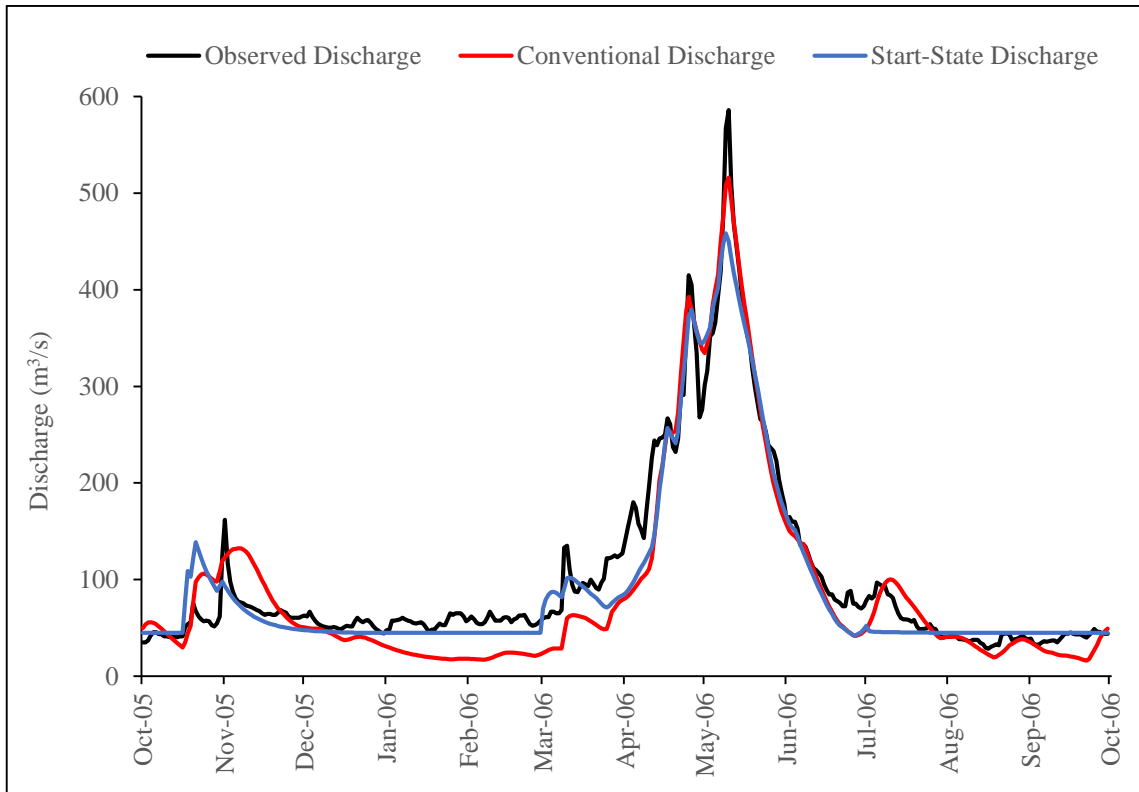


**Figure A.5.** Observed and simulated flows for Karasu Basin, 2006.

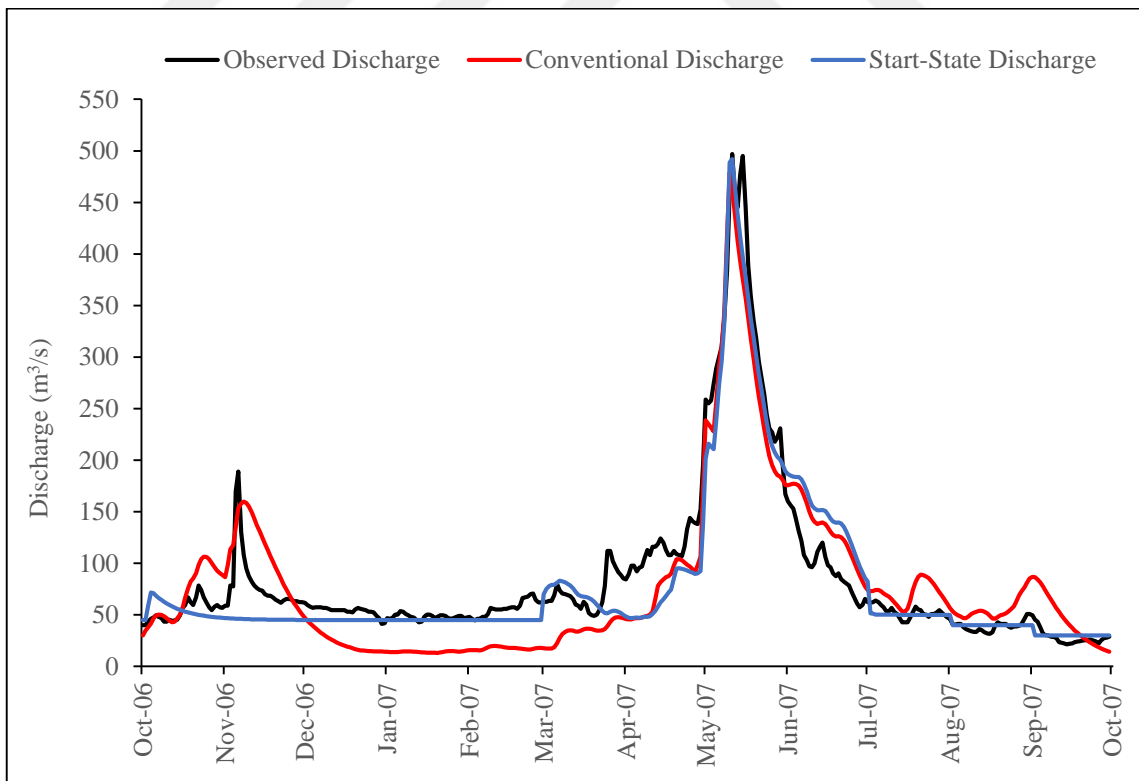


**Figure A.6.** Observed and simulated flows for Karasu Basin, 2007.

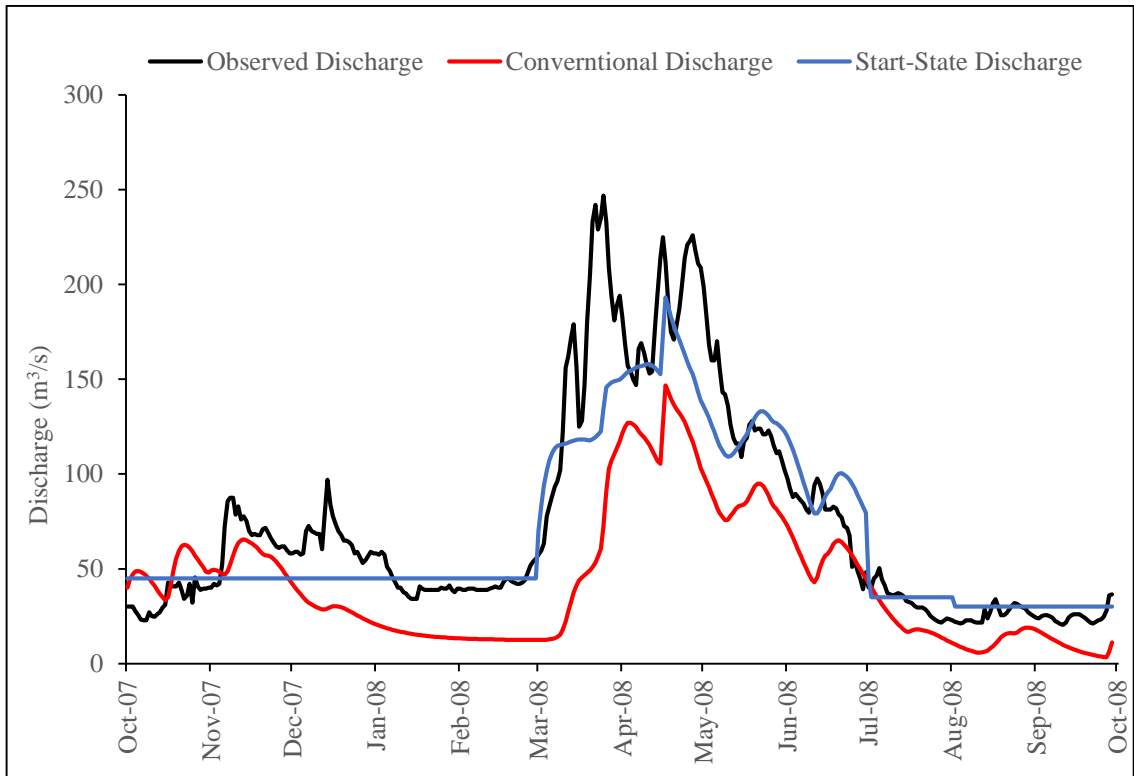


**Figure A.7.** Observed and simulated flows for Karasu Basin, 2008.

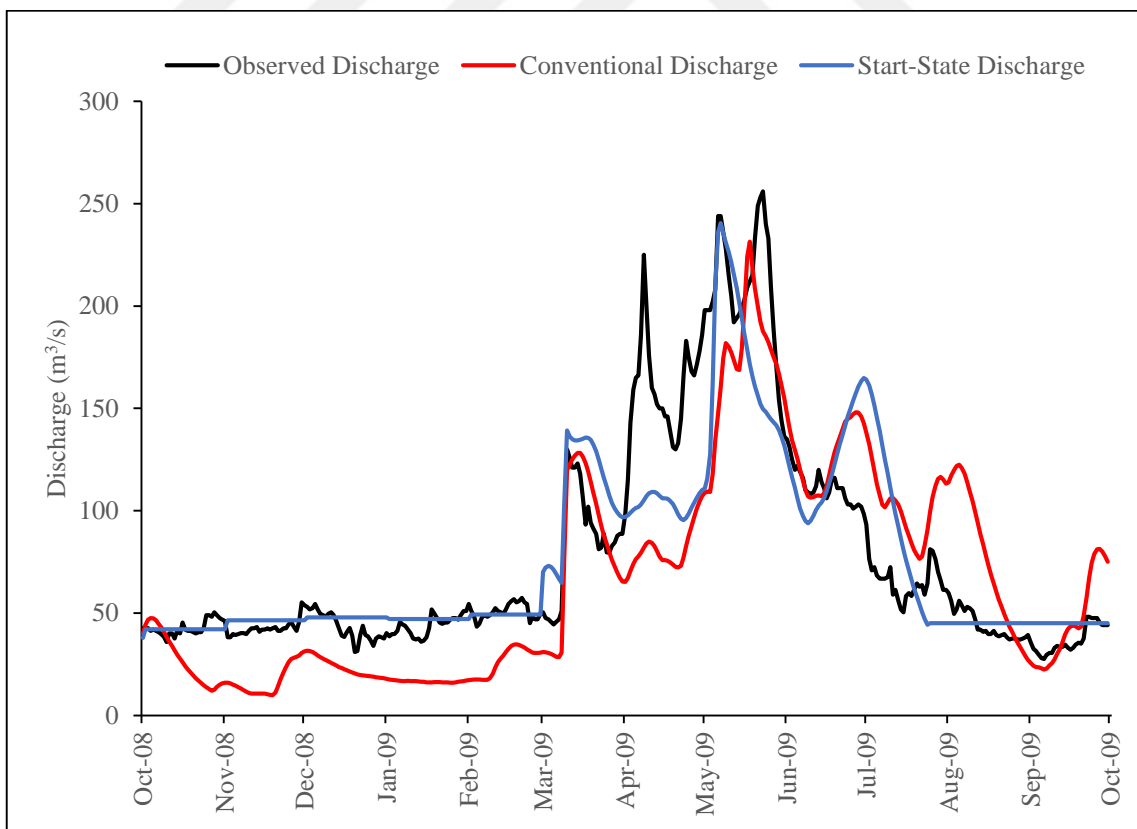


**Figure A.8.** Observed and simulated flows for Karasu Basin, 2009.

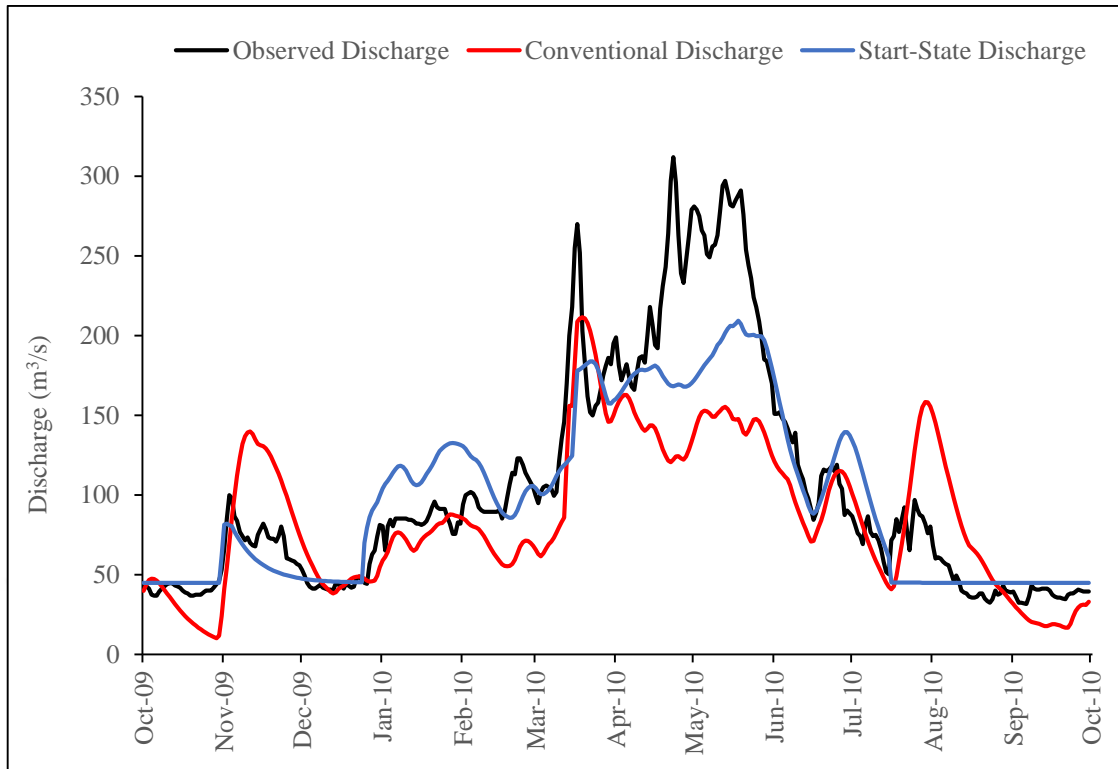


**Figure A.9.** Observed and simulated flows for Karasu Basin, 2010.

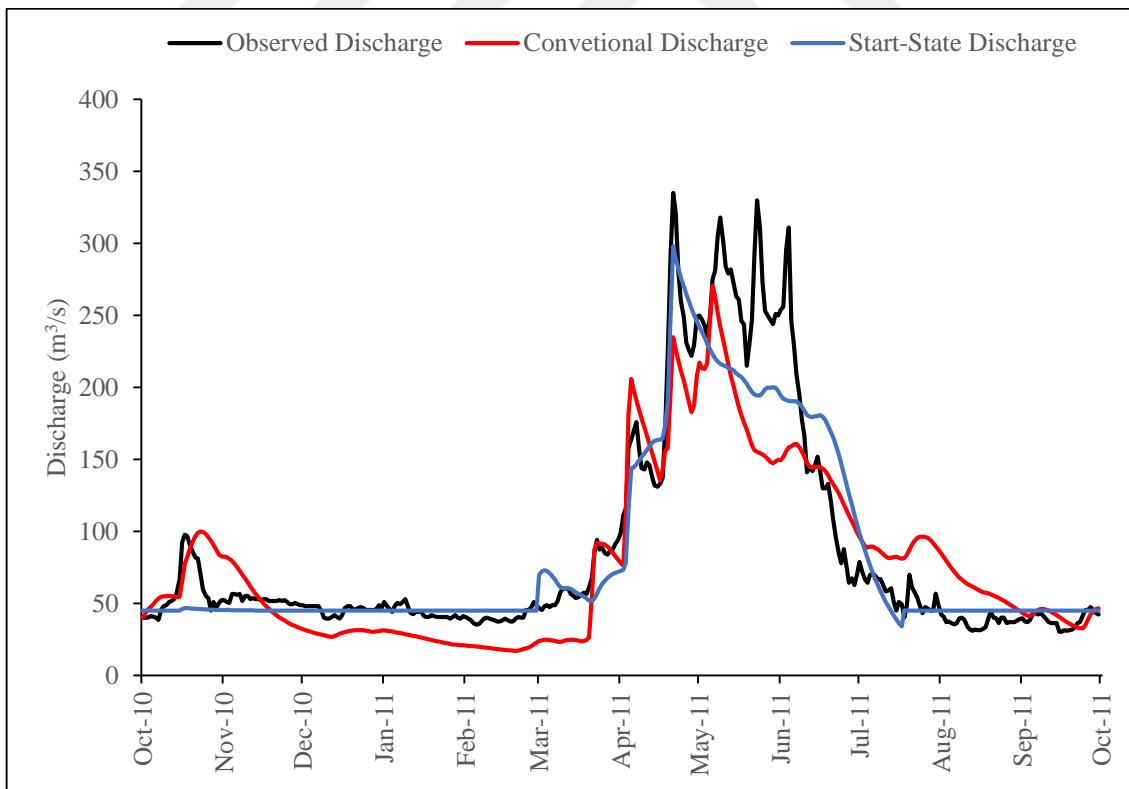


**Figure A.10.** Observed and simulated flows for Karasu Basin, 2011.



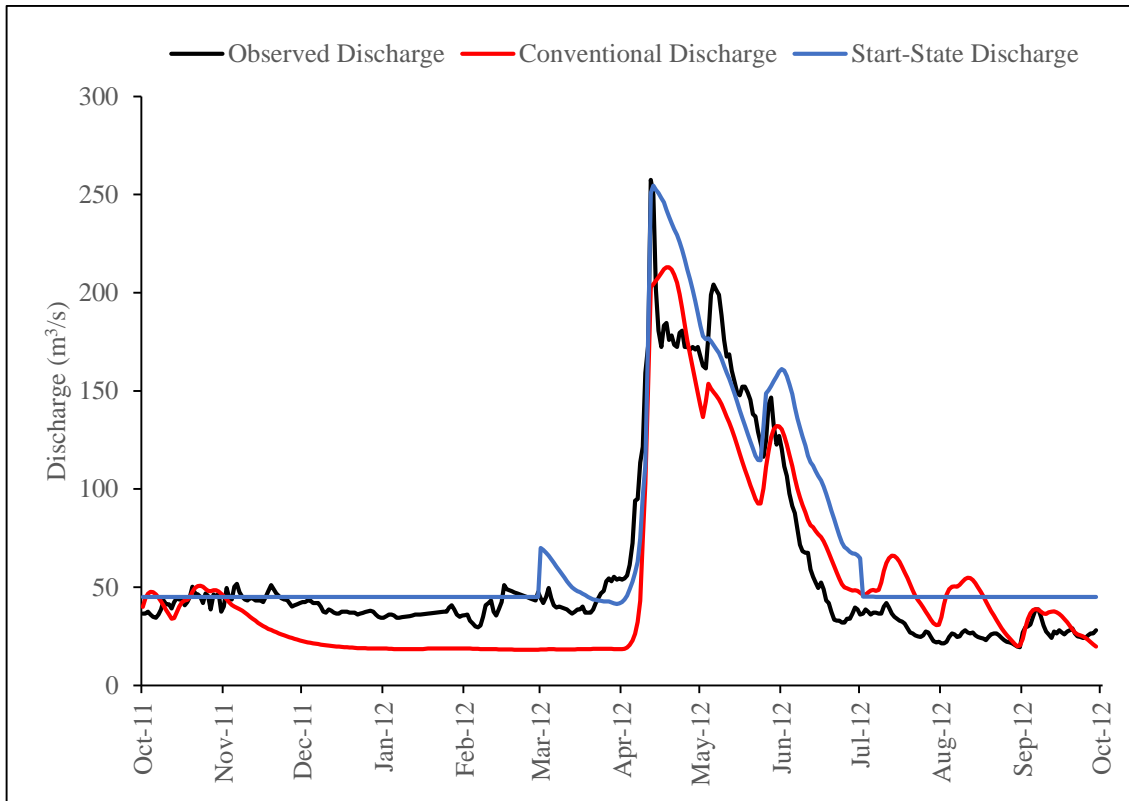


**Figure A.11.** Observed and simulated flows for Karasu Basin, 2012.

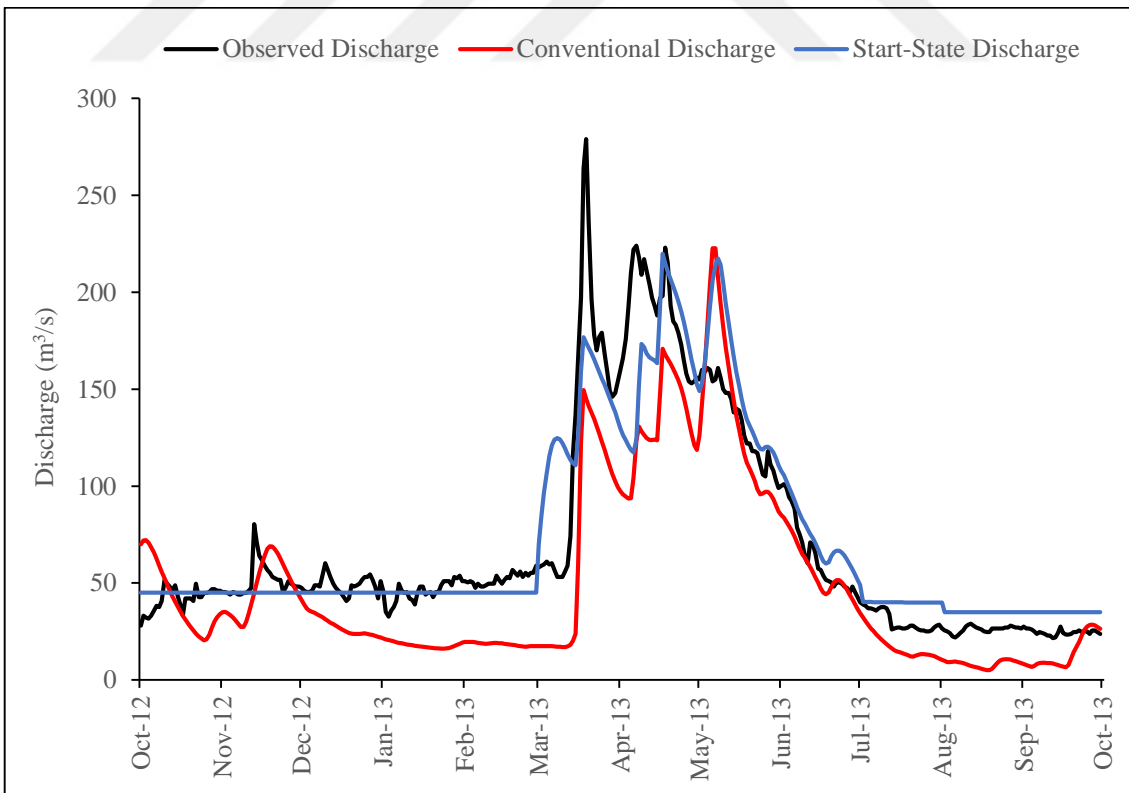


**Figure A.12.** Observed and simulated flows for Karasu Basin, 2013.

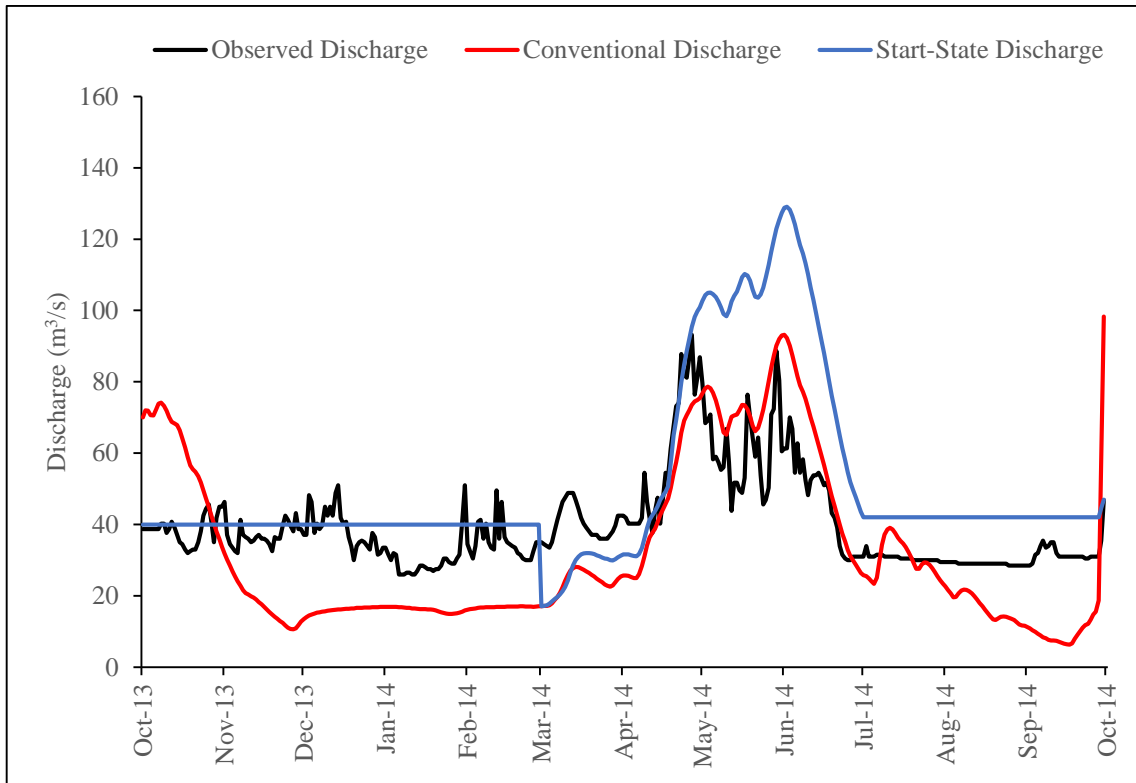


**Figure A.13.** Observed and simulated flows for Karasu Basin, 2014.

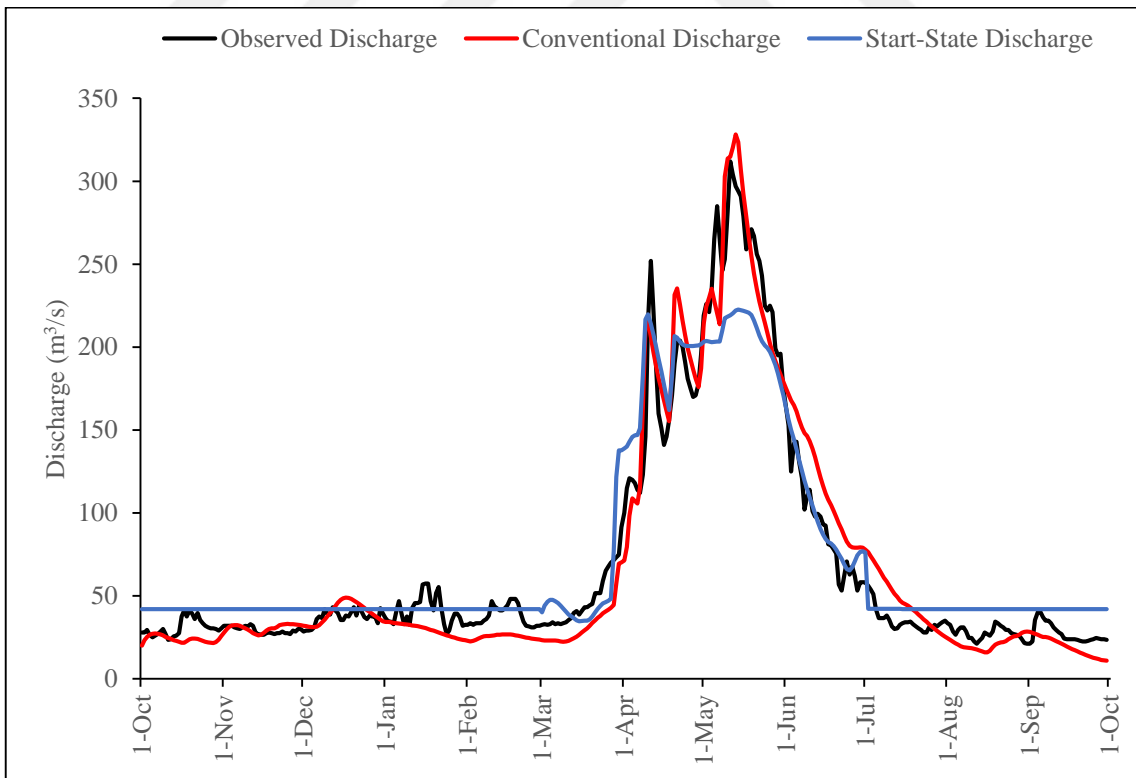


**Figure A.14.** Observed and simulated flows for Karasu Basin, 2015.

## CV

Name-Surname : Bahlakoana Daniel KIKINE  
Foreign Languages : English, Turkish, Zulu and Xhosa  
Place of Birth and Year : Lesotho / 1990  
Email : danielkikine@gmail.com

### Education and Vocational Background:

- 2014, Eskişehir Anadolu University, Civil Engineering Department, Bachelor's Degree

### Publications and Scientific Activities:

- Kikine, D., Şensoy, A. and Şorman, A. (2016). Modeling the Soil Moisture Parametrization in a Snow Dominated Mountainous Region. EGU General Assembly Conference Abstracts (Vol. 18, p. 16846-1).